



POLITECNICO DI TORINO

Master's Degree in Civil Engineering
A.a. 2024/2025

Structural Design of a Cycle- Pedestrian Footbridge Using BIM Methodology

A Case Study in Verbania, Italy

Supervisors

Prof. Rosario Ceravolo

Prof. Anna Osello

Ing. PhD Andrea Alberto

Ing. PhD Davide Lorenzo Dino Aschieri

Candidate:

Anastasia Fanelli

*Alla mia famiglia,
e a tutte le anime gentili che mi hanno accompagnato in questo percorso.*

CONTENTS

Introduction	6
1 BIM METHODOLOGY	7
1.1 Goals and approach.....	7
1.2 BIM Regulations in Italy and Europe	8
1.3 Workflow	9
1.4 Interoperability.....	10
2 PRELIMINARY DESIGN.....	11
2.1 Location and site analysis.....	11
2.2 Footbridge type and material.....	14
2.3 Design considerations: geometric and functional constraints.....	15
3 STRUCTURAL ANALYSIS.....	17
3.1 Calculation criteria and Codes.....	17
3.2 Materials.....	18
3.2.1 Steel.....	18
3.2.2 Wood	19
3.3 Load Analysis	21
3.3.1 Permanent load	21
3.3.2 Variable traffic load	22
3.3.3 Snow load	22
3.3.4 Wind load	24
3.3.5 Thermal load.....	34
3.3.6 Seismic load	37
3.3.7 Load combinations	42
3.4 Modelling in Advance Design	46
3.5 ULS verifications	51
3.5.1 Arch	62
3.5.2 Transverse deck beams	72
3.5.3 Longitudinal deck beams.....	74
3.5.4 Bracings	77
3.5.5 Vertical members	79
3.5.6 Diagonals	81
3.5.7 Secondary longitudinal beams	82
3.5.8 Hangers.....	84
3.5.9 Timber decking	88
3.6 SLS verifications.....	90

3.7 Human comfort	91
3.7.1 Pedestrian loading.....	92
3.7.2 Workflow	95
3.7.3 Dynamic analysis	96
3.8 Support devices	105
4 CONNECTIONS	111
4.1 Theory of Bolted Joints.....	112
4.2 Theory of Welded Joints.....	119
4.3 Connection Design Using IDEA StatiCa.....	121
4.3.1 Joint 1: Longitudinal beams – Vertical members – Diagonals – Bracings – Transversal beams	121
4.4.2 Joint 2: Beam-beam connection.....	130
4.4 Joint 3: Bracing connection	134
5 ARCHITECTURAL MODEL	137
6 COST ANALYSIS (5th Dimension)	139
7 RENDER.....	148
Conclusions.....	150
Table of figures	152
Bibliography amd Webography.....	155

Introduction

The objective of this thesis is to carry out the design of a bridge using the BIM methodology, namely Building Information Modelling. The project was conceived and developed within the professional context of L.G.A. Engineering, a company that has been investing in BIM for years and which is progressively gaining increasing relevance throughout the civil engineering sector.

The case study at the core of the design process is a pedestrian and cycle bridge located in Verbania, specifically near the port of Intra, with a total length of 160 meters.

Particular attention was dedicated to the design of steel structures, drawing on the experience gained during this period at L.G.A. The project began with the definition of a specific structural solution; based on the technical documentation provided, it was then possible to proceed with the development of the model, the dimensioning of sections and profiles, and finally, the verification of the structural elements. Following these phases, the construction details were defined, and a render of the bridge was produced.

The entire process was carried out by taking advantage of the key benefit offered by BIM: the interoperability and information sharing between software tools and across the various phases of the project.

This experience has certainly enabled me to apply in practice the knowledge acquired during the master's program, while also allowing me to gain insight into the professional world and into the roles involved in the various design and decision-making processes required for the realization of an engineering work — from the simplest to the most complex.

1 BIM METHODOLOGY

1.1 Goals and approach

Building Information Modelling (BIM) is a digital process for the design, construction and management of buildings and infrastructure. The acronym BIM refers both to the process and the digital models that are generated and used throughout a project's lifecycle. In fact, BIM involves creating a digital representation of the physical and functional characteristics of a facility, but it also allows all stakeholders—architects, engineers, contractors and owners—to collaborate within a shared, data-rich model.

Unlike traditional 2D drawings, BIM models contain detailed, multi-dimensional information (3D geometry, materials, cost, time, maintenance schedules and more). These models can be used across the entire lifecycle of a project: from early design through construction and operation, to demolition or repurposing.

BIM has revolutionized the AEC (Architecture, Engineering, Construction) industry due to its wide array of applications:

- Design visualization: Enables better understanding of the project before construction begins.
- Clash detection: Identifies spatial conflicts between systems (e.g., mechanical vs structural).
- Time scheduling: Integrates project timelines and logistics (4D BIM).
- Cost estimation: Supports quantity take-offs and cost planning (5D BIM).
- Facility management: Provides accurate as-built data for maintenance and operations (6D/7D BIM).

The main advantages of using BIM include:

- Improve coordination between disciplines
- Reduce errors and rework
- Faster decision-making
- Greater transparency throughout the project
- Enhanced sustainability and lifecycle management

The concept of Level of Development (LOD) defines the degree of detail and reliability of a BIM element. It is used to communicate how much information is included in a model component at different project stages.

Here's a brief summary of the most common LODs:

- LOD 100 – Conceptual: Elements are represented symbolically; approximate geometry.
- LOD 200 – Schematic: Elements have approximate geometry and location.
- LOD 300 – Detailed Design: Accurate geometry, location, and component data suitable for

coordination.

- LOD 350 – Construction Details: Includes interfaces with other building elements.
- LOD 400 – Fabrication: Includes details for manufacturing or construction.
- LOD 500 – As-built: Reflects the final, constructed conditions, used for operation and maintenance.

Each LOD stage supports decision-making and model usability during specific phases of the project.

In this thesis, the goal is to achieve a LOD 400.

LoD USA	LoD UK	LoD Ita
LOD 100 - Concept	LOD 1 - Preparation and Brief	LOD A - oggetto SIMBOLICO
LOD 200 - Design Development	LOD 2 - Concept	LOD B - oggetto GENERICO
LOD 300 - Documentation	LOD 3 - Developed Design	LOD C - oggetto DEFINITO
LOD 350 - Construction	LOD 4 - Technical Design	LOD D - oggetto DETTAGLIATO
LOD 400 - Construction	LOD 5 - Construction	LOD E - oggetto SPECIFICO
LOD 500 - Facilities	LOD 6 - Handover	LOD F - oggetto ESEGUITO
	LOD 7 - Mantainance	LOD G - oggetto AGGIORNATO

Figure 1: LOD in different countries

1.2 BIM Regulations in Italy and Europe

In Italy, the use of BIM is progressively becoming mandatory for public procurement. The main legal references are:

- Ministerial Decree DM 560/2017 (“Decreto BIM”) – Outlines the gradual introduction of BIM in public works, depending on project complexity and cost
- Ministerial Decree 312/2021 which updated and strengthened the guidelines of the previous DM 560/2017, according to which the mandatory to use BIM will be progressive:
 - From 2022 for public works over €15 million.
 - From 2025, all public works over 2 million euros will have to adopt BIM.

This means that right now BIM is becoming a standard for public works.
- Codice dei Contratti Pubblici (D.Lgs. 36/2023) which provides the establishment of a commission to carry out monitoring activities and identify corrective or preventive measures to overcome difficulties encountered by contractors.
- UNI 11337 – The Italian standard defining BIM processes, roles, LOD, data exchange, etc.

At the European level, BIM adoption is encouraged by:

- The EU Directive 2014/24/EU on public procurement, which suggests the use of tools such as BIM for public works.
- EN ISO 19650 – “Organization and digitization of information about buildings and civil engineering works, including BIM”. This standard provides a framework for information management in a collaborative BIM environment, helping align processes across borders.

Building Information Modelling is not just a design tool, but a comprehensive methodology that transforms how construction projects are conceived, built and operated. Through the integration of data-rich models, standardized processes, and collaborative workflows, BIM supports more efficient, accurate, and sustainable project delivery.

1.3 Workflow

Below it's described the process followed for the footbridge study, highlighting the methodology and software used:

1. Structural sizing, starting from the two-dimensional drawing on Autocad, importing it as a .dxf file to Advance Design where the structural model was developed for profile selection.
2. Verification of the profiles constituting the entire structure on Advance Design
3. Nodes verification on Idea Statica, importing the .ifc file from Advance Design to Idea Statica
4. Realization of the architectural model on Revit, exporting the .gtcx file from Advance Design
5. Placement in context and rendering, through the “direct link” function from Revit to Twinmotion

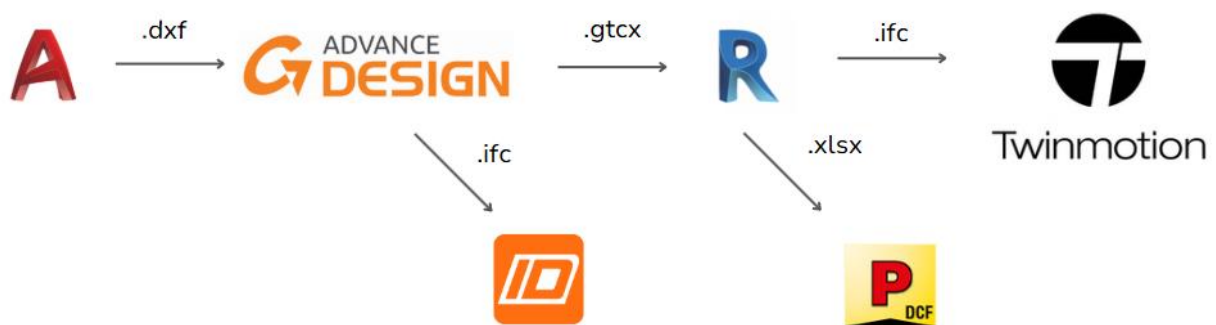


Figure 2: Workflow

1.4 Interoperability

During the design phase of a civil engineering project, two distinct types of interoperability can be identified:

- Interoperability between people

This is fundamental as it facilitates communication among the various professionals involved in the project, who often work together as a team. However, this aspect has not been explored in depth in this thesis, as it represents an individual work.

- Interoperability between software

Software and data interoperability is of great importance, as it allows for the transfer of files between different models, thereby streamlining the workflow and information exchange. An example of this is the transition from a global structural model to local node models, or from a structural model to an architectural one. It should be noted that some data loss may occur during the transfer between software platforms. Therefore, it is essential to assess what information is effectively transferred and how well interoperability functions across the various programs.

In order to illustrate the level of interconnection between the software tools used, at the end of the paper, the interoperability matrix will be developed.

2 PRELIMINARY DESIGN

2.1 Location and site analysis

Site analysis is a preliminary phase of architectural and urban design processes dedicated to the study of the climatic, geographical, historical, legal, and infrastructural context of a specific site. It involves gathering data and studying the site's context and surrounding features that might impact the design. The case study being designed is a 160 m long cycle-pedestrian footbridge located in Verbania, on the western shore of Lake Maggiore and capital of the province of Verbano-Cusio-Ossola. In particular, the intervention is part of the theoretical proposal within the call ITALIA CITY BRANDING 2020, whose winning cities include Verbania, for the realisation of an integrated intermodal system of sustainable mobility and public infrastructures. The final objective of the call is to increase the attractiveness of the territories with respect to investments, enhancing the most identifying aspects of the productive, cultural and social fabric (the brand) of the beneficiary cities.

Precisely for this reason, the preliminary design of the new infrastructure includes not only the initial dimensioning of the elements constituting the supporting structure, but also a careful analysis of the territory on which the bridge under consideration will be built.

The footbridge under consideration will have to stand alongside an existing vehicular bridge located near the Intra Heliport, crossing the San Bernardino torrent.

The following is a bird's eye view of the site of the intervention under examination as seen from satellite (Google Maps), followed by some photos taken on site by drone.



Figure 3: Top view of the site of the intervention



Figure 4: Top view photo of the site taken with a drone



Figure 5: Photo of the site taken with a drone

As can be seen from the photos, the footbridge is placed next to the Theatre THE MAJOR, characterised by curved forms covered in titanium zinc, evoking the stones of the banks and the adjacent river. Modern architecture of this kind can be found in various new urban areas of European cities; we can't help but think, for example, of the Neuer Zollhof complex in Dusseldorf overlooking the Rhine, with its sometimes angular, sometimes rounded forms. Or the more famous Guggenheim Museum in Bilbao, which, seen from the river, seems to have the shape of a ship.



Figure 6: Neuer Zollhof complex in Dusseldorf



Figure 7: Guggenheim Museum in Bilbao

What do these new urban areas have in common that makes them so appealing? The element of water in the form of a river, round shapes that fit sinuously into their surroundings, the use of materials such as steel/titanium and a great visual impact.

The proposal for the footbridge is inspired by this type of architecture; in addition, given the considerable length of the deck and in order to avoid introducing new piers into the riverbed, the decision was made for a through arch bridge made of steel, with a wooden deck.

2.2 Footbridge type and material

The chosen typology is an arch bridge with intermediate deck, also called "half-through arch" bridge. An arch bridge with an intermediate deck is a structural design where the bridge deck is positioned between the apex and the base of the arch. The arch primarily bears compressive forces, transferring loads from the deck to the foundations. The deck, situated at an intermediate level, is typically suspended from the arch using vertical. This arrangement allows for efficient load distribution and provides structural stability. The intermediate deck placement offers advantages such as reduced material usage and aesthetic appeal.

There are notable examples of arch bridges with Intermediate decks in literature:



Figure 8: Tyne Bridge, UK



Figure 9: Las Llamas Bridge, Spain



Figure 10: Chaotianmen Bridge, China

Bridge Name	Main Length	Span	Span-to-Rise Ratio	Materials	Location	Year of Completion
Las Llamas Bridge	120 m		5.0	Reinforced Concrete	Santander, Spain	2007
Tyne Bridge	162 m		2.95	Steel	Newcastle upon Tyne, UK	1928
Chaotianmen Bridge	552 m		3.89	Steel	Chongqing, China	2009

2.3 Design considerations: geometric and functional constraints

According to Article 7 of Ministerial Decree 557/1999, we have:

"The minimum width of a cycle lane, including edge markings, is 1.50 m; this width may be reduced to 1.25 m in the case of two adjacent lanes, either in the same or opposite direction, resulting in a minimum total width of 2.50 m."

Another important design constraint concerns the maximum overall dimensions of bicycles allowed to use the footbridge, as established by Article 50 of the Italian Highway Code. The prescribed limits are as follows:

- Maximum width: 1.30 m
- Maximum length: 3.00 m
- Maximum height: 2.20 m

Based on these parameters, the footbridge has been designed with a minimum vertical clearance of 2.20 meters. This allows the safe transit of larger bicycles, such as cargo bikes or tandems, and ensures adequate headroom for pedestrian users.

To facilitate traffic flow, it was decided to place the two directions of the cycle path adjacent to each other so we must have a minimum total width of 2.5 meters. In the present case, the decision was made to adopt a deck width of 6.00 meters, which is significantly greater than the minimum regulatory requirements. This ensures a comfortable and safe passage for both cyclists and pedestrians, while also providing adequate space for benches.

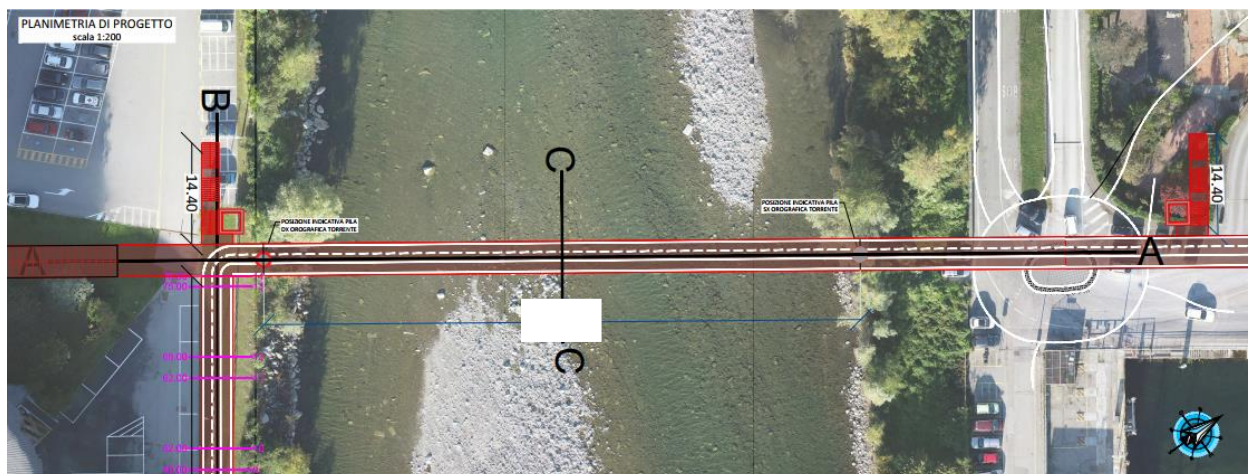


Figure 11: Site plan

3 STRUCTURAL ANALYSIS

The structural analysis, after determining the actions acting on the structure according to the reference standard, will be structured in the following steps:

- Global analysis at SLUs of strength and stability;
- Global analysis at SLEs of deformation;
- Analysis of the human comfort;

3.1 Calculation criteria and Codes

The standards used in this project are:

- D.M. January 17, 2018
"Update of "Technical Standards for Construction"
- Circular n° 7, January 21, 2019
"Instructions for the application of the "Update of the "Technical Standards for constructions"
- CNR-DT 207/2008
"Instructions for the evaluation of wind actions and effects on constructions"
- UNI EN 1991 Eurocodice 1
"Actions of structures"
- UNI EN 1993 Eurocodice 3
"Design of steel structures"
- UNI 11035-2:2022
"Structural wood - Visual classification of Italian timbers according to mechanical strength"
- D.M. n° 557, November 30, 1999
"Regulation containing standards for the definition of technical characteristics of bicycle paths"

3.2 Materials

The materials used for the structural elements of the footbridge are presented below.

3.2.1 Steel

The main characteristics that a steel intended for structural applications must possess are the following:

- Strain hardening
- Ductility
- Weldability
- Workability

The stress-strain constitutive relationship describes the deformation behavior of steel in response to a given stress state. It is symmetrical in both tension and compression, providing a significant technical advantage over concrete.

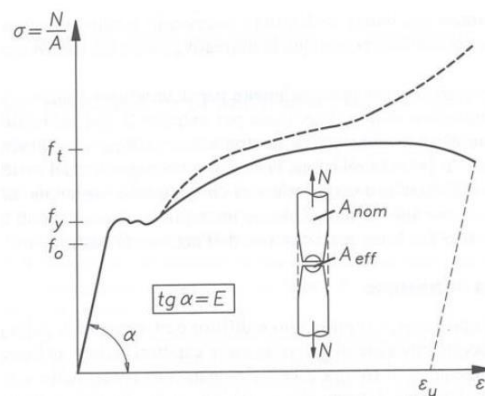


Figure 12: Stress-strain curve

The steel chosen is the S355J0WP (Corten). The meaning of the designation S355J0WP is:

- S = Structural steel
- 355 = Minimum yield strength of 355 MPa for thicknesses less than 16 mm
- J0 = Guaranteed impact toughness at 0°C (minimum absorbed energy ≥ 27 J)
- W = Weathering steel, i.e., steel with enhanced atmospheric corrosion resistance
- P = Phosphorus-alloyed, improving the protective patina formation and corrosion resistance

The suffix "WP" in S355J0WP indicates that this is a structural steel with enhanced resistance to atmospheric corrosion, due to the addition of phosphorus, which promotes the formation of a stable and protective surface patina. This type of steel is commonly used in the construction of bridges,

architectural facades, sculptures, road barriers, and other structures exposed to the elements, without the need for protective painting. Below there's a table with the mechanical characteristics:

Classification	S355 J0 WP Corten Steel (EN10025-5)	
Elastic Modulus	$E = 210000$	MPa
Poisson's Ratio	$\nu = 0.3$	[-]
Shear Modulus	$G = 81000$	MPa
Thermal Expansion Coefficient	$\alpha = 12 \cdot 10^{-6}$	$^{\circ}\text{C}^{-1}$
Yield Strength	$f_y = 355$	MPa
Ultimate Tensile Strength	$f_u = 510$	MPa
Partial Safety Factor	$\gamma_{M0} = 1.05$	[-]
Design Yield Strength	$f_{y,d} = f_y / \gamma_m = 355 / 1.0 = 355$	MPa

3.2.2 Wood

From a structural point of view, solid wood is characterized by an anisotropic fibrous composition, which results in different mechanical properties along its main directions. Due to its ability to work well in compression and tension, it is used in numerous works, from roofing to pedestrian bridges, providing good static and dynamic performance. One of the distinctive aspects of solid wood is its durability, which is influenced by factors such as moisture, temperature and exposure to weathering. The solid wood chosen is chestnut wood of strength class 28; it is valued for its durability, resistance to moisture, and is easy to work with. Due to its high tannin content, chestnut wood is naturally resistant to weathering and pests, even without chemical treatment.

Below there's a table with the mechanical characteristics:

Tabella 18-3-Classi di resistenza secondo EN 11035, per specie legnose di provenienza italiana (continua)

Proprietà		Castagno / Italia	Querce caducifoglie / Italia	Pioppo e Ontano / Italia	Altre Latifoglie / Italia
		<i>S</i>	<i>S</i>	<i>S</i>	<i>S</i>
Flessione (5-percentile), MPa	$f_{m,k}$	28	42	26	27
Trazione parallela alla fibratura (5-percentile), MPa	$f_{t,0,k}$	17	25	16	16
Trazione perpendicolare alla fibratura (5-percentile), MPa	$f_{t,90,k}$	0.5	0.8	0.4	0.5
Compressione parallela alla fibratura (5-percentile), MPa	$f_{c,0,k}$	22	27	22	22
Compressione perpendi-colare alla fibratura (5-percentile), MPa	$f_{c,90,k}$	3.8	5.7	3.2	3.9
Taglio (5-percentile), MPa	$f_{v,k}$	2.0	4.0	2.7	2.0
Modulo di elasticità parallelo alla fibratura (medio), MPa ($\times 10^3$)	$E_{0,mean}$	11	12	8	11.5
Modulo di elasticità parallelo alla fibratura (5-percentile), MPa ($\times 10^3$)	$E_{0,05}$	8	10.1	6.7	8.4
Modulo di elasticità perpen dicolare alla fibratura -(medio), MPa ($\times 10^2$)	$E_{90,mean}$	7.3	800	5.3	7.7
Modulo di taglio (medio), MPa ($\times 10^2$)	G_{mean}	9.5	750	5	7.2
Massa volumica (5-percentile), kg/m ³	ρ_k	465	760	420	515
Massa volumica (media), kg/m ³	ρ_{mean}	550	825	460	560

3.3 Load Analysis

According to paragraph §5.1.3. of NTC2018, the actions to be considered in the design of road bridges are:

- permanent actions;
- impressed distortions and deformations;
- the variable actions of traffic;
- the variable actions (thermal variations, hydrodynamic thrusts, wind, snow and the actions on parapets);
- the passive resistances of constraints;
- the impacts on the road safety barriers of swerving vehicles;
- the seismic actions;
- the exceptional actions.

In the present case, since the bridge is for pedestrian and bicycle use, the impacts on the barriers of swerving vehicles and all actions that would be caused by the passage of motor vehicles are not considered.

3.3.1 Permanent load

Permanent actions are those that act throughout the design life of the construction; this category includes structural and nonstructural permanent weight.

3.3.1.1 Structural Permanent Load -G1

The self-weight of the structural elements consists of the metallic carpentry.

3.3.1.2 Non- structural Permanent Load -G2

Non-structural elements considered are:

- Wooden plank deck: 0,3 kN/ m²
- Parapet: 1kN/m

3.3.2 Variable traffic load

In the present case, since the bridge is for pedestrian and bicycle use, the variable traffic actions are to be understood exclusively as a distributed load of 5 kN/m² as provided in the paragraph §5.1.3.14 NTC18.

Tab. 5.1.IV – Valori caratteristici delle azioni dovute al traffico

	Carichi sulla superficie carrabile					Carichi su marciapiedi e piste ciclabili non sormontabili
	Carichi verticali			Carichi orizzontali		Carichi verticali
Gruppo di azioni	Modello principale (schemi di carico 1, 2, 3, 4 e 6)	Veicoli speciali	Folla (Schema di carico 5)	Frenatura	Forza centrifuga	Carico uniformemente distribuito
1	Valore caratteristico					Schema di carico 5 con valore di combinazione 2,5kN/m ²
2a	Valore frequente			Valore caratteristico		
2b	Valore frequente				Valore caratteristico	
3 (*)						Schema di carico 5 con valore caratteristico 5,0kN/m ²
4 (**)			Schema di carico 5 con valore caratteristico 5,0kN/m ²			Schema di carico 5 con valore caratteristico 5,0kN/m ²
5 (***)	Da definirsi per il singolo progetto	Valore caratteristico o nominale				
(*) Ponti pedonali						
(**) Da considerare solo se richiesto dal particolare progetto (ad es. ponti in zona urbana)						
(***) Da considerare solo se si considerano veicoli speciali						

Load pattern 5: consisting of the compact crowd, acting with a nominal intensity, including dynamic effects, of 5.0 kN/m². The crowd load shall be applied to all significant areas of the influence surface.

3.3.3 Snow load

The snow load is evaluated according to §3.4.1 NTC18, by the following expression

$$q_s = q_{sk} \cdot \mu_i \cdot C_E \cdot C_t$$

where:

- q_{sk} is the reference value of the snow load on the ground which depends on the local conditions of climate and exposure. To calculate this value, the 4 zones into which the national territory is divided are considered; the city of Verbania belongs to *zone I - Alpine*, with an altitude of 197 m above sea level ; since it is less than 200 m , a value of snow on the ground is considered to be:

$$q_{sk} = 1.50 \text{ kN/m}^2$$

- $\mu_i = 0.8$ is the roof shape coefficient for pitched roofs with $\alpha < 30^\circ$ (for a bridge, the surface is assimilated to that of a flat roof)
- $C_E = 1$ is the exposure coefficient that takes into account the specific characteristics of the area where the is located;
- $-C_t = 1$ s the thermal coefficient takes into account the reduction in snow load. In the absence of a specific documented study, $C_t = 1$ must be set.

It is assumed that the snow load acts in the vertical direction and refers it to the horizontal projection of the roof surface.

Therefore, the following table shows the result of snow load:

a_s [m]	q_{sk} [kN/m ²]	μ_i [-]	C_E [-]	C_t [-]	q_s [kN/m ²]
197	1.5	0.8	1	1	1.2

The characteristic design value of snow on the ground used will be 1.20 kN/m^2 equal to 120 kg/m^2

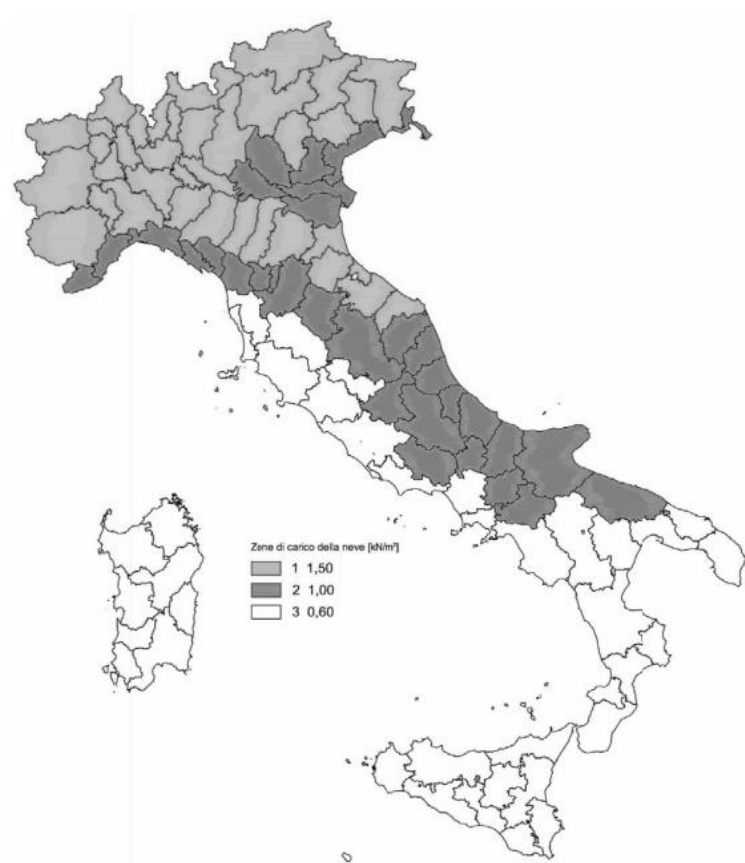


Figure 13: Snow load zones

3.3.4 Wind load

According to §5.1.3.7 NTC18 wind action can conventionally be assimilated to a system of static loads, the main component of which is horizontal and directed orthogonally to the axis of the. This principal component is considered to be acting on the projection in the vertical plane of the invested surfaces, including parapets, road safety barriers and noise barriers, where provided.

Referring to Chapter 3 of NTC2018, the maximum horizontal static wind action is evaluated. In particular, as stated in §3.3.4. the wind pressure can be identified with the expression:

$$p = q_r * c_e * c_p * c_d$$

Where:

- q_r is the reference kinetic pressure;
- c_e is the exposure coefficient;
- c_p is the pressure coefficient;
- c_d is the dynamic coefficient.

The value of the reference kinetic pressure can be calculated as follows:

$$q_r = \frac{1}{2} \rho v_r^2$$

As a design assumption we assume an air density of 1.25 kg/m³; v_r is the reference velocity, which is the average value over 10 minutes at 10 metres ground level on level ground, this value is given:

$$v_r = v_b \cdot c_r$$

Where:

- c_r is the return coefficient, a function of the return period T_R . $T_R = 50$ is assumed, to which $c_r = 1$ corresponds.

- v_b is the reference base velocity, evaluated as:

$$v_b = v_{b,0} \cdot c_a$$

Where:

- $v_{b,0}$ is the reference velocity at sea level, depending on the region showed below
- c_a is the altitude coefficient, equal to 1 in case the altitude of the structure does not exceed the corresponding value of a_0 .

Tab. 3.3.I -Valori dei parametri $v_{b,0}$, a_0 , k_s

Zona	Descrizione	$v_{b,0}$ [m/s]	a_0 [m]	k_s
1	Valle d'Aosta, Piemonte, Lombardia, Trentino Alto Adige, Veneto, Friuli Venezia Giulia (con l'eccezione della provincia di Trieste)	25	1000	0,40
2	Emilia Romagna	25	750	0,45
3	Toscana, Marche, Umbria, Lazio, Abruzzo, Molise, Puglia, Campania, Basilicata, Calabria (esclusa la provincia di Reggio Calabria)	27	500	0,37
4	Sicilia e provincia di Reggio Calabria	28	500	0,36
5	Sardegna (zona a oriente della retta congiungente Capo Teulada con l'Isola di Maddalena)	28	750	0,40
6	Sardegna (zona a occidente della retta congiungente Capo Teulada con l'Isola di Maddalena)	28	500	0,36
7	Liguria	28	1000	0,54
8	Provincia di Trieste	30	1500	0,50
9	Isole (con l'eccezione di Sicilia e Sardegna) e mare aperto	31	500	0,32

Parameter values $v_{b,0}$, a_0 e k_s

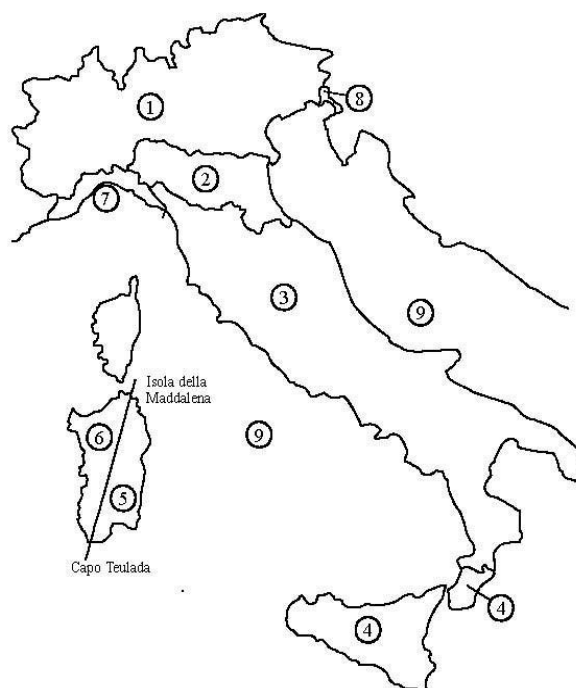


Figure 14: Map of the zones into which the Italian territory is divided

The city of Verbania belongs to Zone 1, to which corresponds a v_b value of 25.00 m/s .

The following values are obtained:

$$v_r = v_b \cdot C_r = 25 \text{ m/s}$$

$$q_r = \frac{1}{2} \rho v_r^2 = \frac{1}{2} * 1.25 * 25^2 = 390.62 \text{ N/m}^2$$

The value of the exposure coefficient depends on the height z above ground of the point in question, the topography of the soil and the exposure category of the site where the building stands. In the absence of specific analyses that take into account the direction of origin of the wind and the actual roughness and topography of the terrain surrounding the construction, for heights above ground not greater than $z = 200 \text{ m}$, it is given by the formula:

$$\begin{aligned} c_e(z) &= k_t^2 c_t \ln(z/z_0) [7 + c_t \ln(z/z_0)] && \text{per } z \geq z_{\min} \\ c_e(z) &= c_e(z_{\min}) && \text{per } z < z_{\min} \end{aligned}$$

The topography coefficient c_t is generally set equal to 1.

To evaluate the parameter c_e we must locate the site exposure category; considering the proximity to the lake, the area is classified as soil roughness class D and exposure category I as showed in the tables below.

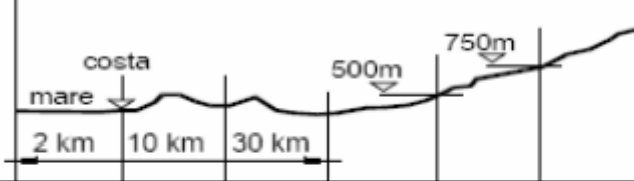
Tab. 3.3.II - Parametri per la definizione del coefficiente di esposizione

Categoria di esposizione del sito	K_t	z_0 [m]	z_{\min} [m]
I	0,17	0,01	2
II	0,19	0,05	4
III	0,20	0,10	5
IV	0,22	0,30	8
V	0,23	0,70	12

Tab. 3.3.III - Classi di rugosità del terreno

Classe di rugosità del terreno	Descrizione
A	Aree urbane in cui almeno il 15% della superficie sia coperto da edifici la cui altezza media superi i 15 m
B	Aree urbane (non di classe A), suburbane, industriali e boschive
C	Aree con ostacoli diffusi (alberi, case, muri, recinzioni,...); aree con rugosità non riconducibile alle classi A, B, D
D	a) Mare e relativa fascia costiera (entro 2 km dalla costa); b) Lago (con larghezza massima pari ad almeno 1 km) e relativa fascia costiera (entro 1 km dalla costa) c) Aree prive di ostacoli o con al più rari ostacoli isolati (aperta campagna, aeroporti, aree agricole, pascoli, zone paludose o sabbiose, superfici innevate o ghiacciate,)

L'assegnazione della classe di rugosità non dipende dalla conformazione orografica e topografica del terreno. Si può assumere che il sito appartenga alla Classe A o B, purché la costruzione si trovi nell'area relativa per non meno di 1 km e comunque per non meno di 20 volte l'altezza della costruzione, per tutti i settori di provenienza del vento ampi almeno 30°. Si deve assumere che il sito appartenga alla Classe D, qualora la costruzione sorga nelle aree indicate con le lettere a) o b), oppure entro un raggio di 1 km da essa vi sia un settore ampio 30°, dove il 90% del terreno sia del tipo indicato con la lettera c). Laddove sussistano dubbi sulla scelta della classe di rugosità, si deve assegnare la classe più sfavorevole (l'azione del vento è in genere minima in Classe A e massima in Classe D).

ZONE 1,2,3,4,5						
						
A	--	IV	IV	V	V	V
B	--	III	III	IV	IV	IV
C	--	*	III	III	IV	IV
D	I	II	II	II	III	**
* Categoria II in zona 1,2,3,4 Categoria III in zona 5						
** Categoria III in zona 2,3,4,5 Categoria IV in zona 1						

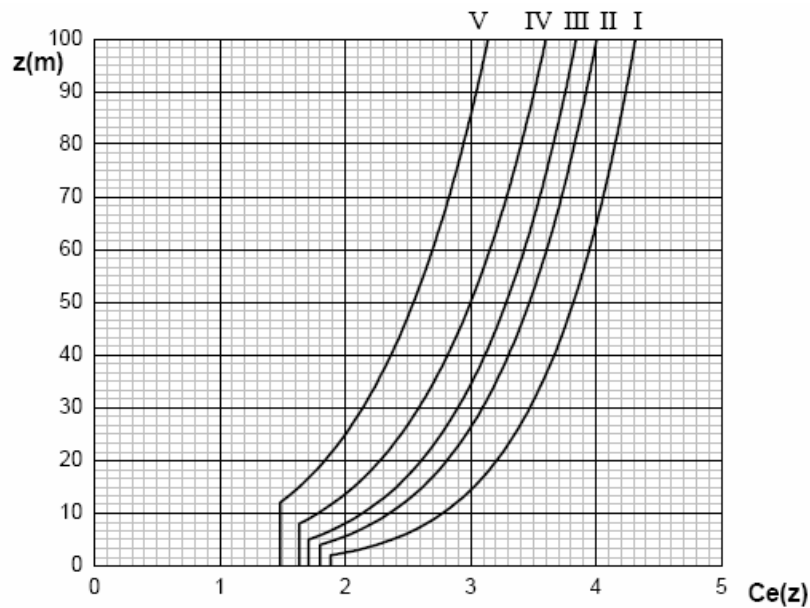


Figure 15: -Evolution of the exposure coefficient c_e as a function of height above ground (for $ct = 1$)

Since c_e varies according to the height considered, we have different values of wind pressure acting on the bridge; for safety and simplicity reasons the value of the maximum height of the bridge (23m) will be used for vertically developed elements.

The dynamic coefficient c_d takes into account the reductive effects associated with the non-contemporaneity of the maximum local pressures and the amplifying effects due to the dynamic response of the structure.

It can be cautiously assumed to be equal to 1.

Without considering the contribution made by the pressure coefficient, the wind pressure on the different elements of the bridge results:

Element	z [m]	c_e	$q_p(\text{kN/m}^2)$
Deck	$z = 5$	2,373	0,93
Arch	$z \leq 23$	3,298	1,29
Vertical hangers	$z \leq 23$	3,298	1,29

However, as the structure is a bridge, the shape of the deck and the other elements influences the wind pressure distribution, which is why further analyses should be carried out in order to determine the pressure coefficient more precisely. The standard considered to conduct the analyses is CNR-DT 207 R1/2018, Appendix G.

The standard specifies that the criteria given in the paragraph are not applicable to arched bridges, but since it was not possible to conduct more in-depth analyses in this regard, it was decided to use the guidelines in the standard for calculating the shape and aerodynamic coefficients anyway.

It is possible to consider the deck as isolated. The basic hypothesis is that the wind acts in a predominantly horizontal direction and orthogonally to the axis of the deck, exerting in the plane of the section a system of aerodynamic actions per unit length which can be traced back to a force parallel to the wind direction, f_x , a vertical force, f_y , and a moment about the axis line, m_z . These actions are:

$$f_x(z) = q_p(z) \cdot l \cdot c_{fx}$$

$$f_y(z) = q_p(z) \cdot l \cdot c_{fy}$$

$$m_z(z) = q_p(z) \cdot l^2 \cdot c_{mz}$$

- q_p is the peak wind kinetic pressure calculated before;

- z is the reference height, equal to the maximum value of the height of the centre of the deck with respect to the lowest point of the ground below, increased by $h_{tot}/2$.

- l is the reference dimension associated with the force coefficients, equal to the width of the deck;

- c_{fy} and c_{fx} are force coefficients, c_{mz} is the moment coefficient. These values are provided by the relations:

$$c_{fx} = \begin{cases} \frac{1,85}{d/h_{tot}} - 0,10 & 2 \leq d/h_{tot} \leq 5 \\ \frac{1,35}{d/h_{tot}} & d/h_{tot} > 5 \end{cases}$$

$$c_{fy} = \begin{cases} \pm \left(0,7 + 0,1 \frac{d}{h_{tot}} \right) & 0 \leq d/h_{tot} \leq 5 \\ \mp 1,2 & d/h_{tot} > 5 \end{cases}$$

$$c_{mz} = \pm 0,2$$

where: d is the width of the deck in the wind direction, h_{tot} is the total deck height (including parapets).

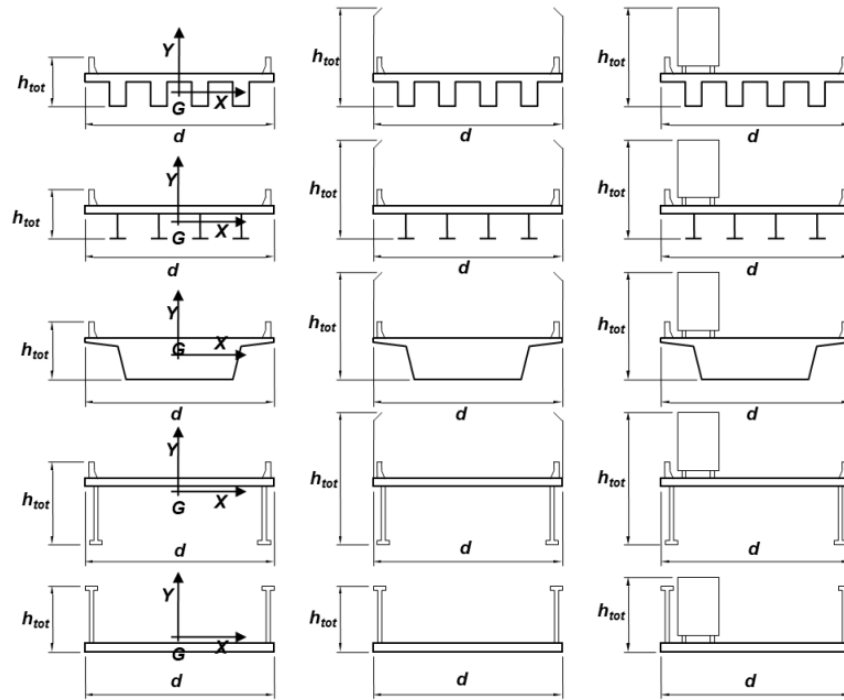


Figure 16: Deck shapes proposed by the CNR -DT 207 R1/2008

An h_{tot} of 2 m is assumed, consisting of a parapet height of 1.10 m and a height of approximately one metre for the deck structure.

Therefore, the first of the two formulations for c_{fx} and c_{fy} is used.

d [m]	h [m]	d/h _{tot} [-]	c _{fx} [-]	c _{fy} [-]	c _{mz} [-]	f _x [kN/m]	f _y [kN/m]	m _z [kNm/m]
6	2	3	0.52	± 1,1	± 0.2	2,9	5,6	6,7

The aerodynamic actions f_x , f_y and m_z are normally considered simultaneous and combined with the signs producing the most onerous effects. The wind actions to be applied to each main beam of the deck are equal to:

$$F_{x,i} := \frac{f_{xi}}{2} = 1,4 \frac{\text{kN}}{\text{m}}$$

$$F_{y,1} := \frac{f_{yi}}{2} + \frac{m_{zi}}{d} = 3,9 \frac{\text{kN}}{\text{m}}$$

$$F_{y,2} := \left(\frac{f_{yi}}{2} - \frac{m_{zi}}{d} \right) = 1,7 \frac{\text{kN}}{\text{m}}$$

Regarding the analysis of the global aerodynamic coefficients of the vertical hangers, which are elements with a circular cross-section, the wind exercises a force on them per unit length in the direction of flow X dependent on the coefficient c_{fx} , which can be calculated as stated in §G.10.6 CNR -DT 207 R1/2018):

$$c_{fx} = c_{fx0} * \psi_\lambda$$

Considering negligible edge effects and thus taking the term ψ_λ to be equal to 1, the coefficient of force c_{fx0} is a function of the Reynolds number Re and the ratio k/b , where k is the surface roughness and b the diameter of the section.

Reynolds number is a fundamental dimensionless quantity that expresses the relationship between the force of inertia and viscous forces, a characteristic dimension of the structure and a characteristic dimension of the flow.

Its value at a height z above the ground is expressed by the following expression:

$$Re(z) = \frac{l \cdot v_m(z)}{\nu}$$

Where:

- l is the characteristic dimension of the element, in the case under consideration it will be equal to the diameter of the circular section;
- $v_m(z)$ is the average wind speed;
- ν is the kinetic viscosity of the air, which, in the absence of precise estimates related to local site conditions, can be assumed to be equal to $\nu=15 \cdot 10^{-6} \text{ m}^2/\text{s}$.

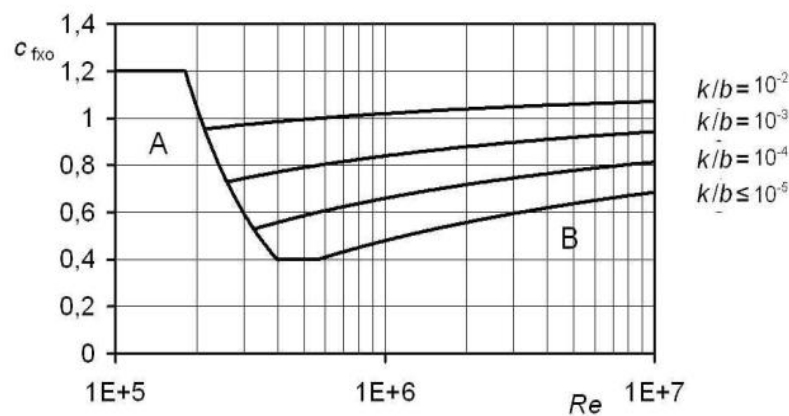


Figure 17: Force coefficient c_{fx0} for structures and elements with circular cross-section (Fig. G.53 CNR)

$$c_{f_{\text{Ro}}} = \frac{0,11}{(Re/10^6)^{1,4}} \leq 1,2 \quad (\text{curva A}) \quad (\text{G.23a})$$

$$c_{f_{\text{Ro}}} = 1,2 + \frac{0,18 \cdot \log_{10}(10 \cdot k/b)}{1 + 0,4 \cdot \log_{10}(Re/10^6)} \geq 0,4 \quad (k/b \geq 10^{-5}) \quad (\text{curva B}) \quad (\text{G.23b})$$

Roughness values k are given by the following table:

CNR-DT 207 R1/2018

Tabella G.XVIII – Scabrezza k della superficie.

Superficie	k [mm]
Vetro	0,0015
Metalli lucidati	0,002
Pittura liscia	0,006
Pittura a spruzzo	0,02
Acciaio lucido	0,05
Ghisa	0,2
Acciaio galvanizzato	
Calcestruzzo lisciato	
Legno levigato	0,5
Calcestruzzo ruvido	1,0
Legno grezzo	2,0
Superfici arrugginite	
Murature	3,0

The average wind speed is given by the relation:

$$v_m(z) = v_r * c_m(z)$$

where:

- v_r is the reference velocity evaluated before;

- c_m is the mean wind profile coefficient, evaluated through the following diagram:

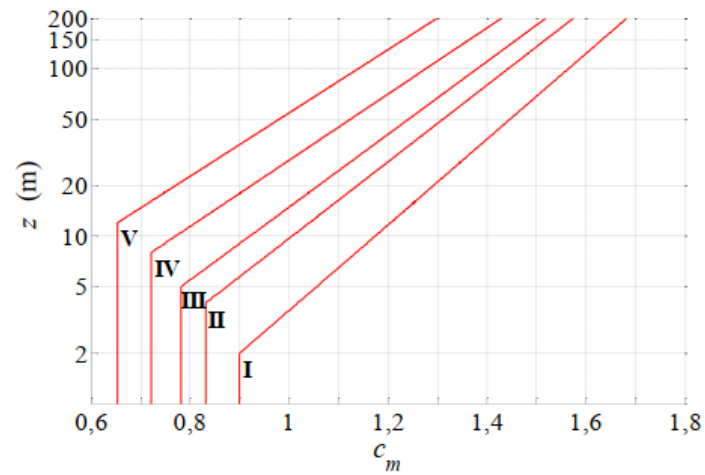


Figure 18: Values of $c_m(z)$ for different exposure categories, in case $c_r(z)=1$

Considering that the vertical hangers develop along a height between 5 and 23 m, an intermediate value of $c_m=1,15$ has been chosen, so that the average wind speed is 29 m/s.

Element	b [m]	k [mm]	k/b [-]	v_m [m/s]	v_m [m ² /s]	Re [-]	c_{fx} [-]	f_x
Vertical Hanger	0.06	0.05	0.0008	30	$15 \cdot 10^{-6}$	$1.15 \cdot 10^5$	0.62	0.05

The transverse force coefficient c_{fy0} and the torque coefficient c_{mz0} , since the cross-section is circular, can be assumed equal to zero.

3.3.5 Thermal load

For the calculation of thermal actions, reference is made to the formulations proposed in paragraph 3.5 NTC18 and 6.1 UNI EN 1991.1.5, in which the daily and seasonal variations in temperature, solar radiation and convection are considered. The severity of the thermal actions is generally influenced by several factors, such as the climatic conditions of the site, the exposure, the overall mass of the structure and the possible presence of non-structural insulating elements.

For bearings and expansion joints the design values of the uniform thermal variation for the SLU assessment of the maximum expansion/contraction can be expressed as follows:

- $\Delta T_{exp,d} = \Delta T_{N,exp} + \Delta T_0$
- $\Delta T_{con,d} = \Delta T_{N,con} + \Delta T_0$

Where:

- $\Delta T_{N,exp} = T_{e,max} - T_0$
- $\Delta T_{N,con} = -T_{e,min} + T_0$

The initial bridge temperature T_0 at the time that the structure is restrained can be assumed equal to 15 °C, as stated in §3.5.4. of NTC2018. A value $\Delta T_0=20^\circ\text{C}$ is assumed.

Following the indications proposed by UNI EN 1991-1-5, the values of minimum and maximum uniform bridge temperature components $T_{e,max}$ and $T_{e,min}$ are calculated as:

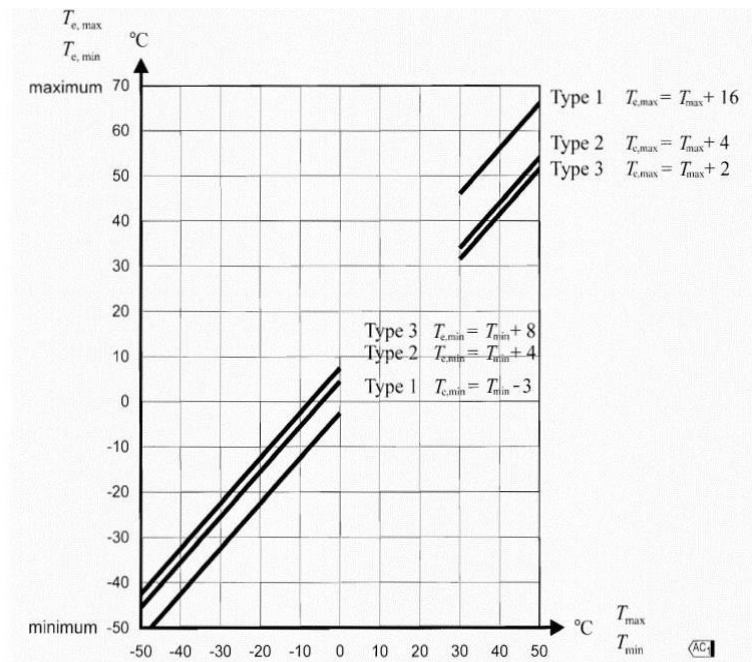


Figure 19: Maximum and minimum temperatures for bridges

T_{\max} and T_{\min} are the shade air temperatures, defined respectively as the maximum summer and minimum winter air temperature at the building site, with reference to a return period of 50 years. It can be evaluated considering the zoning shown in the image below, in particular the city of Verbania is within *Zone I*.



Figure 20: Thermal zones according to external air temperature

Zona I

Valle d'Aosta, Piemonte, Lombardia, Trentino-Alto Adige, Veneto, Friuli-Venezia Giulia, Emilia Romagna:

$$T_{\min} = -15 - 4 \cdot a_s / 1000 \quad [3.5.1]$$

$$T_{\max} = 42 - 6 \cdot a_s / 1000 \quad [3.5.2]$$

Considering the altitude $a_s = 197$ m :

$$T_{\min} = -15 - 4 \cdot a_s / 1000 = -15.8^\circ C$$

$$T_{\max} = 42 - 6 \cdot a_s / 1000 = +40.8^\circ C$$

$$\Delta T = 56.61^\circ C$$

The bridge is made of a steel deck, so it is identified as Type 1. Now, based on the previous diagram, we obtain:

$$T_{e,max} = T_{max} + 4 = 41 + 16 = 57^{\circ}C$$

$$T_{e,min} = T_{min} + 4 = -16 + 16 = 0^{\circ}C$$

In conclusion, the following results are obtained:

$T_0[^{\circ}C]$	$\Delta T_0[^{\circ}C]$	$T_{min}[^{\circ}C]$	$T_{max}[^{\circ}C]$	$T_{e,min}[^{\circ}C]$	$T_{e,max}[^{\circ}C]$	$\Delta T_{exp}[^{\circ}C]$	$\Delta T_{con}[^{\circ}C]$	$\Delta T_{exp,d}[^{\circ}C]$	$\Delta T_{con,d}[^{\circ}C]$
15	20	-16	41	0	57	60	27	80	47

The overall range of the uniform bridge temperature component is:

$$\Delta T_N = T_{e,max} - T_{min} = 45 + 12 = 57^{\circ}C$$

This temperature variation will be applied to all the elements of the deck and the arch.

With regard to the vertical pendants, the thermal variations will be assumed to be $\pm 25^{\circ}C$, as suggested in Tab.3.5.II in §3.5. of the NTC2018.

Tab. 3.5.II – Valori di ΔT_u per gli edifici

Tipo di struttura	ΔT_u
Strutture in c.a. e c.a.p. esposte	$\pm 15^{\circ}C$
Strutture in c.a. e c.a.p. protette	$\pm 10^{\circ}C$
Strutture in acciaio esposte	$\pm 25^{\circ}C$
Strutture in acciaio protette	$\pm 15^{\circ}C$

The effects of these temperature variations result in uniform axial tensile or compressive stresses as a function of temperature variation, evaluated as follows:

$$\sigma = E * \alpha_T * \Delta T$$

Where α_T is the coefficient of thermal expansion at ambient temperature, which is $12 \cdot 10^{-6}^{\circ}C^{-1}$.

Tab. 3.5.III - Coefficienti di dilatazione termica a temperatura ambiente

Materiale	$\alpha_T [10^{-6}/^{\circ}\text{C}]$
Alluminio	24
Acciaio da carpenteria	12
Calcestruzzo strutturale	10
Strutture miste acciaio-calcestruzzo	12
Calcestruzzo alleggerito	7
Muratura	6 ÷ 10
Legno (parallelo alle fibre)	5
Legno (ortogonale alle fibre)	30 ÷ 70

Element	$\Delta T [^{\circ}\text{C}]$	$\sigma [\text{Mpa}]$
Deck, arch	57	144
Hanger	25	63

In order to prevent stresses resulting from thermal loads, the bearing configuration is designed in such a way that horizontal and transversal sliding are permitted. This topic is discussed in more detail in the chapter “Support devices”.

3.3.6 Seismic load

With reference to §3.2NTC18 the seismic action is defined starting from the ‘basic seismic risk’ of the construction site and is a function of the morphological and stratigraphic characteristics that determine the local seismic response.

The seismic risk is defined in terms of the maximum expected horizontal acceleration a_g in free field conditions on a rigid reference site with a horizontal topographical surface, as well as the ordinates of the spectrum of the elastic acceleration response spectrum $S_e(T)$ corresponding to it, with reference to predefined exceedance probabilities PVR , in the reference period V_R . The spectral shapes are defined, for each of the exceedance probabilities PVR in the reference period V_R , from the values of the following parameters on a rigid horizontal reference site:

- a_g maximum horizontal acceleration at the site;
- F_0 maximum value of the amplification factor of the spectrum in horizontal acceleration;
- T_C^* reference value for the determination of the starting period of the constant velocity section of the spectrum in horizontal acceleration

For the values of a_g , F_0 and T_C^* required for the determination of seismic actions, reference is made to Annexes A and B of the ‘Decreto del Ministro delle Infrastrutture 14 gennaio 2008’.

The nominal life of the structure, defined according to the minimum duration provided for in NTC18 §2.4.1, is equal to 50 years. The use class is 2 (buildings whose use involves normal crowding), to which corresponds a unitary use coefficient C_u . As a result, there is a reference period for the construction:

$$V_R = V_N \cdot C_u = 50 \cdot 1 = 50 \text{ years}$$

The return period TR used for the definition of the seismic action depends on the limit state considered.

With respect to seismic actions, both operating limit states (SLE) and ultimate limit states (SLU) are identified by referring to the performance of the construction as a whole.

Operational limit states are subdivided into:

- Operational Limit State (SLO)
- Damage Limit State (SLD)

Ultimate limit states, on the other hand, consist of:

- Life Preservation Limit State (SLV)
- Collapse Prevention Limit State (SLC)

Stati limite di esercizio - SLE	SLO - $P_{VR} = 81\%$	30
	SLD - $P_{VR} = 63\%$	50
Stati limite ultimi - SLU	SLV - $P_{VR} = 10\%$	475
	SLC - $P_{VR} = 5\%$	975

FASE 1. INDIVIDUAZIONE DELLA PERICOLOSITÀ DEL SITO

☒ Ricerca per coordinate

LONGITUDINE
8,57069

LATITUDINE
45,93200

☐ Ricerca per comune

REGIONE
Piemonte

PROVINCIA
Verbanio Cusio Oss

COMUNE

Elaborazioni grafiche

Grafici spettri di risposta
Variabilità dei parametri

Elaborazioni numeriche

Tabella parametri

Nodi del reticolo intorno al sito

Reticolo di riferimento

Controllo sul reticolo
☐ Sito esterno al reticolo
☒ Interpolazione su 3 nodi
☐ Interpolazione corretta

Interpolazione
superficie rigata

La "Ricerca per comune" utilizza le ... coordinate ISTAT del comune per identificare il sito. Si sottolinea che ... all'interno del territorio comunale le azioni sismiche possono essere significativamente diverse da quelle così individuate e si consiglia, quindi, la "Ricerca per coordinate".

INTRO

FASE 1

FASE 2

FASE 3

FASE 2. SCELTA DELLA STRATEGIA DI PROGETTAZIONE

Vita nominale della costruzione (in anni) - V_N info

Coefficiente d'uso della costruzione - C_U info

Valori di progetto

Periodo di riferimento per la costruzione (in anni) - V_R info

Periodi di ritorno per la definizione dell'azione sismica (in anni) - T_R info

Stati limite di esercizio - SLE

- SLO - $P_{VR} = 81\%$ info
- SLD - $P_{VR} = 63\%$ info

Stati limite ultimi - SLU

- SLV - $P_{VR} = 10\%$ info
- SLC - $P_{VR} = 5\%$ info

Elaborazioni

- Grafici parametri azione
- Grafici spettri di risposta
- Tabella parametri azione

Strategia di progettazione

LEGENDA GRAFICO

- Strategia per costruzioni ordinarie
- Strategia scelta

INTRO FASE 1 **FASE 2** FASE 3

FASE 3. DETERMINAZIONE DELL'AZIONE DI PROGETTO

Stato Limite

Stato Limite considerato info

Risposta sismica locale

Categoria di sottosuolo info

Categoria topografica info

$S_S = 1,500$ $C_C = 1,593$ info

$h/H = 0,000$ $S_T = 1,000$ info
(h=quota sito, H=altezza rilievo topografico)

Compon. orizzontale

☐ Spettro di progetto elastico (SLE) Smorzamento ξ (%) $\eta = 1,000$ info

☒ Spettro di progetto inelastico (SLU) Fattore q_s Regol. in altezza info

Compon. verticale

Spettro di progetto Fattore q_v $\eta = 1,000$ info

Elaborazioni

- Grafici spettri di risposta
- Parametri e punti spettri di risposta

Spettri di risposta

— Spettro di progetto - componente orizzontale

— Spettro di progetto - componente verticale

— Spettro elastico di riferimento (Cat. A-T1, $\xi = 5\%$)

INTRO FASE 1 FASE 2 **FASE 3**

Parametri indipendenti

STATO LIMITE	SLV
a_g	0,043 g
F_{q_s}	2,651
T_C	0,283 s

These parameters are entered into the calculation software in order to evaluate the seismic action on the structure.

The analysis of structures subjected to seismic action can be linear or nonlinear; in this case, it was conducted using the linear approach, which consists of determining the modes of vibration through the use of modal analysis, calculating the effects of seismic action in each of the modes, and finally combining the effects.

The modes to be considered, as the standard indicates, must have significant involvement of the participating mass :all modes with a participating mass greater than 5 percent and a number of modes such that the total participating mass, given by the sums of the participating masses of the individual mode, that is greater than 85 percent (in this thesis a value of 95% has been chosen). The combination of the effects of individual modes must be carried out through the use of proposed statistical methods of proven validity, the one proposed by the NTC and used is called CQC or Complete Quadratic Combination whose formulation is:

$$E = \sqrt{\sum \sum \rho_{ij} \cdot E_i \cdot E_j}$$

Where E_j corresponds to the value of the effect related to the j -th mode, E_i to the value of the effect of the

i -th mode and ρ_{ij} the correlation coefficient between the i -th mode and the j -th mode, which is calculated with the formulation proposed by the NTC18.

$$\rho_{ij} = \frac{8 \cdot \sqrt{\xi_i \cdot \xi_j} \cdot (\beta_{ij} \cdot \xi_i + \xi_j) \cdot \beta_{ij}^{3/2}}{(1 - \beta_{ij}^2)^2 + 4 \cdot \xi_i \cdot \xi_j \cdot \beta_{ij} \cdot (1 + \beta_{ij}^2) + 4 \cdot (\xi_i^2 + \xi_j^2) \cdot \beta_{ij}^2}$$

If the modes i and j have the same damping ratio ξ we have:

$$\rho_{ij} = \frac{8 \cdot \xi^2 \cdot \beta_{ij}^{3/2}}{(1 + \beta_{ij}) \cdot [(1 - \beta_{ij})^2 + 4 \cdot \xi^2 \cdot \beta_{ij}]}$$

β_{ij} is the ratio of the inverse of the periods of each i - j pair of modes:

$$\beta_{ij} = \frac{T_i}{T_j}$$

The following is the seismic action menu in the model on Advance Design:

Proprietà 🔍 ✕

Tutte le proprietà

Famiglia

Nome	Sisma NTC 2018
Nr.	6
Spettro	Calcolo

Impianto

Accelerazione terreno agr m...	0.43
Fattore di amplificazione F0	2.651
Periodo Tc*	0.28 s
Categoria topografica	T1
Tipo di terreno	C
Ss - parametro del terreno	1.50
Valore imposto Tb	0.15
Valore imposto Tc	0.45
Valore imposto Td	1.78

Struttura

γI - coefficiente di importan...	1
q orizzontale (x)	1
q orizzontale (y)	1
q verticale	1
Correzione dello smorzame...	<input type="checkbox"/> Disabilitato
Coefficiente β	0.2
Classe di duttilità	DCM

Spettro

Spettro orizzontale (x)	Spettro NTC 2018
Spettro orizzontale (y)	Spettro NTC 2018
Spettro verticale	Spettro NTC 2018

Sovrapposizione dei modi

Metodo	CQC
Modi residui	<input type="checkbox"/> Disabilitato

Caso di carico modale

Titolo	
Nome	Modi
Nr.	0
Codice	CAS

Metodo

Tipo	Carico Dipendente dai Vettori di...
Tipologia matrice massa	Concentrata

Modi

Obiettivo	Tasso di partecipazione
Numero	1
Tasso di partecipazione	95 %

Masse

Impostazione	masse ottenuto dalla combinaz...
Combinazioni	$1.00 \cdot 1G + 1.00 \cdot 2G + 0.14 \cdot 4Q$
Percentuale Dir.X	100 %
Percentuale Dir.Y	100 %
Percentuale Dir.Z	100 %

Convergenza

Tolleranza	1e-06
Iterazioni Max	300

Smorzamento per sisma

Calc. auto	<input type="checkbox"/> Disabilitato
Smorzamento imposto	4 %

Eccentricità dinamica delle masse

Eccentricità delle masse	<input type="checkbox"/> Disabilitato
Sisma X	0
Sisma Y	0
Percentuale della distanza i...	5 %
Percentuale della distanza i...	5 %

3.3.7 Load combinations

A structure reaches a limit state when it ceases to perform one or all of the functions for which it was designed, thus violating, partially or completely, the design requirements. According to this definition, a distinction is made between ultimate limit states, related to the structure's ability to resist design actions, and service limit states, corresponding to the structure's ordinary use and durability.

For each limit state identified, a combination of the actions acting on the structure must be defined, for which the stress levels of the structural elements must be calculated to verify the levels of satisfaction of the requirements.

At the SLU the characteristic value of the loads acting on the structure is multiplied by the respective partial safety coefficient greater than one, according to Tab 2.6.I - NTC 18, as well as the resistances of the materials which are divided by a partial safety coefficient greater than unity so as to use a lower value for precautionary purposes.

Combination coefficients are also introduced in the combination of actions, to take into account the low probability that variable actions can exert their effects simultaneously with maximum intensity.

Having defined the characteristic values of the actions (load analysis), the different combinations of actions can be symbolically represented as follows ((+ symbol stands for 'combined with').)

ULTIMATE LIMIT STATE

- in persistent or transient situations, the calculation values of the dominant actions and the combination values of the other actions are considered, so we have:

$$\sum_{j \geq 1} \gamma_{Gj} G_{K,j} + \sum_{j \geq 1} \gamma_G^* G_{K,j}^* + \gamma_P P_K + \gamma_{Q,1} Q_{K,1} + \sum_{i > 1} \gamma_{Q,i} \psi_{0,i} \cdot Q_{K,i}$$

G_{Kj} : is the characteristic value of the permanent actions;

G_{Kj}^* : is the characteristic value of permanent actions of variable intensity;

P_K : is the characteristic value of the prestressing action;

$Q_{K,1}$: is the characteristic value of the dominant variable action;

$\psi_{0,i} Q_{K,i}$: is the combination value of the variable actions concomitant with the dominant action.

Load combinations are thus generated which consider a variable action as dominant.

- In accidental situations, the calculation values of the permanent actions combined with the frequent values of the dominant variable action, with quasi-permanent values of the other variable actions and the calculation value of a possible accidental action are considered:

$$\sum_{j \geq 1} \gamma_{Gi} G_{Kj} + \sum_{j \geq 1} \gamma_G^* G_{K,j}^* + \gamma_P P_K + \gamma_A A_K + \gamma_{Q,1} \psi_{1,1} Q_{K,1} + \sum_{i > 1} \gamma_{Q,i} \psi_{2,i} Q_{K,i}$$

where

A_K characteristic value of the incidental actions;

$\psi_{1,1} Q_{K,1}$ frequent value of the dominant action;

$\psi_{2,i} Q_{K,i}$ quasi-permanent values of the variable actions concomitant with the dominant variable action or the accidental action.

SERVICEABILITY LIMIT STATE

- Rare combination:

$$\sum_{j \geq 1} G_{Kj} + \sum_{j \geq 1} G_{K,j}^* + P_K + Q_{K,1} + \sum_{i \geq 1} \psi_{0,i} Q_{K,i}$$

- Frequent combination:

$$\sum_{j \geq 1} G_{Kj} + \sum_{j \geq 1} G_{K,j}^* + P_K + \psi_{1,1} \cdot Q_{K,1} + \sum_{i \geq 1} \psi_{2,i} \cdot Q_{K,i}$$

- Quasi – permanent combination:

$$\sum_{j \geq 1} G_{Kj} + \sum_{j \geq 1} G_{K,j}^* + P_K + \sum_{i \geq 1} \psi_{2,i} Q_{K,i}$$

PARTIAL SAFETY COEFFICIENTS USED IN VERIFICATIONS:

Tab. 5.1.V – Coefficienti parziali di sicurezza per le combinazioni di carico agli SLU

		Coefficiente	EQU ⁰¹	A1	A2
Azioni permanenti g_1 e g_3	favorevoli	γ_{G1} e γ_{G3}	0,90	1,00	1,00
	sfavorevoli		1,10	1,35	1,00
Azioni permanenti non strutturali ⁽²⁾ g_2	favorevoli	γ_{G2}	0,00	0,00	0,00
	sfavorevoli		1,50	1,50	1,30
Azioni variabili da traffico	favorevoli	γ_Q	0,00	0,00	0,00
	sfavorevoli		1,35	1,35	1,15
Azioni variabili	favorevoli	γ_{Qi}	0,00	0,00	0,00
	sfavorevoli		1,50	1,50	1,30
Distorsioni e presollecitazioni di progetto	favorevoli	γ_{t1}	0,90	1,00	1,00
	sfavorevoli		1,00 ⁽³⁾	1,00 ⁽⁴⁾	1,00
Ritiro e viscosità, Cedimenti vincolari	favorevoli	$\gamma_{t2}, \gamma_{t3}, \gamma_{t4}$	0,00	0,00	0,00
	sfavorevoli		1,20	1,20	1,00

COMBINATION COEFFICIENTS OF ACTIONS:

Tab. 5.1.VI - Coefficienti ψ per le azioni variabili per ponti stradali e pedonali

Azioni	Gruppo di azioni (Tab. 5.1.IV)	Coefficiente ψ_0 di combinazione	Coefficiente ψ_1 (valori frequenti)	Coefficiente ψ_2 (valori quasi permanenti)
Azioni da traffico (Tab. 5.1.IV)	Schema 1 (carichi tandem)	0,75	0,75	0,0
	Schemi 1, 5 e 6 (carichi distribuiti)	0,40	0,40	0,0
	Schemi 3 e 4 (carichi concentrati)	0,40	0,40	0,0
	Schema 2	0,0	0,75	0,0
	2	0,0	0,0	0,0
	3	0,0	0,0	0,0
	4 (folla)	–	0,75	0,0
	5	0,0	0,0	0,0
Vento	a ponte scarico SLU e SLE	0,6	0,2	0,0
	in esecuzione	0,8	0,0	0,0
	a ponte carico SLU e SLE	0,6	0,0	0,0
Neve	SLU e SLE	0,0	0,0	0,0
	in esecuzione	0,8	0,6	0,5
Temperatura	SLU e SLE	0,6	0,6	0,5

PARTIAL SAFETY COEFFICIENTS FOR MATERIALS

Cap. 11 – NTC '18

Structural steel	$\gamma_M = 1,05$
Ordinary reinforcing steel	$\gamma_S = 1,15$
Concrete	$\gamma_C = 1,50$

The actions are combined in order to identify the most unfavourable condition for each individual element under verification. From these combinations, the stress envelopes are constructed. The dimensioning and verifications are carried out on these envelopes, which show, section by section, the maximum and minimum value of the action.

3.4 Modelling in Advance Design

To make the model on Advance Design, we started from the drawing on Autocad, importing the .dxf file. Having thus obtained a 2D drawing, it was rotated by 90 degrees so that we're in the xz plane:

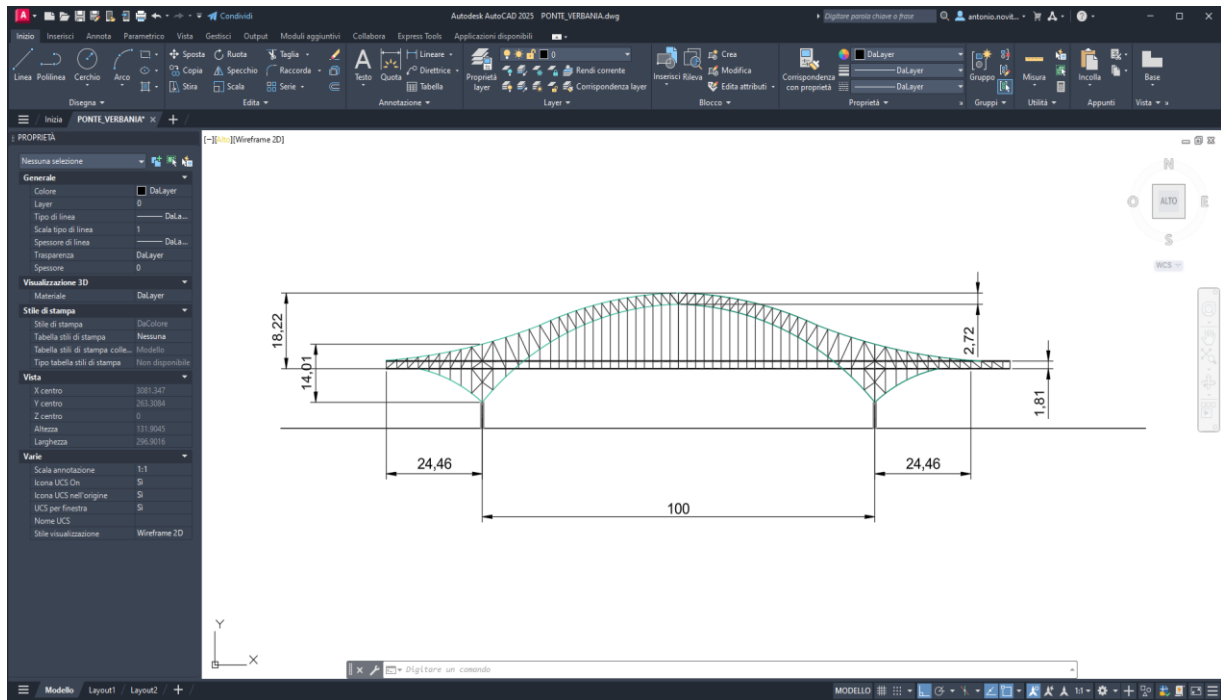


Figure 21: 2D Design in Autocad

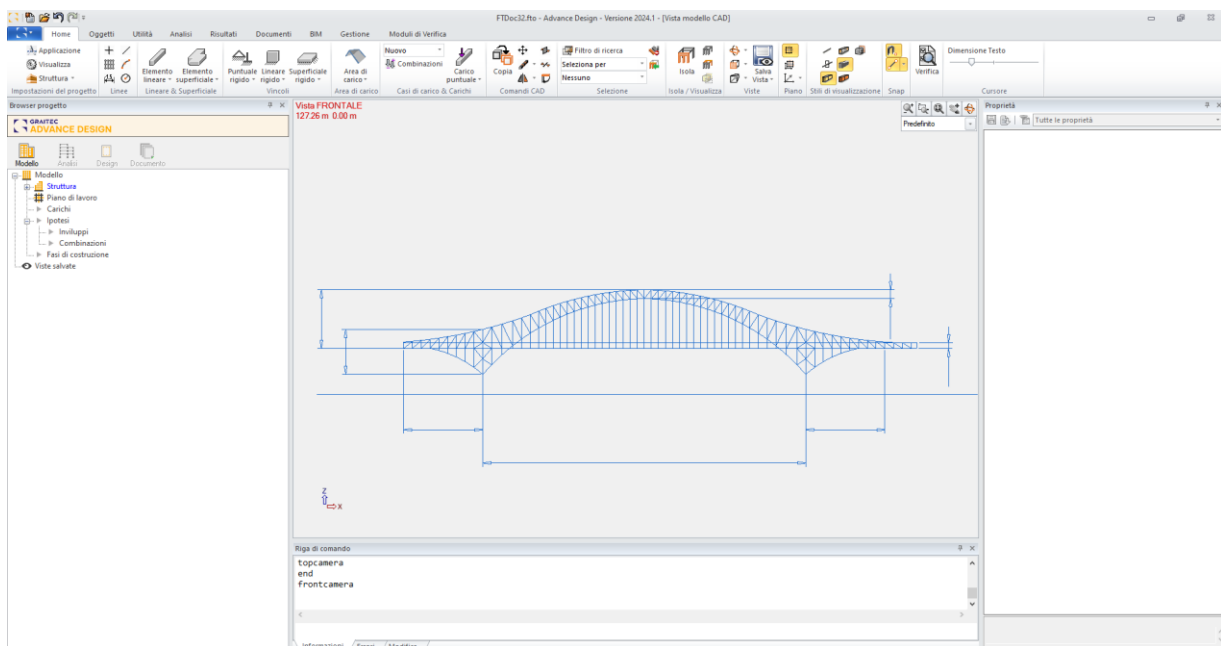


Figure 22: 2D Design in Advance Design

Then each line element was replaced with a linear element, modeled as a beam or truss depending on function, and constraints were added. Beam elements are capable of resisting axial stress, shear and bending moments, resulting in being suitable for representing structural components subject to bending, such as the deck and arch. In contrast, truss elements are ideal for modeling components that work exclusively at axial stresses (tension or compression), such as vertical hangers or bracing elements.

Then the model has been copied in the y-direction at a distance of 6 m equal to the width of the deck, and transverse element added.

The complete model used for analysis and verification is shown below:

Vista UTENTE
170.98 m 6.00 m 103.89 m

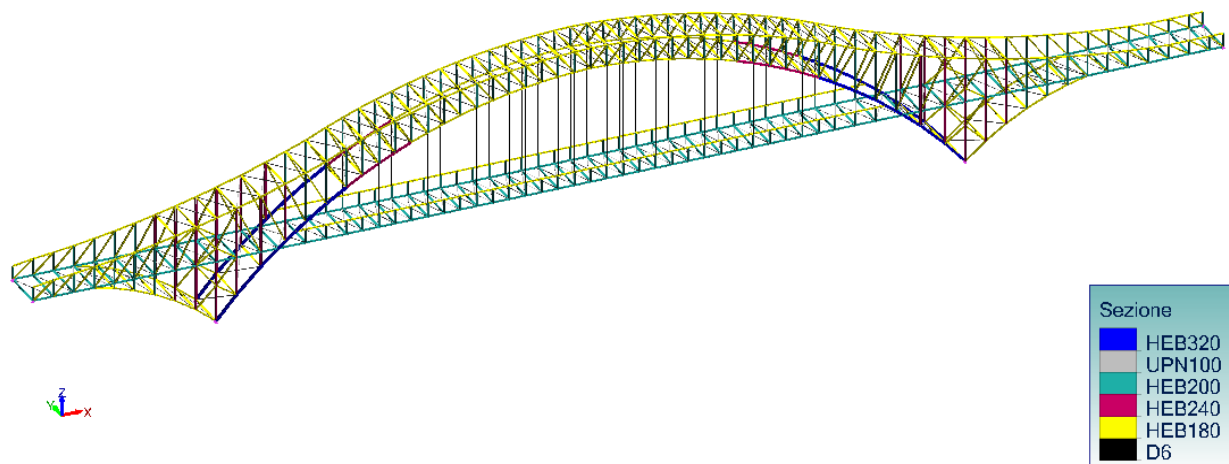


Figure 23: 3D Model in Advance Design

To verify that the model was working properly, the model was run with only its own weight before inserting the loads, verifying, as shown in the figure, that the arch (bottom) goes into compression and that the truss elements work only at normal stress (zero moment). The sign conventions of the program are such that normal compressive stress is present at negative.

Vista FRONTALE
Analisi: 1 G
Lineare : Fx
Assi locali

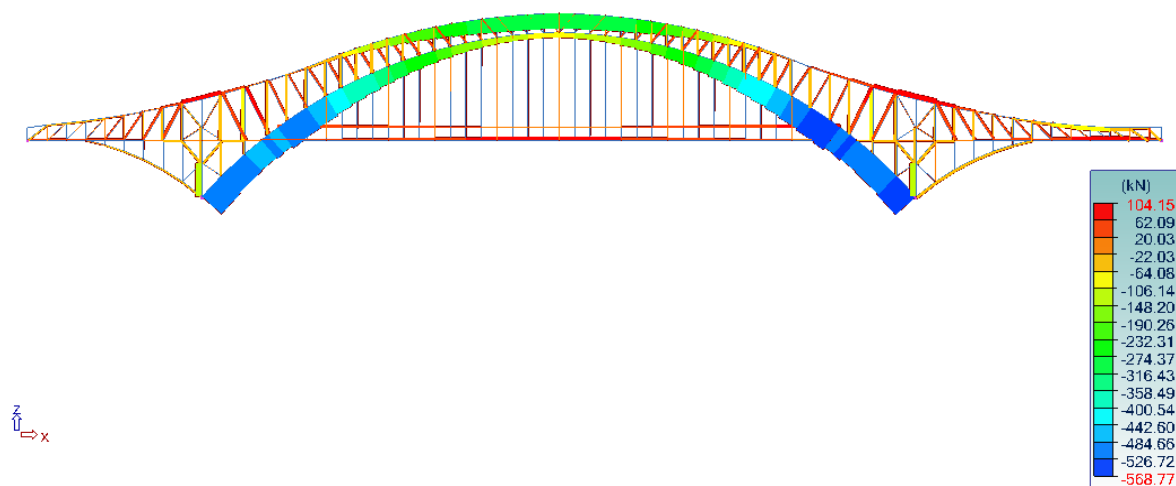


Figure 24: Axial forces under self-weight

Vista FRONTALE
Analisi: 1 G
Lineare : My
Assi locali

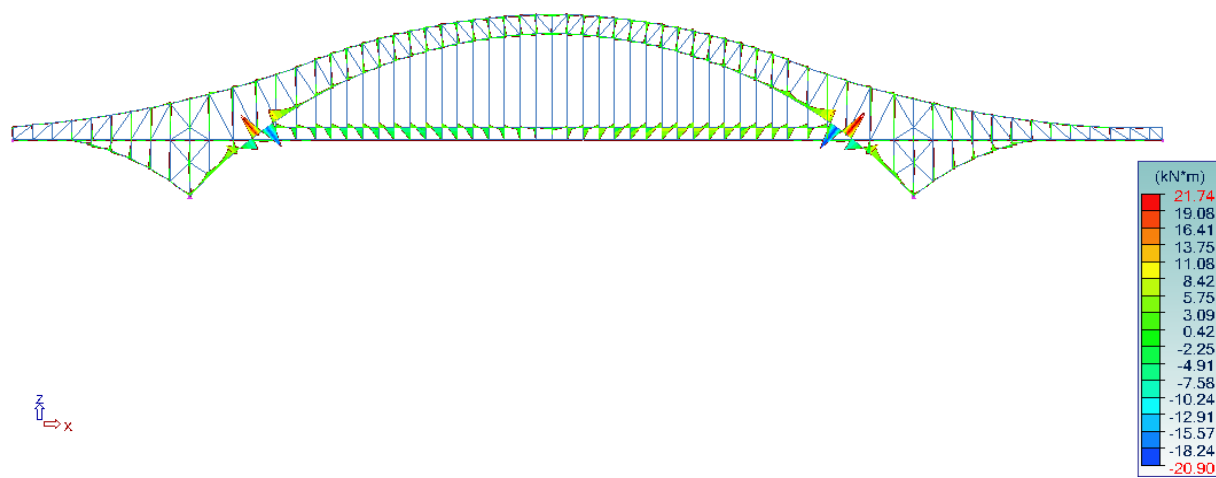


Figure 25: Bending moment under self-weight

Is now reported the complete model of all loads that will be properly combined as explained in the previous paragraphs:

Vista UTENTE
170.98 m 6.00 m 103.89 m

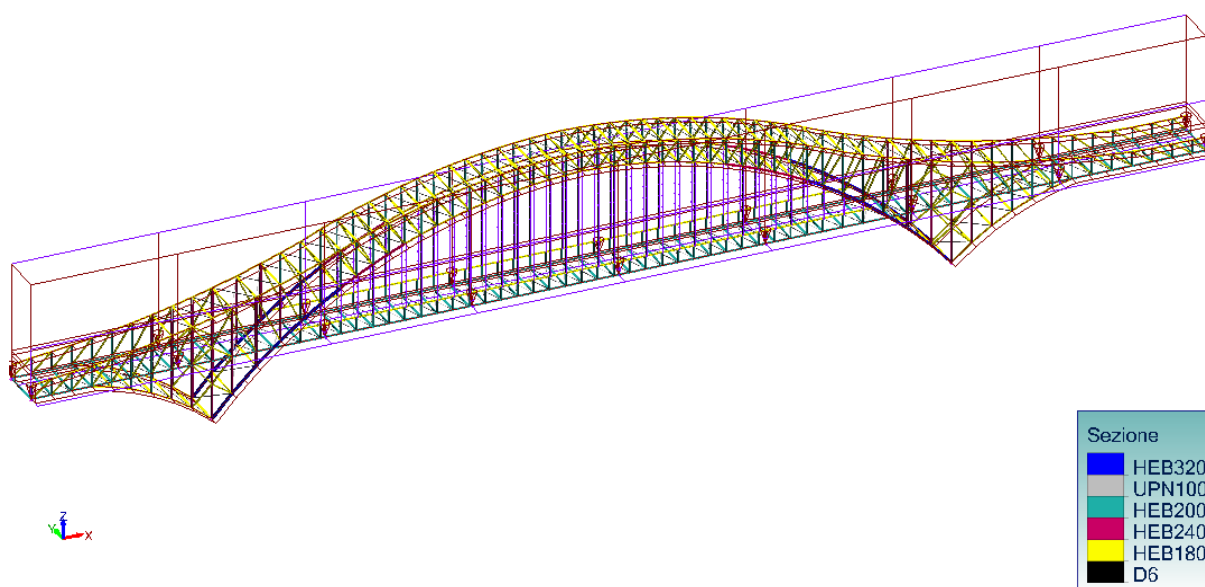


Figure 26: 3D Model with loads

Vista UTENTE
266.27 m 0.00 m 97.82 m
L = 1.77 m

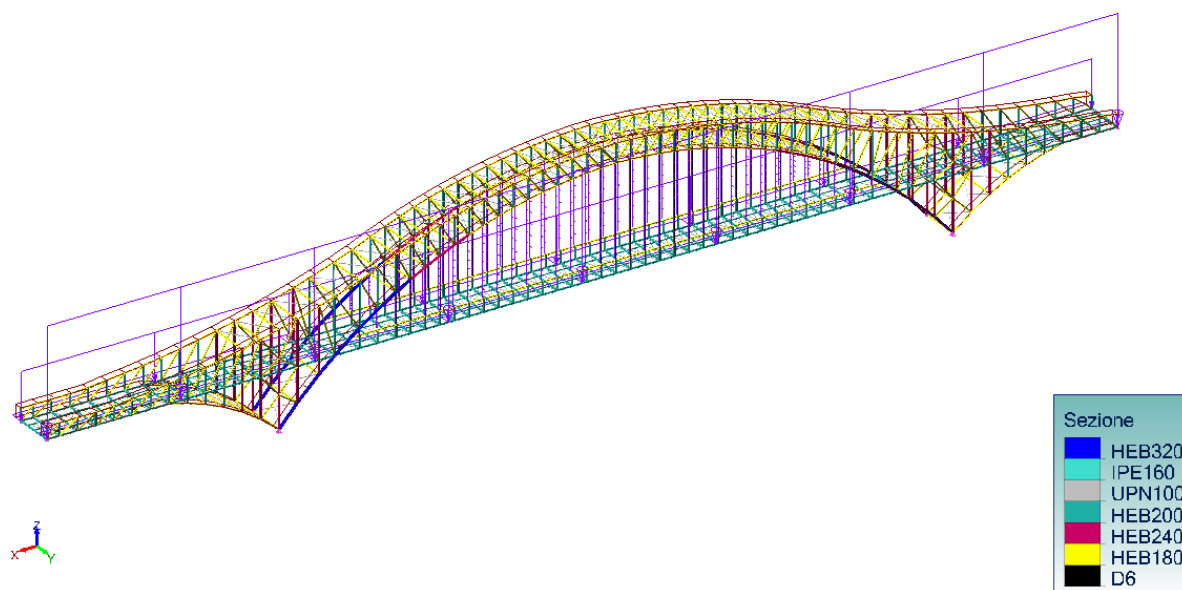
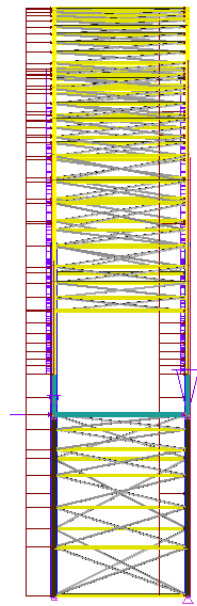


Figure 27: 3D Model with wind loads

Vista DESTRA
266.27 m 0.00 m 97.82 m
L = 1.77 m



Sezione	
HEB320	
IPE160	
UPN100	
HEB200	
HEB240	
HEB180	
D6	

Figure 28: 3D Model with wind load, lateral view

The conventions adopted by the Advance Design software are given on the following page, in order to make the graphs and values more understandable. Advance Design 2024® calculation software expresses finite element calculation results in the local coordinate system of the relevant element. Only the constraining forces are expressed in the global coordinate system. It should be noted that tensile forces occur in the case of positive forces, while positive moments are those that stretch the upper fibers in the elements.

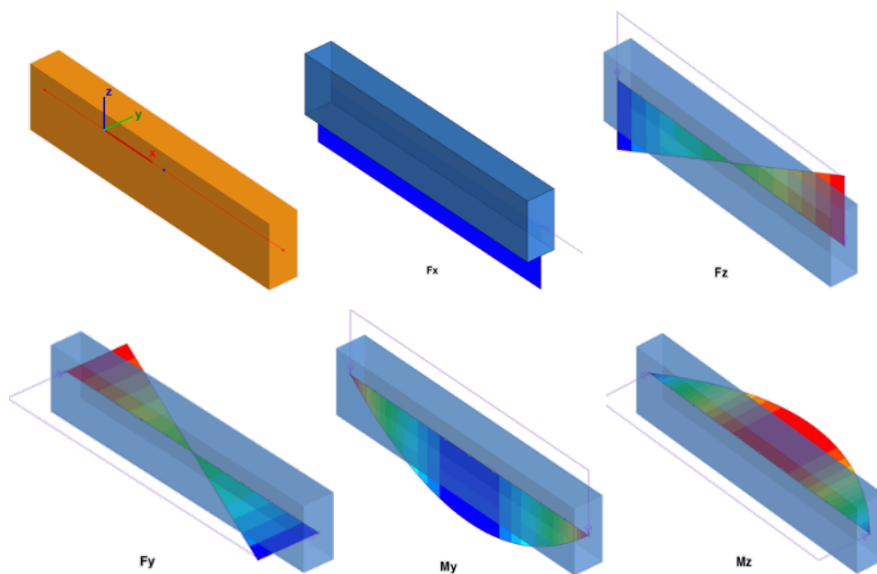


Figure 29: Advance Design Conventions

3.5 ULS verifications

In ultimate limit state verifications, it is evaluated that each acting action, appropriately derived for each element and for each combination, is lower than the corresponding resistant action offered by profile.

$$E \leq R$$

Where E denotes the effects of actions, evaluated in the global analysis while R denotes the resisting capacity.

The calculation of actions and strengths can be carried out by three distinct methodologies:

- Elastic Method (E) - assumption of linear elastic σ - ϵ bond until yielding
- Plastic Method (P) - assumption of rigid-plastic σ - ϵ bond, neglecting elastic deformation and considering complete plasticization of the material
- Elasto-plastic (EP) method - assumption of bi-linear σ - ϵ bonding

Based on the classification of the sections under consideration, a different method should be used. Finite element software uses the elastic method as the global analysis method and the elasto-plastic method for calculating the section resisting capacity, which is valid for all types of sections.

Tab. 4.2.VI - Metodi di analisi globali e relativi metodi di calcolo delle capacità e classi di sezioni ammesse

Metodo di analisi globale	Metodo di calcolo della capacità resistente della sezione	Tipo di sezione
(E)	(E)	tutte (*)
(E)	(P)	classi 1 e 2
(E)	(EP)	tutte (*)
(P)	(P)	classe 1
(EP)	(EP)	tutte (*)

(*) per le sezioni di classe 4 la capacità resistente può essere calcolata con riferimento alla sezione efficace.

The structural analysis software Advance Design automatically performs all the checks related to each steel member. The figure below shows the utilization ratios calculated by the software, based on the most critical load combination and resistance verification for each structural element.

Vista UTENTE
Tasso di lavoro massimo
Lineare : Tasso di lavoro massimo - Resistenza



Figure 30: Maximum resistance utilization ratio

Vista UTENTE
Tasso di lavoro massimo
Lineare : Tasso di lavoro massimo - Stabilità

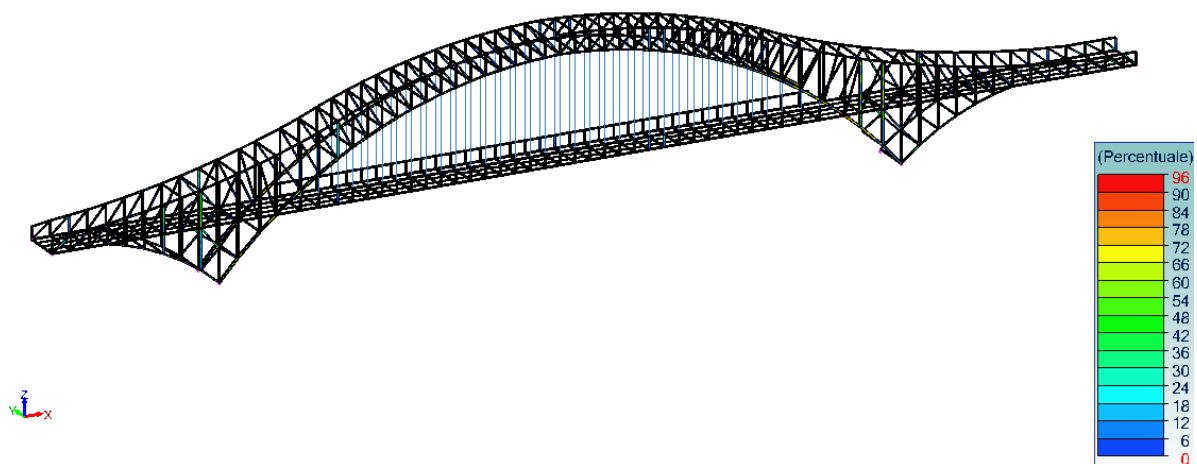


Figure 31: Maximum stability utilization ratio

The following paragraphs present all types of members used in the design of the bridge under study. For each member type, the most critically loaded element was selected, and the most relevant

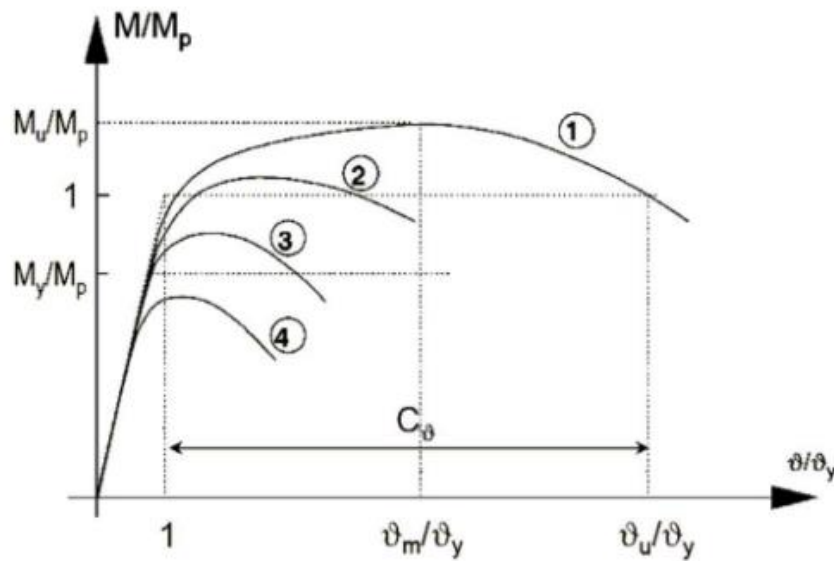
verification checks are reported. In order to validate the results obtained from the structural analysis software, some manual verifications were carried out.

Classification section

Steel is a material with a symmetrical constitutive bond, however, the response of a structural element may not be symmetrical due to buckling phenomena in some of its parts. Specifically, the most insidious phenomenon is local buckling, which can prevent the section from drawing on all its plastic resources, effectively reducing the load-bearing capacity of the structural element. The NTC2018 proposes, in §4.2.3.1, a classification of steel cross-sections in function of their rotational capacity defined as follows:

$$C_{\vartheta} = \vartheta_r / \vartheta_y - 1$$

Where ϑ_r and ϑ_y are the rotations corresponding to reaching ultimate deformation and yielding, respectively.



"The classification of cross-sections of structural elements is made according to their ability to deform in the plastic field.

The following classes of sections can be distinguished:

- Class 1-if the section is capable of developing a plastic hinge having the rotational capacity required for the structural analysis conducted by the plastic method in § 4.without

suffering reductions in strength. Sections with rotational capacity $C\theta \geq 3$ can generally be classified as class 1;

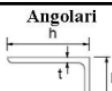


- Class 2 if the section is capable of developing its own plastic resistant moment, but with limited rotational capacity. Sections with rotational capacity $C\theta \geq 1.5$ can generally be classified as class 2;
- Class 3 if in the section the calculated stresses in the extreme compressed fibers can reach the yield stress, but local buckling prevents the development of the plastic resistant moment;
- Class 4 if, in order to determine its bending, shear or normal strength, it is necessary to take into account the effects of local buckling in the elastic phase in the compressed parts that make up the section. In that case, the geometric effective section may be substituted for an effective section in the strength calculation.

Class 1 sections are called ductile, Class 2 compact, Class 3 semi-compact and Class 4 slender.

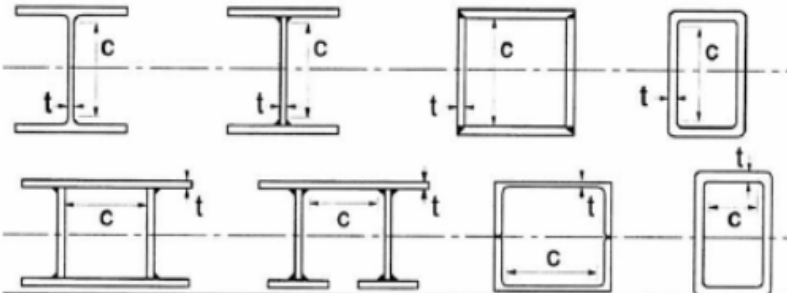
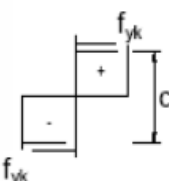
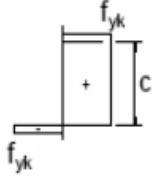
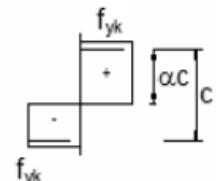
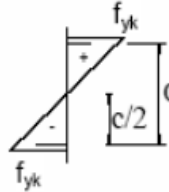
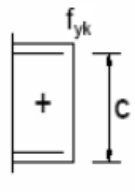
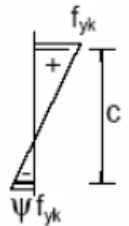
For the most common cases of section shapes and stress modes, the following Tables 4.2.III, 4.2.IV and 4.2.V provide guidance for classifying sections. The class of a compound section corresponds to the highest class value among those of its component elements.

The class to which the section belongs is defined by the dimensional relationship between the width and thickness of the component parts of the section, the state of stress (compression, bending or bending-compression) and the strength class of the material. Practically, to evaluate the class of a cross-section, the tables found in the above paragraph of NTC2018 are used:

Tab. 4.2.V - Massimi rapporti larghezza spessore per parti compresse

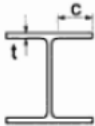


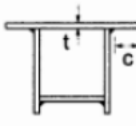
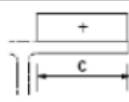

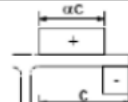
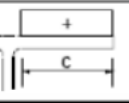
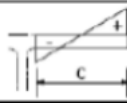
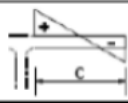
<p style="text-align: center;"> Angolari</p> <p>Riferirsi anche alle piattabande esterne (v. Tab 4.2.II) Non si applica agli angoli in contatto continuo con altri componenti</p>						
Classe		Sezione in compressione				
Distribuzione delle tensioni sulla sezione (compressione positiva)		 f_{yk}				
3		$h/t \leq 15\varepsilon \qquad \frac{b+h}{2t} \leq 11,5\varepsilon$				
<p style="text-align: center;"> Sezioni Tubolari</p>						
Classe		Sezione inflessa e/o compressa				
1		$d/t \leq 50\varepsilon^2$				
2		$d/t \leq 70\varepsilon^2$				
3		$d/t \leq 90\varepsilon^2$ (Per $d/t > 90 \varepsilon^2$ vedere EN 1993-1-6)				
$\varepsilon = \sqrt{235/f_{yk}}$	f_{yk}	235	275	355	420	460
	ε	1,00	0,92	0,81	0,75	0,71
	ε^2	1,00	0,85	0,66	0,56	0,51

Tab. 4.2.III - Massimi rapporti larghezza spessore per parti compresse

						
Parti interne compresse						
Classe	Parte soggetta a flessione	Parte soggetta a compressione		Parte soggetta a flessione e a compressione		
Distribuzione delle tensioni nelle parti (compressione positiva)						
1	$c/t \leq 72\epsilon$	$c/t \leq 33\epsilon$		quando $\alpha > 0,5: c/t \leq \frac{396\epsilon}{13\alpha - 1}$ quando $\alpha \leq 0,5: c/t \leq \frac{36\epsilon}{\alpha}$		
2	$c/t \leq 83\epsilon$	$c/t \leq 38\epsilon$		quando $\alpha > 0,5: c/t \leq \frac{456\epsilon}{13\alpha - 1}$ quando $\alpha \leq 0,5: c/t \leq \frac{41,5\epsilon}{\alpha}$		
Distribuzione delle tensioni nelle parti (compressione positiva)						
3	$c/t \leq 124\epsilon$	$c/t \leq 42\epsilon$		quando $\psi > -1: c/t \leq \frac{42\epsilon}{0,67 + 0,33\psi}$ quando $\psi \leq -1: c/t \leq 62\epsilon(1 - \psi)\sqrt{(-\psi)}$		
$\epsilon = \sqrt{235/f_{yk}}$	f_{yk}	235	275	355	420	460
	ϵ	1,00	0,92	0,81	0,75	0,71

*) $\psi \leq -1$ si applica se la tensione di compressione $\sigma \leq f_{yk}$ o la deformazione a trazione $\epsilon_y > f_{yk}/E$

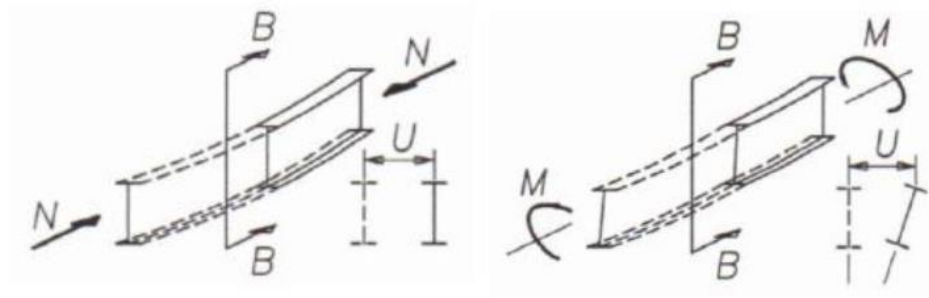
Tab. 4.2.IV - Massimi rapporti larghezza spessore per parti compresse

Piattabande esterne						
						
						
Profilati laminati a caldo			Sezioni saldate			
Classe	Piattabande esterne soggette a compressione	Piattabande esterne soggette a flessione e a compressione				
		Con estremità in compressione		Con estremità in trazione		
Distribuzione delle tensioni nelle parti (compressione positiva)						
1	$c/t \leq 9\epsilon$	$c/t \leq \frac{9\epsilon}{\alpha}$		$c/t \leq \frac{9\epsilon}{\alpha\sqrt{\alpha}}$		
2	$c/t \leq 10\epsilon$	$c/t \leq \frac{10\epsilon}{\alpha}$		$c/t \leq \frac{10\epsilon}{\alpha\sqrt{\alpha}}$		
Distribuzione delle tensioni nelle parti (compressione positiva)						
3	$c/t \leq 14\epsilon$	$c/t \leq 21\epsilon\sqrt{k_\epsilon}$ Per k_ϵ vedere EN 1993-1-5				
$\epsilon = \sqrt{235/f_{yk}}$	f_{yk}	235	275	355	420	460
	ϵ	1,00	0,92	0,81	0,75	0,71

Stability

When dealing with steel structures, the phenomenon of buckling must be taken into account; in contrast to reinforced concrete structures, instead of having limitations on the strength side, one mainly encounters stability problems in compressed and inflected elements. This is due to the fact that steel, compared to concrete, has a high strength but more compact and significantly slimmer sections. It is precisely slenderness that is an important parameter in stability verification. Buckling can be of three types:

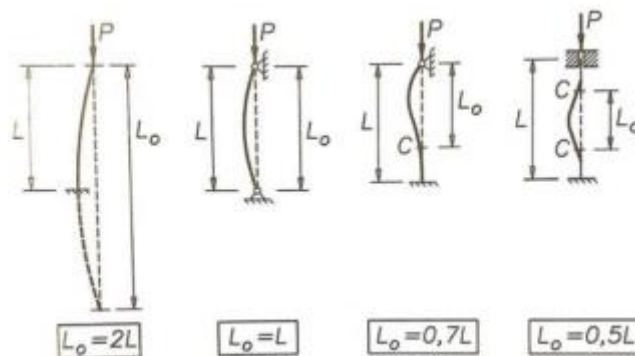
- flexural: the cross-section undergoes displacements in only one plane and is governed by the flexural stiffness of the element in that plane.
- torsional: represented by rotations along the axis of the element, it is governed by the primary torsional stiffness GJ and secondary torsional stiffness EI_ω
- flexural-torsional: union of the two phenomena described above; in fact, there is a dual displacement and torsion along the longitudinal axis.



In a compressed element, under the assumption of geometric imperfections, a critical elastic load N_{cr} can be defined that triggers the buckling phenomenon:

$$N_{cr} = \frac{\pi^2 \cdot EI}{l_0^2}$$

Where E is the elastic modulus of the material, I is the moment of inertia of the section, l_0 is the free length of deflection, i.e. the distance between two successive deflections of the deformation, so it varies as the static scheme changes. Both parameters can be evaluated for bending with respect to the strong axis as well as for bending with respect to the weak axis.

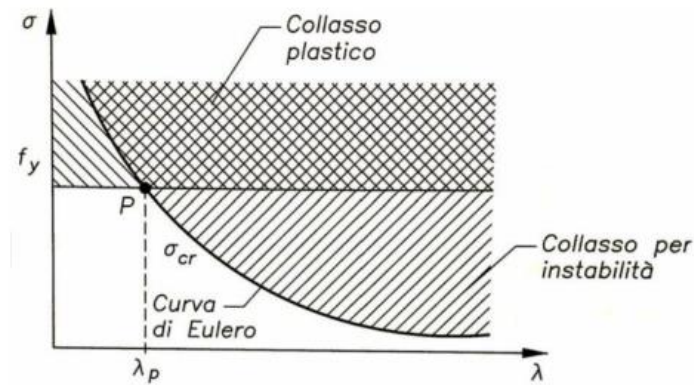


Dividing the Eulerian critical load by the cross-sectional area yields the critical normal stress

$$\sigma_{cr} = \frac{N_{cr}}{A}$$

The figure below shows a graph called the Euler curve, which relates the critical stress to the slenderness. Equalising the critical stress with the yield stress gives the slenderness of proportionality

$\lambda_{(p)}$ (.)



For values of $\lambda \leq \lambda_p$, a plastic-type collapse occurs, otherwise a brittle-type buckling collapse occurs. However, it must be taken into account that geometric and mechanical imperfections 'lower' the Euler curve. To account for such imperfections, the imperfection parameter ϕ is used:

$$\phi = \frac{[1 + \alpha \cdot (\lambda - 0.2) + \lambda^2]}{2}$$

With λ dimensionless slenderness:

$$\lambda = \sqrt{\frac{f_y \cdot A}{N_{cr}}}$$

E α imperfection factor associated with the buckling curves: Eurocode *EC3* proposes four curves depending on the type of steel, geometric characteristics of the profile and axis of inflection. Below is the table from which the imperfection factor values have been derived.

Sezione trasversale		Limiti		Inflexione intorno all'asse	Curva di instabilità	
					S235, S275, S355, S420	S460
Sezioni laminate		$h/b > 1,2$	$t_f \leq 40 \text{ mm}$	y-y z-z	a b	a ₀ a ₀
			$40 \text{ mm} < t_f \leq 100 \text{ mm}$	y-y z-z	b c	a a
		$h/b \leq 1,2$	$t_f \leq 100 \text{ mm}$	y-y z-z	b c	a a
			$t_f > 100 \text{ mm}$	y-y z-z	d d	c c
Sezioni ad I saldate		$t_f \leq 40 \text{ mm}$		y-y z-z	b c	b c
		$t_f > 40 \text{ mm}$		y-y z-z	c d	c d
Sezioni cave		Sezione formata "a caldo"		qualunque	a	a ₀
		Sezione formata "a freddo"		qualunque	c	c
Sezioni scatolari saldate		In generale		qualunque	b	b
		saldature "spesse": $a > 0,5t_f$ $b/t_f < 30$; $h/t_w < 30$		qualunque	c	c
Sezioni piene, ad U e T				qualunque	c	c
Sezioni ad L				qualunque	b	b
Curva di instabilità		a ₀	a	b	c	d
Fattore di imperfezione α		0,13	0,21	0,34	0,49	0,76

It is therefore possible to calculate the reduction coefficient χ , which precisely reduces the resistance capacity of the element.

$$\chi = \frac{1}{\phi + \sqrt{\phi^2 - \lambda^2}}$$

Paragraph §4.2.4.1.3.3. of NTC18 for the verification of elements at deflection refers to formulae of proven validity; therefore, methodology B found in the application circular in paragraph §4.2.3.1.3.1. has been evaluated, which is shown below:

$$\frac{N_{Ed}}{\chi_y \cdot \frac{N_{Rk}}{\gamma_{M1}}} + k_{yy} \cdot \frac{M_{y,ED} + \Delta M_{y,Ed}}{\chi_{LT} \cdot \frac{M_{y,Rk}}{\gamma_{M1}}} + k_{yz} \cdot \frac{M_{z,ED} + \Delta M_{z,Ed}}{\frac{M_{z,Rk}}{\gamma_{M1}}} \leq 1$$

$$\frac{N_{Ed}}{\chi_y \cdot \frac{N_{Rk}}{\gamma_{M1}}} + k_{zy} \cdot \frac{M_{y,ED} + \Delta M_{y,Ed}}{\chi_{LT} \cdot \frac{M_{y,Rk}}{\gamma_{M1}}} + k_{zz} \cdot \frac{M_{z,ED} + \Delta M_{z,Ed}}{\frac{M_{z,Rk}}{\gamma_{M1}}} \leq 1$$

With:

$$N_{Rk} = f_y \cdot A_i$$

$$M_{y,Rk} = W_y \cdot A_i$$

$\chi_{(LT)}$ and $\phi_{(LT)}$ are respectively the reduction coefficient and the imperfection parameter with respect to flexural-torsional buckling, calculated as previously but referring to the dimensionless slenderness λ_{LT} :

$$\lambda_{LT} = \sqrt{W_y \cdot \frac{f_y}{M_{cr}}}$$

In the present case, the free deflection lengths are equal to the distance between the transverse connection elements, which is the same as the distance between the pendants. The values of plastic moments and moment increments to be used depending on the class of steel used for the calculation of the resistant moment are given.

Classe	1	2	3	4
A_i	A	A	A	A_{eff}
W_y	$W_{pl,y}$	$W_{pl,y}$	$W_{el,y}$	$W_{eff,y}$
W_z	$W_{pl,z}$	$W_{pl,z}$	$W_{el,z}$	$W_{eff,z}$
$\Delta M_{y,Ed}$	0	0	0	$e_{N,y} \cdot N_{ed}$

Since the profiles adopted are class one, with reference to the table above the contribution of the additional moment in the two directions is considered to be zero.

The EC3 approach proposes, in the case of a doubly symmetrical section, for assumed varus applied in the shear centre and if there are no joints at the ends, to calculate M_{cr} with the following:

$$M_{cr} = \frac{C_1(\pi^2 E I_z)}{L^2} \left[\sqrt{\frac{I_w}{I_z} + \frac{L^2 G I_t}{\pi^2 E I_z}} \right]$$

The value of C1 was obtained by double interpolation, ψ being the ratio of moments, denoted as y , and the direction orthogonal to that axis, denoted as z . Please refer to Tables C4.2.IV-VI and in general to Eurocode EC8 for the evaluation of these parameters. In the above relationship I_w corresponds to the engulfment constant is equal to:

$$I_w = I_z \cdot \frac{(h - t_f)^2}{4}$$

In which the terms composing it are I_z , moment of inertia about the weak axis, h is profile height, t_f the thickness of the wings.

All structural verifications performed for each type of element are reported below. In order to assess the reliability of the results obtained from the FEM model, it was decided to perform all the verifications of one element by hand, specifically the lower arch element that is most stressed at the base.

3.5.1 Arch

The profile chosen for the lower part of the arch is HEB320, the section of which is shown in the image below:

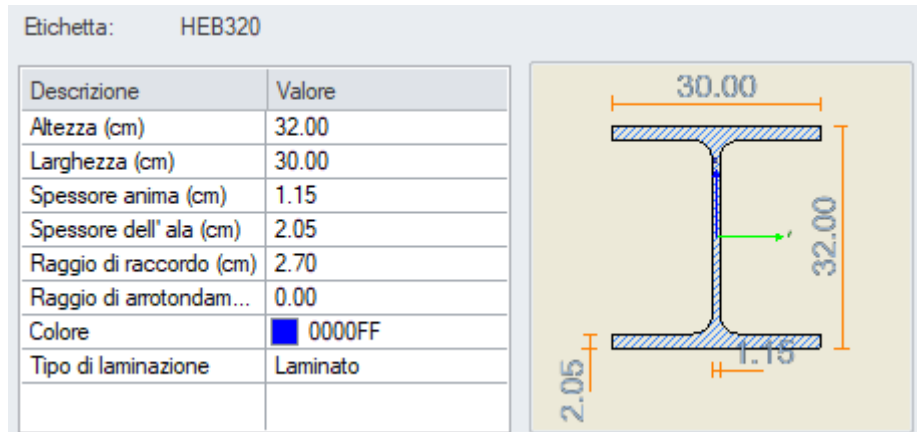


Figure 32: HEB 320 section taken from Advance Design profiler

As a first step, the class classification of the cross-section is carried out. The element is subjected to both compression and bending. Section classification is based on the evaluation of the shape ratios of both the web and the compressed wings. Specifically, following the indications found in Tab.4.2.III and Tab.4.2.IV, the arch element thus results in class 1. The internal forces acting on the arch are reported.

Vista FRONTALE
Analisi:1-10, 101-135, 137, 138, 141, 142, 145, 146, 149-169, 180-287 (Involuppo grafico - MaxAbs)
Lineare : Fx
Assi locali

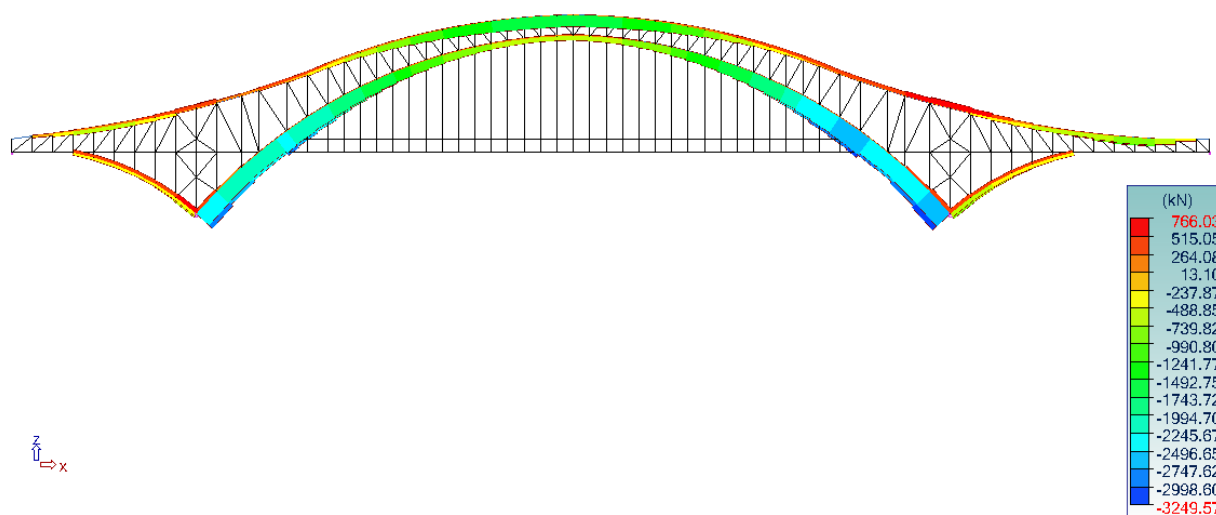


Figure 33: Axial forces F_x on arch

Vista UTENTE
Analisi:1-8, 101-135, 137, 138, 141, 142, 145, 146, 149-169, 180-261 (Involuppo grafico - MaxAbs)
Lineare : F_y
Assi locali

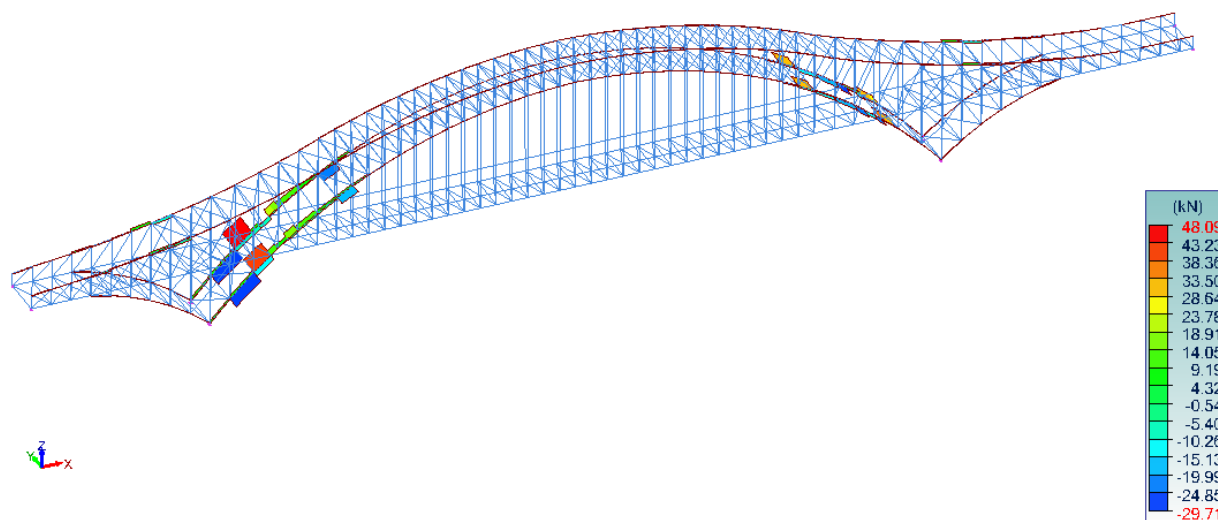


Figure 34: Shear forces F_y on the arch

Vista UTENTE
Analisi: 1-8, 101-135, 137, 138, 141, 142, 145, 146, 149-169, 180-261 (Involuppo grafico - MaxAbs)
Lineare : Fz
Assi locali

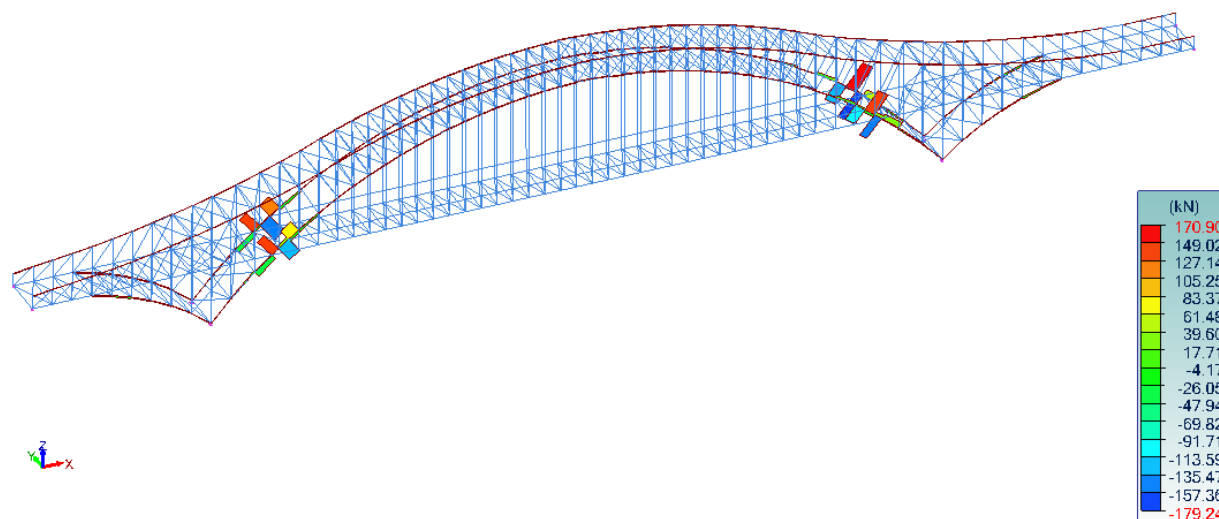


Figure 35: Shear forces F_z on the arch

Vista UTENTE
Analisi: 1-8, 101-135, 137, 138, 141, 142, 145, 146, 149-169, 180-261 (Involuppo grafico - MaxAbs)
Lineare : My
Assi locali

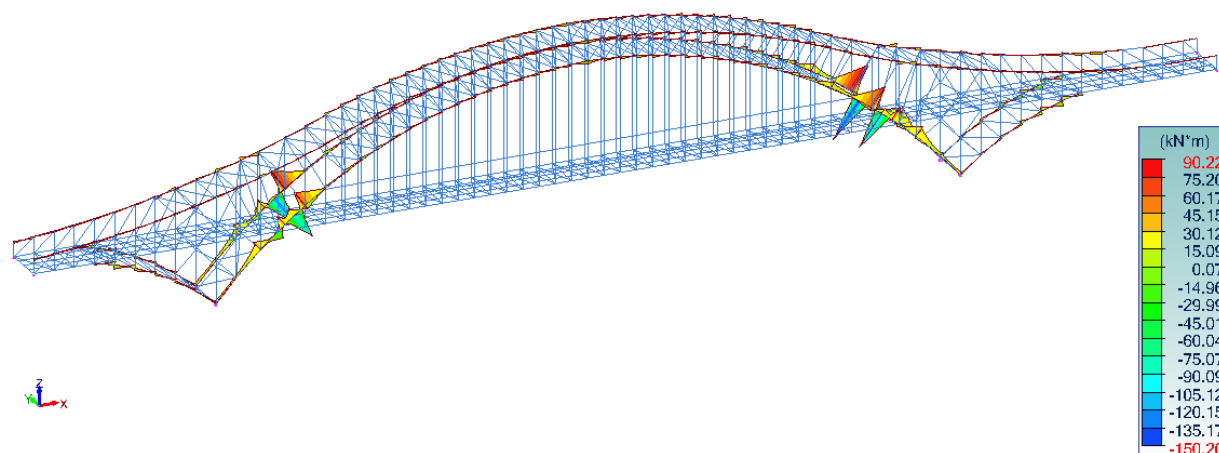


Figure 36: Bending moment on the arch

To validate the software, as an example, the manually performed checks related to one of the most heavily stressed elements of the arch are presented. It is pointed out that the verification is considered satisfied when the utilization ratio is lower than one; the utilization ratio is the ratio between the effects of actions and the resistance. If it's lower than one, it means the resistance is bigger than the acting forces.

Normal stress verification

The design compressive force N_{Ed} must meet the following condition:

$$N_{Ed} \leq N_{c,Rd}$$

With:

$$N_{c,Rd} = \frac{A \cdot f_y}{\gamma_{M0}}$$

This is valid for class 1,2, and 3 sections. If the section were class 4 we would have to consider the effective cross-sectional area instead of the gross cross-sectional area (A_{eff}), since local buckling phenomena would intervene, reducing the resistance.

$$N_{Ed} := 3060,13 \text{ kN}$$

Design axial force

$$\gamma_{M0} := 1,05$$

Partial safety coefficient

$$A = 161,3 \text{ cm}^2$$

Section area

$$f_{yk} := 355 \text{ MPa}$$

Yield strength

$$N_{c,Rd} := \frac{A \cdot f_{yk}}{\gamma_{M0}} = 5453,48 \text{ kN}$$

Plastic axial resistance

$$\rho := \frac{N_{Ed}}{N_{c,Rd}} = 0,56$$

Utilization ratio

Shear verification

The design value of shear action V_{Ed} must meet the following condition:

$$V_{Ed} \leq V_{c,Rd}$$

Where the design shear strength $V_{c,Rd}$ in the absence of torsion holds:

$$V_{c,Rd} = \frac{A_v \cdot f_{yk}}{\sqrt{3} \cdot \gamma_{M0}}$$

$$V_{Ed,y} := 25,53 \text{ kN} \quad \text{Shear force}$$

$$A_{v,y} := 127,43 \text{ cm}^2 \quad \text{Shear resistant area}$$

$$V_{c,Rd,y} := \frac{A_{v,y} \cdot f_{yk}}{\sqrt{3} \cdot \gamma_{M0}} = 2487,43 \text{ kN} \quad \text{Shear resistance}$$

$$\rho := \frac{V_{Ed,y}}{V_{c,Rd,y}} = 0,01 \quad \text{Utilization ratio}$$

$$V_{Ed,z} := 170,90 \text{ kN} \quad \text{Shear force}$$

$$A_{v,z} := 51,77 \text{ cm}^2 \quad \text{Shear resistant area}$$

$$V_{c,Rd,z} := \frac{A_{v,z} \cdot f_{yk}}{\sqrt{3} \cdot \gamma_{M0}} = 1010,55 \text{ kN} \quad \text{Shear resistance}$$

$$\rho := \frac{V_{Ed,z}}{V_{c,Rd,z}} = 0,17 \quad \text{Utilization ratio}$$

Bending verification

The bending verification is determined by the following formula:

$$M_{N,Rd} \leq M_{pl,y,Rd}$$

It can be seen from the previous shear verification that the shear utilization rate is less than 50 percent, so it can be stated, as in §4.2.4.1.2.9 of NTC18, that the flexural strength will not have to be reduced for the interaction between shear and bending by the reductive coefficient ρ .

The verifications are reported along the y- and z-axes, respectively:

$M_{y,Ed} := 147,46 \text{ kN m}$	Design bending moment
$W_{y,pl} := 2149 \text{ cm}^3$	Plastic section modulus
$M_{pl,y,Rd} := \frac{W_{y,pl} \cdot f_{yk}}{Y_{M0}} = 726,57 \text{ kN m}$	Plastic moment resistance
$\rho := \frac{M_{y,Ed}}{M_{pl,y,Rd}} = 0,2$	Utilization ratio
$M_{z,Ed} := 58,65 \text{ kN m}$	Design bending moment
$W_{z,pl} = 939,1 \text{ cm}^3$	Plastic section modulus
$M_{pl,z,Rd} := \frac{W_{z,pl} \cdot f_{yk}}{Y_{M0}} = 317,51 \text{ kN m}$	Plastic moment resistance
$\rho := \frac{M_{z,Ed}}{M_{pl,z,Rd}} = 0,18$	Utilization ratio

Bending and axial compression verification

It is required to verify that the bending moment capacity, reduced due to the presence of axial compressive force, is greater than the applied bending moment. For doubly symmetric Class 1 and 2 I- or H-sections subjected to axial compression or tension combined with bending in the web plane, the corresponding design conventional bending resistance can be evaluated as:

$$M_{N,y,Rd} = M_{pl,y,Rd} (1 - n) / (1 - 0,5 a) \leq M_{pl,y,Rd}$$

$$n = N_{Ed} / N_{pl,Rd}$$

$$a = \frac{(A - 2bt_f)}{A} \leq 0,5$$

$$M_{N,z,Rd} = M_{pl,z,Rd} \text{ per } n \leq a$$

$$M_{N,z,Rd} = M_{pl,z,Rd} \left[1 - \left(\frac{n - a}{1 - a} \right)^2 \right] \text{ per } n > a$$

Where:

-A is the gross area of the section

-b is the width of the wings,

-tf is the thickness of the wings

The following stresses and results occur:

$$N_{Ed} = 3060,13 \text{ kN}$$

Applied axial force

$$\gamma_{M0} := 1,05$$

Partial safety coefficient

$$N_{pl,Rd} := A \cdot \frac{f_{yk}}{\gamma_{M0}} = 5453,5 \text{ kN}$$

Plastic axial resistance

$$n := \frac{N_{Ed}}{N_{pl,Rd}} = 0,56$$

Utilization ratio

$$M_{y,Ed} := 136,03 \text{ kN m}$$

Design bending moment

$$W_{y,pl} := 2149 \text{ cm}^3$$

Plastic section modulus

$$M_{pl,y,Rd} := \frac{W_{y,pl} \cdot f_{yk}}{\gamma_{M0}} = 726,57 \text{ kN m}$$

$$a := \frac{A - 2 \cdot b \cdot t_f}{A} = 0,2374$$

$$M_{N,y,Rd} := \frac{M_{pl,y,Rd} \cdot (1 - n)}{(1 - 0,5 \cdot a)} = 361,82 \text{ kN m}$$

Plastic moment resistance

$$\rho := \frac{M_{y,Ed}}{M_{N,y,Rd}} = 0,38$$

Utilization ratio

$$M_{z,Ed} := 58,65 \text{ kN m}$$

Design bending moment

$$W_{z,pl} := 939,1 \text{ cm}^3$$

Plastic section modulus

$$M_{pl,z,Rd} := \frac{W_{z,pl} \cdot f_{yk}}{\gamma_{M0}} = 317,51 \text{ kN m}$$

$$a := \frac{A - 2 \cdot b \cdot t_f}{A} = 0,24$$

$$M_{N,z,Rd} := M_{pl,z,Rd} \cdot \left(1 - \left(\frac{n - a}{1 - a} \right)^2 \right) = 260,3 \text{ kN m}$$

Plastic moment resistance

$$\rho := \frac{M_{z,Ed}}{M_{N,z,Rd}} = 0,2$$

Utilization ratio

Biaxial bending and axial compression verification

For doubly symmetrical class 1 and 2 I- or H-sections subjected to axial compression or tension combined with biaxial bending, the strength condition can be evaluated as:

$$\left(\frac{M_{y,Ed}}{M_{N,y,Rd}} \right)^2 + \left(\frac{M_{z,Ed}}{M_{N,z,Rd}} \right)^{5n} \leq 1$$

with $n \geq 0,2$ $n = N_{Ed} / N_{pl,Rd}$

In cases where $n < 0,2$, for Class 1 and 2 sections the verification can be carried out using the following expression:

$$\left(\frac{M_{y,Ed}}{M_{N,y,Rd}} \right) + \left(\frac{M_{z,Ed}}{M_{N,z,Rd}} \right) \leq 1$$

In this case $n=0,56$.

$$M_{y,Ed} := 136,03 \text{ kN m}$$

Design bending moment

$$M_{z,Ed} := 58,65 \text{ kN m}$$

Design bending moment

$$n := \frac{N_{Ed}}{N_{pl,Rd}} = 0,56$$

Utilization ratio

$$M_{N,y,Rd} := \frac{M_{pl,y,Rd} \cdot (1 - n)}{(1 - 0,5 \cdot a)} = 361,82 \text{ kN m}$$

Plastic moment resistance

$$M_{N,z,Rd} := M_{pl,z,Rd} \cdot \left(1 - \left(\frac{n - a}{1 - a} \right)^2 \right) = 260,3 \text{ kN m}$$

Plastic moment resistance

$$\left(\frac{M_{y,Ed}}{M_{N,y,Rd}} \right)^2 + \left(\frac{M_{z,Ed}}{M_{N,z,Rd}} \right)^{5 \cdot n} = 0,157 \quad 0,15 \leq 1$$

The following table summarizes the strength verifications for the analyzed element, as obtained using the Advance Design post-processor.

Scheda sezione - Elemento lineare no.467				
Sezione Freccia 0 Resistenza sezioni (56%) Stabilità elementi (99%) Stabilità e Resistenza al fuoco 0				
	Caso sfavorevole	Sezione Classe	Verifica	Tasso di lav...
Trazione Compressione (6.2.4)	n°138	Classe 1	$F_x < N_{c,Rd}$ 3060.13 < 5453.48 kN	56%
Taglio in direzione Y (6.2.6)	n°146	Classe 1	$F_y < V_{ply}$ 25.53 < 2487.43 kN	1%
Taglio in direzione Z (6.2.6)	n°138	Classe 1	$F_z < V_{plz}$ 170.90 < 1010.55 kN	17%
Flessione su Y-Y (4.2.4.1.2.3)	n°138	Classe 1	$M_{y,Ed} < M_{y,Rd}$ 147.46 < 726.57 kN*m	20%
Flessione su Z-Z (4.2.4.1.2.3)	n°146	Classe 1	$M_{z,Ed} < M_{z,Rd}$ 58.65 < 317.51 kN*m	18%
Flessione in Y-Y e sforzo normale (6.2.9)	n°138	Classe 1	$M_{y,Ed} < M_{N,y,Rd}$ (6.31) 136.03 < 361.82 kN*m	38%
Flessione in Z-Z e sforzo normale (6.2.9)	n°146	Classe 1	$M_{z,Ed} < M_{N,z,Rd}$ (6.31) 58.65 < 295.53 kN*m	20%
Flessione deviata (6.2.9)	n°138	Classe 1	$(M_{y,Ed}/M_{N,y,Rd})^a + (M_{z,Ed}/M_{N,z,Rd})^b < 1$ (6.41) 0.15 < 1	15%
Torsione St. Venant (...)	n°146	Classe 1	$M_x < W_t \cdot (F_y/3^{1/2}/gM0)$ 3.77 < 21.43 kN*m	18%

As can be observed, the same utilization ratios were obtained, all of which are below unity. The verifications are therefore fully satisfied.

Stability checks

$$L_{0,y} := 3,41 \text{ m}$$

$$N_{cr,y} := \frac{\pi^2 \cdot E \cdot I_y}{L_{0,y}^2} = 54934,21 \text{ kN}$$

$$L_{0,z} := 3,41 \text{ m}$$

$$N_{cr,z} := \frac{\pi^2 \cdot E \cdot I_z}{L_{0,z}^2} = 16467,79 \text{ kN}$$

$$\lambda_y := \sqrt{\left(\frac{f_{yk} \cdot A}{N_{cr,y}} \right)} = 0,323$$

$$\lambda_z := \sqrt{\left(\frac{f_{yk} \cdot A}{N_{cr,z}} \right)} = 0,5897$$

$$\alpha_y := 0,34$$

$$\alpha_z := 0,49$$

$$\phi_y := \frac{(1) + \alpha_y \cdot (\lambda_y - 0,2) + \lambda_y^2}{2} = 0,57$$

$$\phi_z := \frac{(1) + \alpha_z \cdot (\lambda_z - 0,2) + \lambda_z^2}{2} = 0,77$$

$$\chi_y := \frac{1}{\phi_y + \sqrt{\phi_y^2 - \lambda_y^2}} = 0,96$$

$$\chi_z := \frac{1}{\phi_z + \sqrt{\phi_z^2 - \lambda_z^2}} = 0,79$$

$$k_{yy} := 1,16$$

$$\chi_{LT} := 1$$

$$k_{zz} := 1,06$$

$$k_{zy} := 0,64$$

$$k_{yz} := 0,63$$

$$\frac{N_{Ed} \cdot Y_{M1}}{0,96 \cdot A \cdot f_{yk}} + k_{yy} \cdot \frac{M_{y,Ed} \cdot Y_{M1}}{\chi_{LT} \cdot W_{y,Pl} \cdot f_{yk}} + k_{yz} \cdot \frac{M_{z,Ed} \cdot Y_{M1}}{W_{z,Pl} \cdot f_{yk}} = 0,9$$

$$\frac{N_{Ed} \cdot Y_{M1}}{0,79 \cdot A \cdot f_{yk}} + k_{zy} \cdot \frac{M_{y,Ed} \cdot Y_{M1}}{\chi_{LT} \cdot W_{y,Pl} \cdot f_{yk}} + k_{zz} \cdot \frac{M_{z,Ed} \cdot Y_{M1}}{W_{z,Pl} \cdot f_{yk}} = 0,99$$

Scheda sezione - Elemento lineare no.467	
Sezione	Freccia 0
Resistenza sezioni (56%)	Stabilità elementi (99%)
Stabilità e Resistenza al fuoco 0	
Instabilità Snell. E Lung.	LambdaFy = 0.322 LambdaFz = 0.589 Lfy = 3.41 m Lfz = 3.41 m
Inst flessio-torsionale	LambdaLT = 0.453 Ldi = 3.41 m Lds = 3.41 m
Caso sfavorevole	Caso n°138 : 1.35x[1 G]+1.5x[2 G]+1.5x[4 Q]+0.9x[9 V] Sezione : Classe 1
Fattore di amplificazione	kz=1.00 kw=1.00 C1=1.23 C2=0.84 Xy=0.96 Xz=0.79 XLT=1.00 kyy=1.16 kyz=0.63 kzy=0.64 kzz=1.06 zg=0.00 m Mcr=3722.62 kN*m MbRd=726.57 kN*m NcrT=22226.64 kN
Verifica (6.61)	Ned / (Xy Nrk / gM1) + kyy (My,Ed + DMMy,Ed) / (XLT My,Rk / gM1) + kyz (Mz,Ed + DMz,Ed) / (Mz,Rk / gM1) < 1 0.587 + 0.218 + 0.095 = 0.899 < 1 (90%)
Verifica (6.62)	Ned / (Xz Nrk / gM1) + kzy (My,Ed + DMMy,Ed) / (XLT My,Rk / gM1) + kzz (Mz,Ed + DMz,Ed) / (Mz,Rk / gM1) < 1 0.709 + 0.120 + 0.160 = 0.989 < 1 (99%)

3.5.2 Transverse deck beams

The transverse beams, which support the secondary beams and the wooden decking, have a HEB200 cross-section; the geometric properties are reported below.

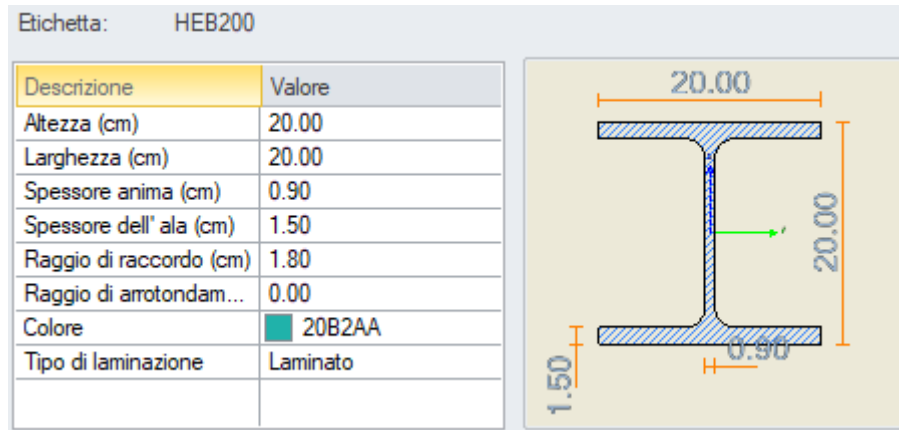


Figure 37: HEB 200 section taken from Advance Design profiler

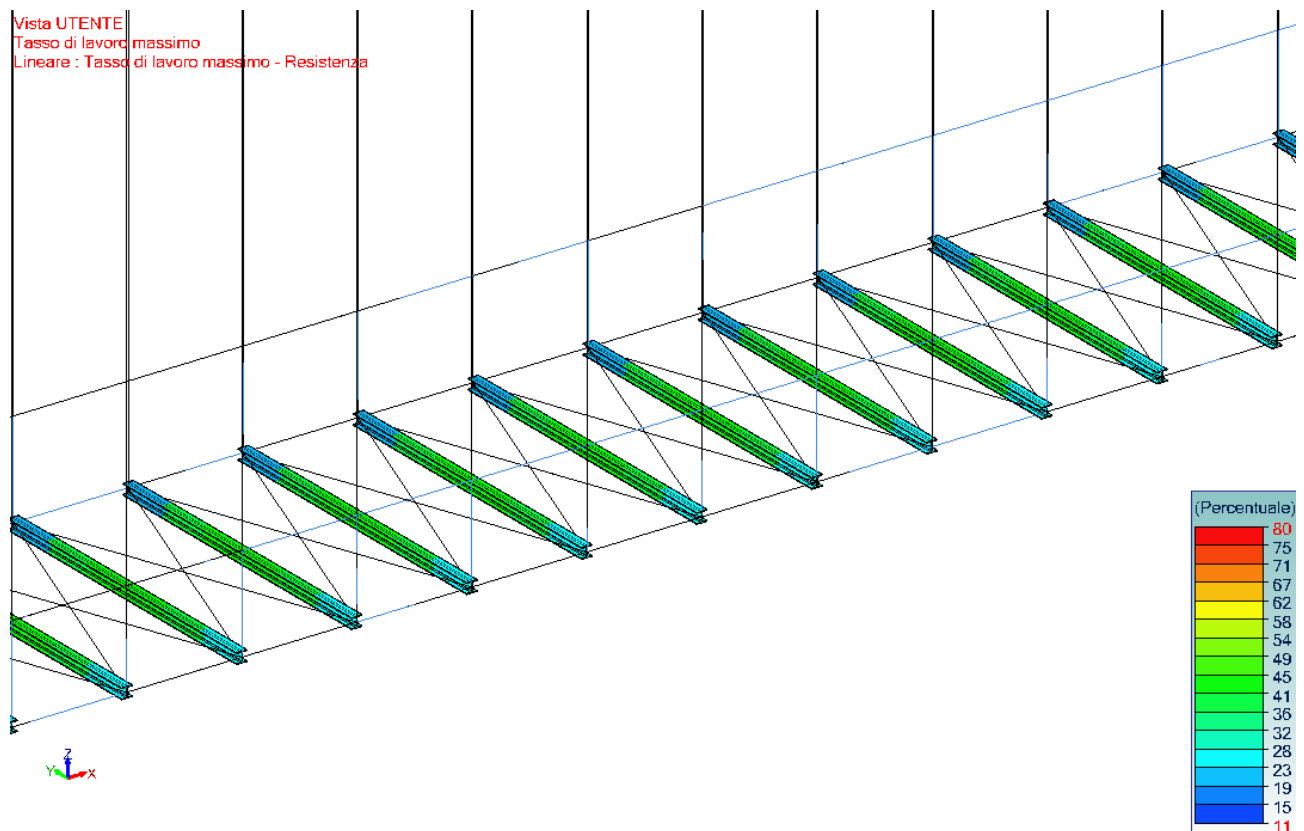


Figure 38: Resistance utilization rate

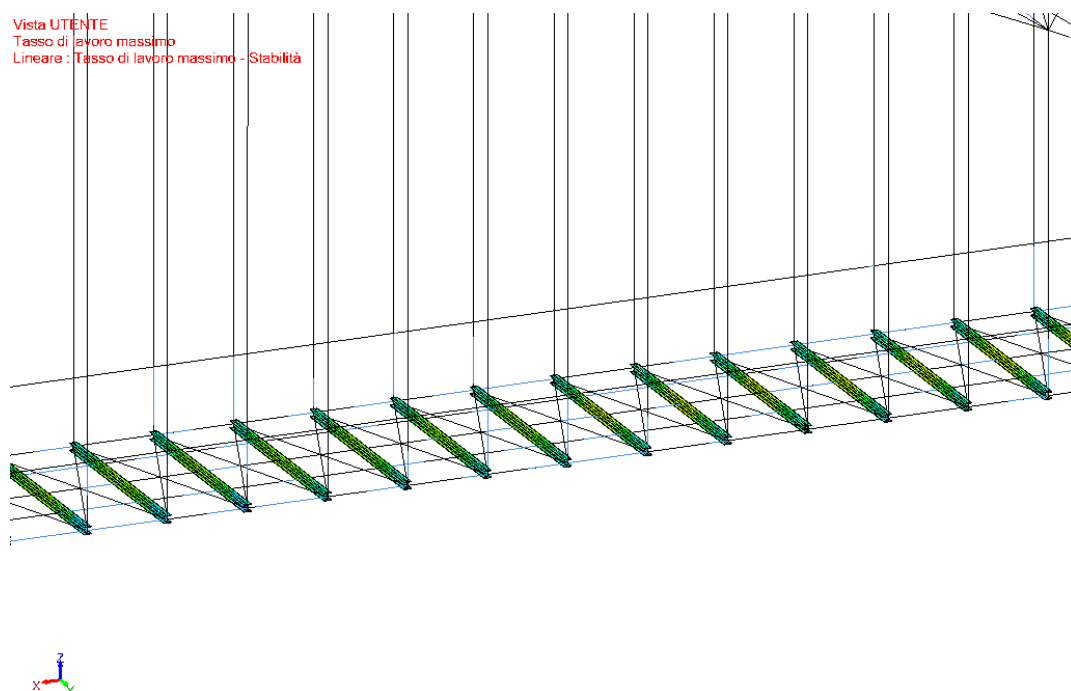


Figure 39: : Stability utilization rate

Sezione	Frecce ()	Resistenza sezioni (80%)	Stabilità elementi (90%)	Stabilità e Resistenza al fuoco ()
	Caso sfavore...	Sezione Classe	Verifica	Tasso di l...
Trazione Compressione (6.2.4)	n°135	Classe 1	$F_x < N_{c,Rd}$ 19.02 < 2639.89 kN	1%
Taglio in direzione Y (6.2.6)	n°267	Classe 1	$F_y < V_{ply}$ 1.99 < 1218.63 kN	0%
Taglio in direzione Z (6.2.6)	n°138	Classe 1	$F_z < V_{plz}$ 106.24 < 484.70 kN	22%
Flessione su Y-Y (4.2.4.1.2.3)	n°146	Classe 1	$M_{yEd} < M_{ycRd}$ 173.36 < 217.24 kN*m	80%
Flessione su Z-Z (4.2.4.1.2.3)	n°267	Classe 1	$M_{zEd} < M_{zcRd}$ 3.83 < 103.39 kN*m	4%
Flessione deviata (6.2.9)	n°146	Classe 1	$(M_{yEd}/M_{N,y}, R_d)^a + (M_{zEd}/M_{N,z}, R_d)^b < 1$ (6.41) 0.64 < 1	64%
Torsione St. Venant (...)	n°146	Classe 1	$M_x < W_t(F_y/3^{1/2}/gM_0)$ 0.009 < 7.74 kN*m	0%

Sezione	Frecce ()	Resistenza sezioni (80%)	Stabilità elementi (90%)	Stabilità e Resistenza al fuoco ()
Instabilità Snell. E Lungh.	$\Lambda_{Fy} = 0.919$ $\Lambda_{Fz} = 1.550$ $L_{fy} = 6.00$ m $L_{fz} = 6.00$ m			
Inst.flesso-torsionale	$\Lambda_{LT} = 0.550$ $L_{di} = 6.00$ m $L_{ds} = 6.00$ m			
Caso sfavorevole	Caso n°146 : 1.35x[1 G]+1.5x[2 G]+1.5x[9 V]+0.6x[4 Q] Sezione : Classe 1			
Fattore di amplificazione	$k_z = 1.00$ $k_w = 1.00$ $C_1 = 2.92$ $C_2 = 0.35$ $X_y = 0.65$ $X_z = 0.30$ $X_{LT} = 0.90$ $k_{yy} = 1.00$ $k_{yz} = 0.70$ $k_{zy} = 0.52$ $k_{zz} = 0.66$ $z_g = 0.00$ m $M_{cr} = 753.93$ kN*m $M_{bRd} = 194.58$ kN*m $N_{crT} = 5875.38$ kN			
Verifica (6.61)	$\frac{N_{ed}}{X_y N_{rk}} + k_{yy} \frac{(M_{y,Ed} + D M_{y,Ed})}{(X_{LT} M_{y,Rk} / g M_1)} + k_{yz} \frac{(M_{z,Ed} + D M_{z,Ed})}{(M_{z,Rk} / g M_1)} < 1$ $0.005 + 0.894 + 0.000 = 0.899 < 1 \quad (90\%)$			
Verifica (6.62)	$\frac{N_{ed}}{X_z N_{rk}} + k_{zy} \frac{(M_{y,Ed} + D M_{y,Ed})}{(X_{LT} M_{y,Rk} / g M_1)} + k_{zz} \frac{(M_{z,Ed} + D M_{z,Ed})}{(M_{z,Rk} / g M_1)} < 1$ $0.011 + 0.466 + 0.000 = 0.477 < 1 \quad (48\%)$			

3.5.3 Longitudinal deck beams

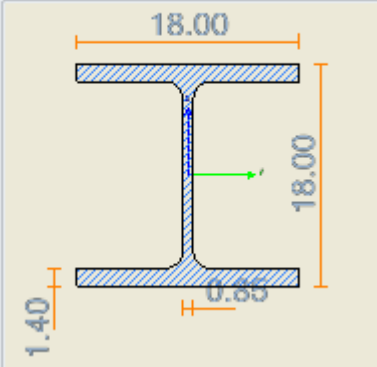
Etichetta: HEB180		
Descrizione	Valore	
Altezza (cm)	18.00	
Larghezza (cm)	18.00	
Spessore anima (cm)	0.85	
Spessore dell'ala (cm)	1.40	
Raggio di raccordo (cm)	1.50	
Raggio di arrotondam...	0.00	
Colore	FFFF00	
Tipo di laminazione	Laminato	

Figure 40: HEB 180 section taken from Advance Design profiler

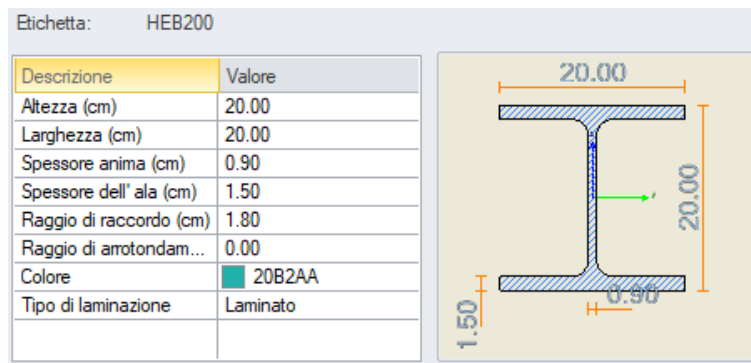


Figure 41: HEB 200 section taken from Advance Design profiler

Vista UTENTE
Tasso di lavoro massimo
Lineare : Tasso di lavoro massimo - Resistenza

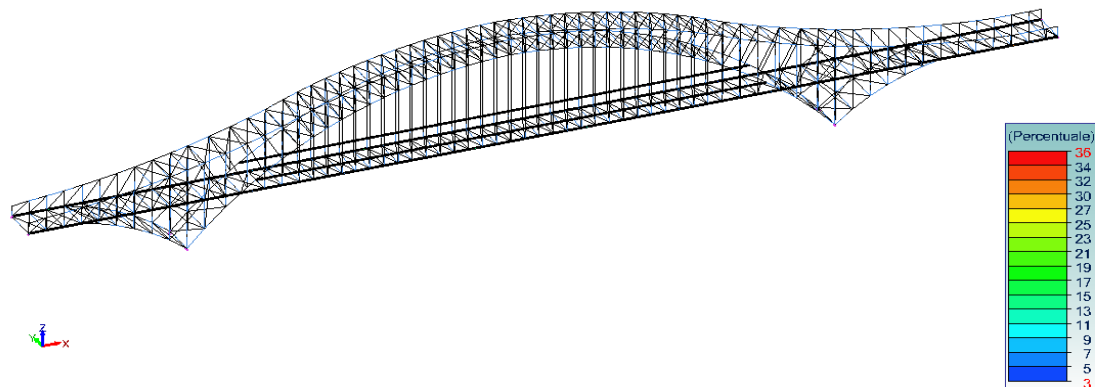


Figure 42: : Resistance utilization rate

	Caso sfavorevole	Sezione Classe	Verifica	Tasso di lav...
Trazione Compressione (6.2.3)	n°138	Classe 1	$F_x < N_{t,Rd}$ $943.84 < 2639.89 \text{ kN}$	36%
Taglio in direzione Y (6.2.6)	n°146	Classe 1	$F_y < V_{ply}$ $1.32 < 1218.63 \text{ kN}$	0%
Taglio in direzione Z (6.2.6)	n°146	Classe 1	$F_z < V_{plz}$ $9.05 < 484.70 \text{ kN}$	2%
Flessione su Y-Y (4.2.4.1.2.3)	n°146	Classe 1	$M_{y,Ed} < M_{y,Rd}$ $6.15 < 217.24 \text{ kN}\cdot\text{m}$	3%
Flessione su Z-Z (4.2.4.1.2.3)	n°146	Classe 1	$M_{z,Ed} < M_{z,Rd}$ $0.90 < 103.39 \text{ kN}\cdot\text{m}$	1%
Flessione in Y-Y e sforzo normale (6.2.9)	n°146	Classe 1	$M_{y,Ed} < M_{N,y,Rd} \text{ (6.31)}$ $6.15 < 180.60 \text{ kN}\cdot\text{m}$	3%
Flessione in Z-Z e sforzo normale (6.2.9)	n°146	Classe 1	$M_{z,Ed} < M_{N,z,Rd} \text{ (6.31)}$ $0.90 < 103.20 \text{ kN}\cdot\text{m}$	1%
Flessione deviata (6.2.9)	n°142	Classe 1	$(M_{y,Ed}/M_{N,y,Rd})^a + (M_{z,Ed}/M_{N,z,Rd})^b < 1 \text{ (6.41)}$ $0.01 < 1$	1%
Torsione St. Venant (4...	n°142	Classe 1	$M_x < W_t \cdot (F_y/3)^{(1/2)} / gM0$ $0.02 < 7.74 \text{ kN}\cdot\text{m}$	0%

Vista UTENTE
Tasso di lavoro massimo
Lineare : Tasso di lavoro massimo - Stabilità

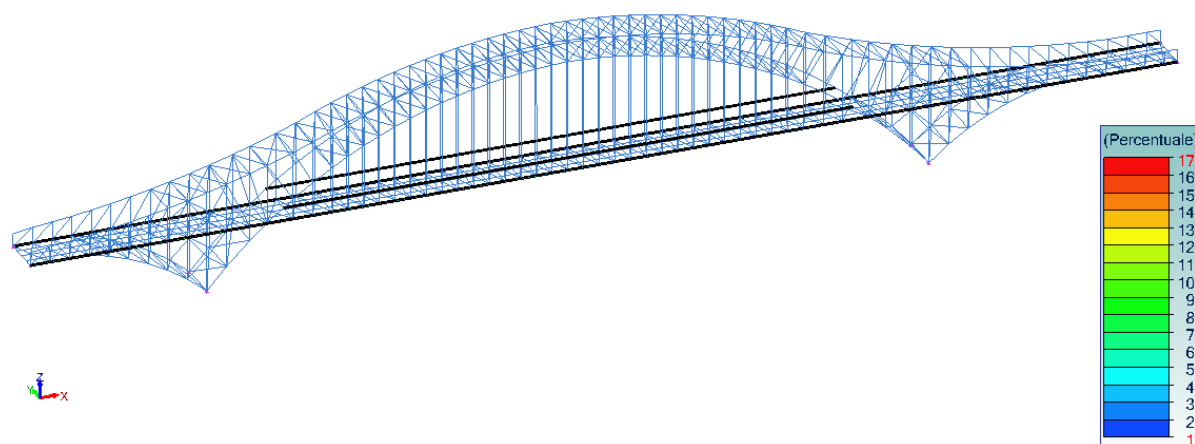


Figure 43: : Stability utilization rate

Sezione	Frecce (10%)	Resistenza sezioni (8%)	Stabilità elementi (17%)	Stabilità e Resistenza al fuoco ()
Sezione lorda				
<input checked="" type="radio"/> Inizio <input type="radio"/> Fine <input type="text" value="HEB200"/>				
Dimensioni(cm)	h = 20.00 b = 20.00 tw = 0.90 tf = 1.50 r = 1.80 r1 = 0.00			
Sezioni(cm2)	Area = 78.0812 Avy = 62.43 Avz = 24.8312			
Momenti d'inerzia(cm4)	It = 59.5128 Iy = 5696.17 Iz = 2003.37 Iyz = 0			
Momenti d'inerzia(cm6)	Iw = 171413			
Moduli d'inerzia(cm3)	Welyinf = 569.617 Welysup = 569.617 Welzinf = 200.337 Welzsup = 200.337 Wply = 642.547 Wplz = 305.812			

3.5.4 Bracings

All the bracing members were designed using UPN 100 profiles.

In the structural analysis software, they were modeled as tie rods, and therefore only tensile checks were carried out.

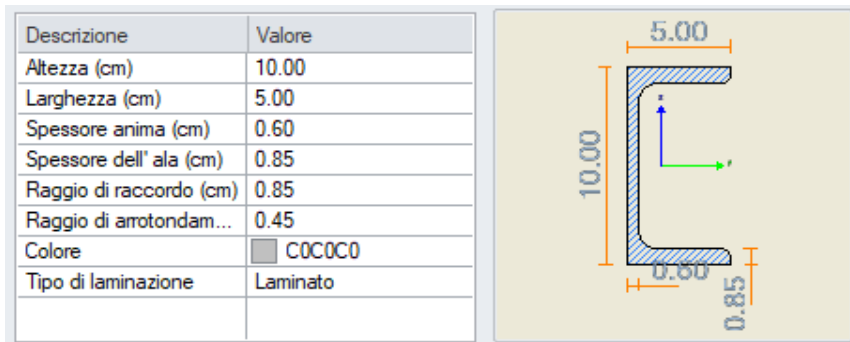
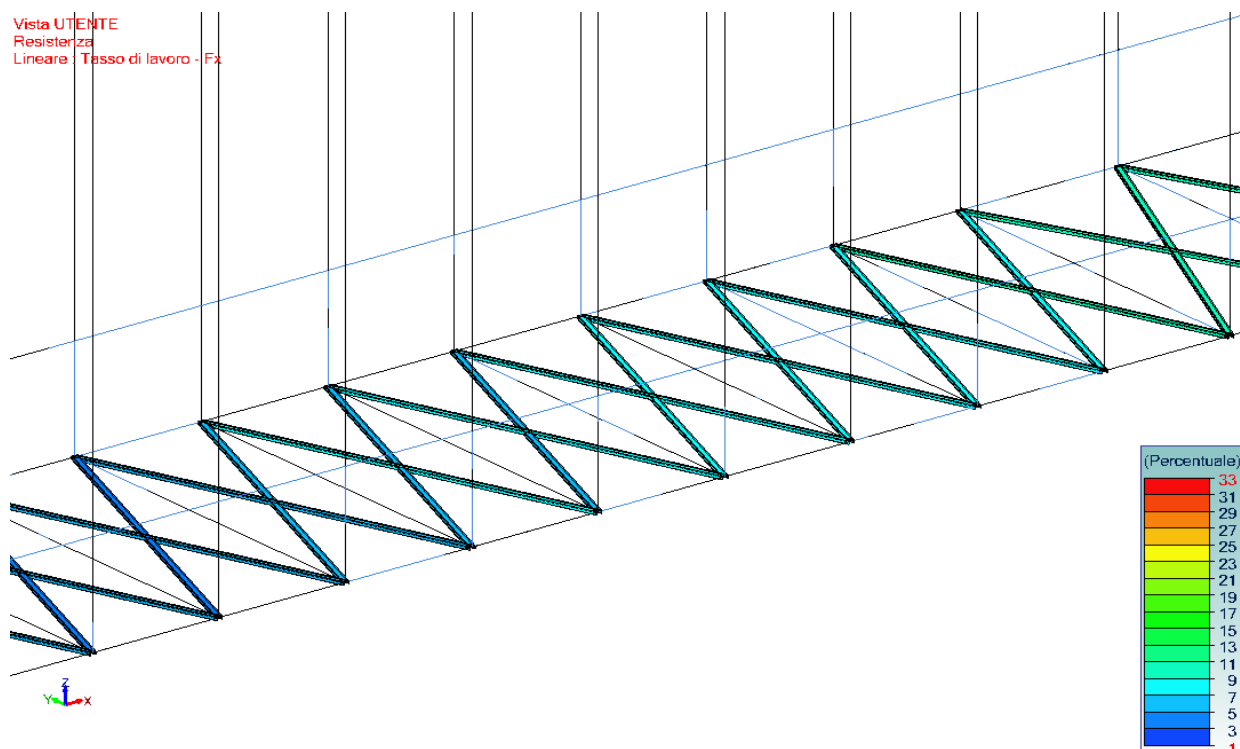


Figure 44: UPN100 section taken from Advance Design proflerl

The bracings were installed as connections between the deck beams and between the two arches; they play a fundamental role in ensuring stability by counteracting mechanisms that could cause relative displacement between the two beams (and the two arches). Therefore, the primary ultimate limit state verification performed on them is the tensile axial force check.



	Caso sfavore...	Sezione Classe	Verifica	Tasso di I...
Trazione Compressione (6.2.4)	n°146	Classe 1	$F_x < N_{c,Rd}$ $152.65 < 466.24 \text{ kN}$	33%

Vista UTENTE

Tasso di lavoro massimo

Lineare : Tasso di lavoro massimo - Resistenza

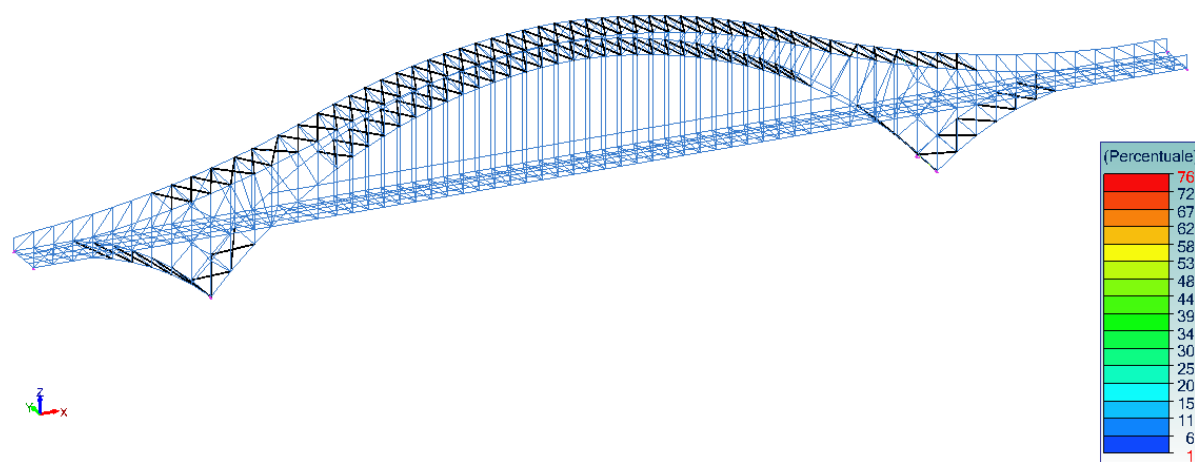
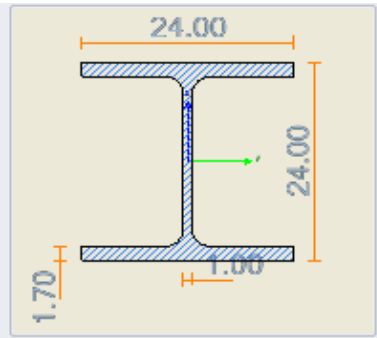


Figure 45: : Resistance utilization rate

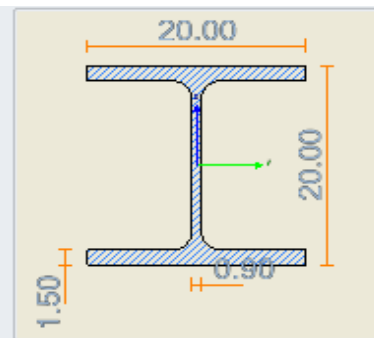
	Caso sfavore...	Sezione Classe	Verifica	Tasso di I...
Trazione Compressione (6.2.4)	n°146	Classe 1	$F_x < N_{c,Rd}$ $357.93 < 466.24 \text{ kN}$	77%

3.5.5 Vertical members

Descrizione	Valore
Altezza (cm)	24.00
Larghezza (cm)	24.00
Spessore anima (cm)	1.00
Spessore dell' ala (cm)	1.70
Raggio di raccordo (cm)	2.10
Raggio di arrotondam...	0.00
Colore	CC0066
Tipo di laminazione	Laminato



Descrizione	Valore
Altezza (cm)	20.00
Larghezza (cm)	20.00
Spessore anima (cm)	0.90
Spessore dell' ala (cm)	1.50
Raggio di raccordo (cm)	1.80
Raggio di arrotondam...	0.00
Colore	20B2AA
Tipo di laminazione	Laminato



Vista UTENTE
Tasso di lavoro massimo
Lineare : Tasso di lavoro massimo - Resistenza

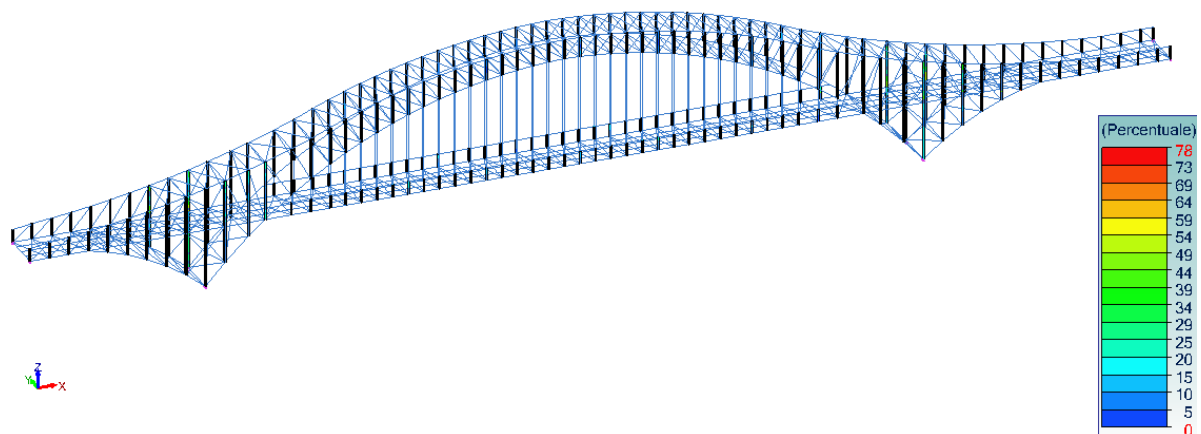
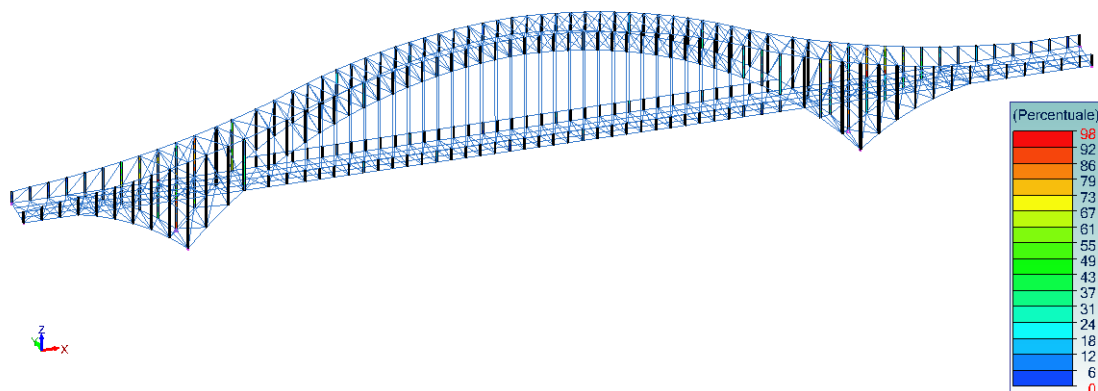


Figure 46: : Resistance utilization rate

Scheda sezione - Elemento lineare no.663				
Sezione	Freccie ()	Resistenza sezioni (78%)	Stabilità elementi (94%)	Stabilità e Resistenza al fuoco ()
	Caso sfavorevole	Sezione Classe	Verifica	Tasso di lavoro
Trazione Compressione (6.2.4)	n°138	Classe 1	$F_x < N_{c,Rd}$ 454.36 < 3583.81 kN	13%
Taglio in direzione Y (6.2.6)	n°146	Classe 1	$F_y < V_{ply}$ 121.85 < 1653.34 kN	7%
Taglio in direzione Z (6.2.6)	n°138	Classe 1	$F_z < V_{plz}$ 3.43 < 648.65 kN	1%
Flessione su Y-Y (4.2.4.1.2.3)	n°138	Classe 1	$M_{y,Ed} < M_{yc,Rd}$ 13.01 < 356.01 kN*m	4%
Flessione su Z-Z (4.2.4.1.2.3)	n°146	Classe 1	$M_{z,Ed} < M_{zc,Rd}$ 130.96 < 168.51 kN*m	78%
Flessione in Y-Y e sforzo normale (6.2.9)	n°138	Classe 1	$M_{y,Ed} < M_{N,y,Rd}$ (6.31) 13.01 < 352.25 kN*m	4%
Flessione deviata (6.2.9)	n°146	Classe 1	$(M_{y,Ed}/M_{N,y,Rd})^a + (M_{z,Ed}/M_{N,z,Rd})^b < 1$ (6.41) 0.78 < 1	78%
Torsione St. Venant (4...)	n°138	Classe 1	$M_x < W_t \cdot (F_y/3)^{1/2} / (gM_0)$ 0.16 < 11.79 kN*m	1%

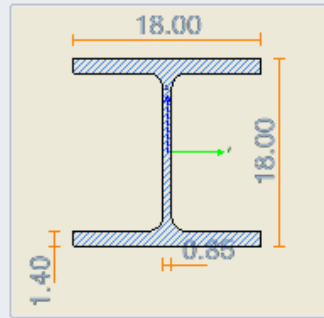
Vista UTENTE
Tasso di lavoro massimo
Lineare : Tasso di lavoro massimo - Stabilità



Sezione	Freccie ()	Resistenza sezioni (53%)	Stabilità elementi (98%)	Stabilità e Resistenza al fuoco ()
Instabilità Snell. E Lungh.		$\Lambda_{bda} F_y = 1.421$ $\Lambda_{bda} F_z = 2.407$ $L_{fy} = 11.19$ m $L_{fz} = 11.19$ m		
Inst.flesso-torsionale		$\Lambda_{bda} L_T = 0.770$ $L_{di} = 11.19$ m $L_{ds} = 11.19$ m		
Caso sfavorevole		Caso n°146 : 1.35x[1 G]+1.5x[2 G]+1.5x[9 V]+0.6x[4 Q] Sezione : Classe 1		
Fattore di amplificazione		$k_z = 1.00$ $k_w = 1.00$ $C_1 = 2.59$ $C_2 = 0.56$ $X_y = 0.37$ $X_z = 0.14$ $X_{LT} = 1.00$ $k_{yy} = 1.17$ $k_{yz} = 0.82$ $k_{zy} = 0.57$ $k_{zz} = 0.74$ $z_g = 0.00$ m $M_{cr} = 631.00$ kN*m $M_{b,Rd} = 356.01$ kN*m $N_{cr,T} = 6354.97$ kN		
Verifica (6.61)		$N_{ed} / (X_y N_{rk} / gM_1) + k_{yy} (M_{y,Ed} + DM_{y,Ed}) / (X_{LT} M_{y,Rk} / gM_1) + k_{yz} (M_{z,Ed} + DM_{z,Ed}) / (M_{z,Rk} / gM_1) < 1$ 0.220 + 0.009 + 0.434 = 0.663 < 1 (66%)		
Verifica (6.62)		$N_{ed} / (X_z N_{rk} / gM_1) + k_{zy} (M_{y,Ed} + DM_{y,Ed}) / (X_{LT} M_{y,Rk} / gM_1) + k_{zz} (M_{z,Ed} + DM_{z,Ed}) / (M_{z,Rk} / gM_1) < 1$ 0.579 + 0.004 + 0.394 = 0.977 < 1 (98%)		

3.5.6 Diagonals

Etichetta: HEB180	
Descrizione	Valore
Altezza (cm)	18.00
Larghezza (cm)	18.00
Spessore anima (cm)	0.85
Spessore dell' ala (cm)	1.40
Raggio di raccordo (cm)	1.50
Raggio di arrotondam...	0.00
Colore	FFFF00
Tipo di laminazione	Laminato



Vista UTENTE
Tasso di lavoro massimo
Lineare : Tasso di lavoro massimo - Resistenza

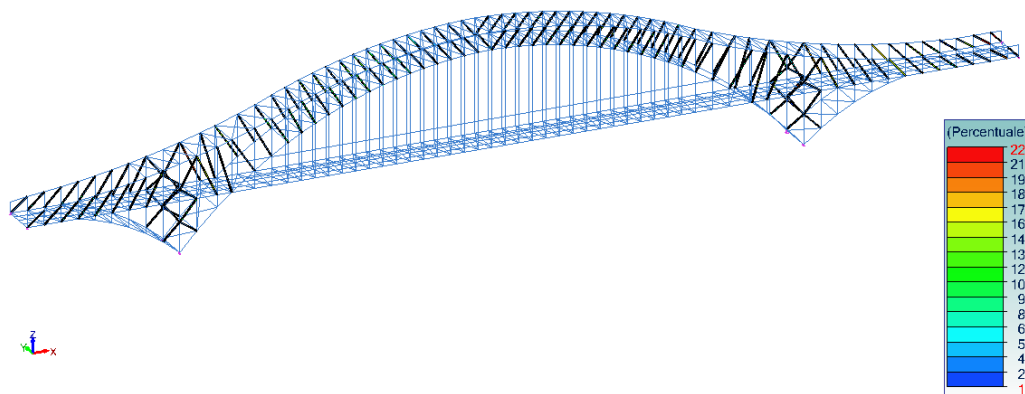


Figure 47: : Resistance utilization rate

	Caso sfavore...	Sezione Classe	Verifica	Tasso di l...
Trazione Compressione (6.2.4)	n°138	Classe 1	$F_x < N_c, R_d$ 476.42 < 2206.12 kN	22%

3.5.7 Secondary longitudinal beams

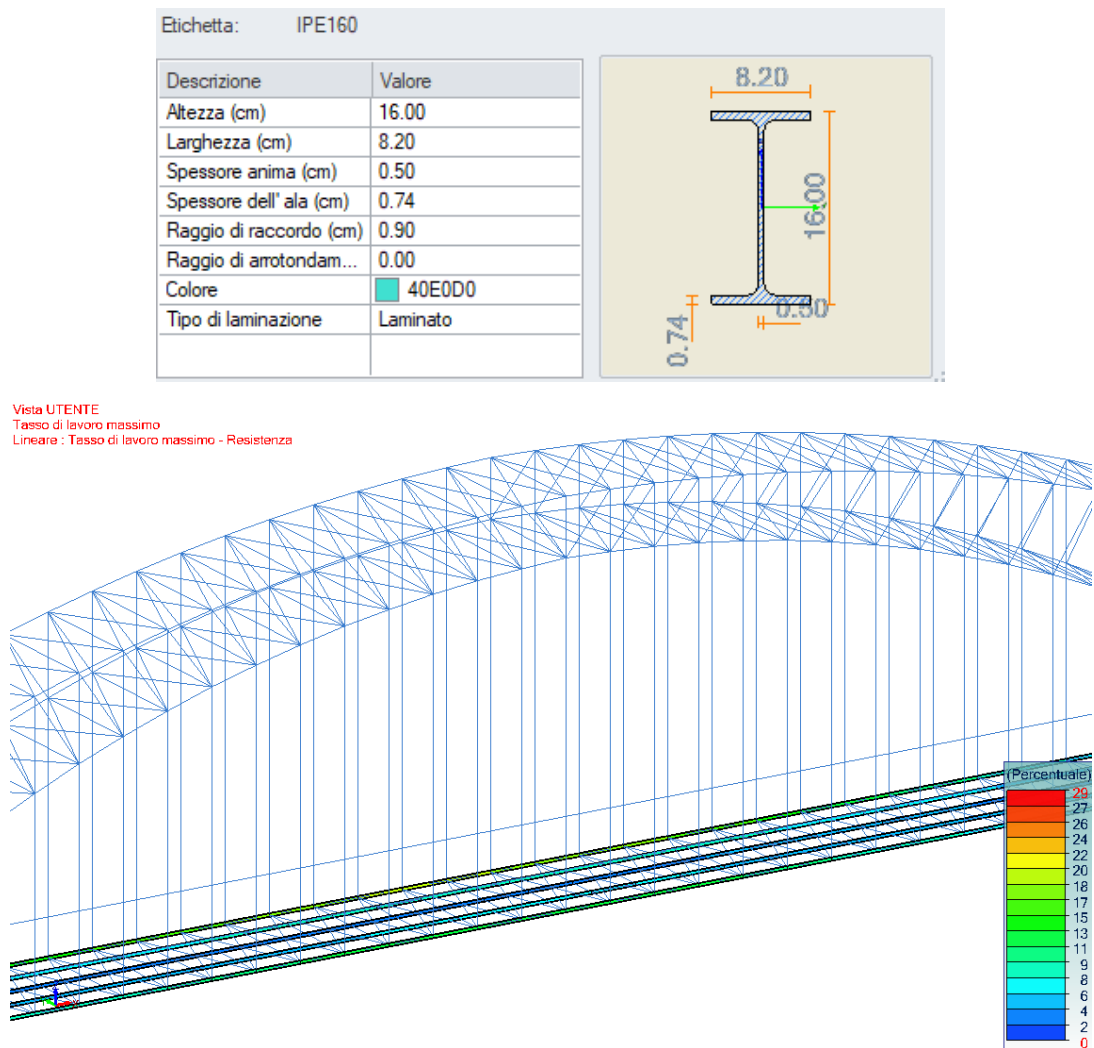


Figure 48:: Resistance utilization rate

	Caso sfavorevole	Sezione Classe	Verifica	Tasso di lav...
Trazione Compressione (6.2.3)	n°138	Classe 1	$F_x < N_{t,Rd}$ $766.62 < 2639.89 \text{ kN}$	29%
Taglio in direzione Y (6.2.6)	n°146	Classe 1	$F_y < V_{ply}$ $1.29 < 1218.63 \text{ kN}$	0%
Taglio in direzione Z (6.2.6)	n°146	Classe 1	$F_z < V_{plz}$ $8.19 < 484.70 \text{ kN}$	2%
Flessione su Y-Y (4.2.4.1.2.3)	n°146	Classe 1	$M_{y,Ed} < M_{y,Rd}$ $5.53 < 217.24 \text{ kN}\cdot\text{m}$	3%
Flessione su Z-Z (4.2.4.1.2.3)	n°146	Classe 1	$M_{z,Ed} < M_{z,Rd}$ $0.88 < 103.39 \text{ kN}\cdot\text{m}$	1%
Flessione in Y-Y e sforzo normale (6.2.9)	n°146	Classe 1	$M_{y,Ed} < M_{N,y,Rd} \text{ (6.31)}$ $5.53 < 192.48 \text{ kN}\cdot\text{m}$	3%
Flessione in Z-Z e sforzo normale (6.2.9)	n°138	Classe 1	$M_{z,Ed} < M_{N,z,Rd} \text{ (6.31)}$ $0.53 < 102.79 \text{ kN}\cdot\text{m}$	1%
Flessione deviata (6.2.9)	n°142	Classe 1	$(M_{y,Ed}/M_{N,y,Rd})^a + (M_{z,Ed}/M_{N,z,Rd})^b < 1 \text{ (6.41)}$ $0.01 < 1$	1%
Torsione St. Venant (...)	n°142	Classe 1	$M_x < W_t \cdot (F_y/3 \cdot (1/2)/gM0)$ $0.02 < 7.74 \text{ kN}\cdot\text{m}$	0%

Vista UTENTE
Tasso di lavoro massimo
Lineare : Tasso di lavoro massimo - Stabilità

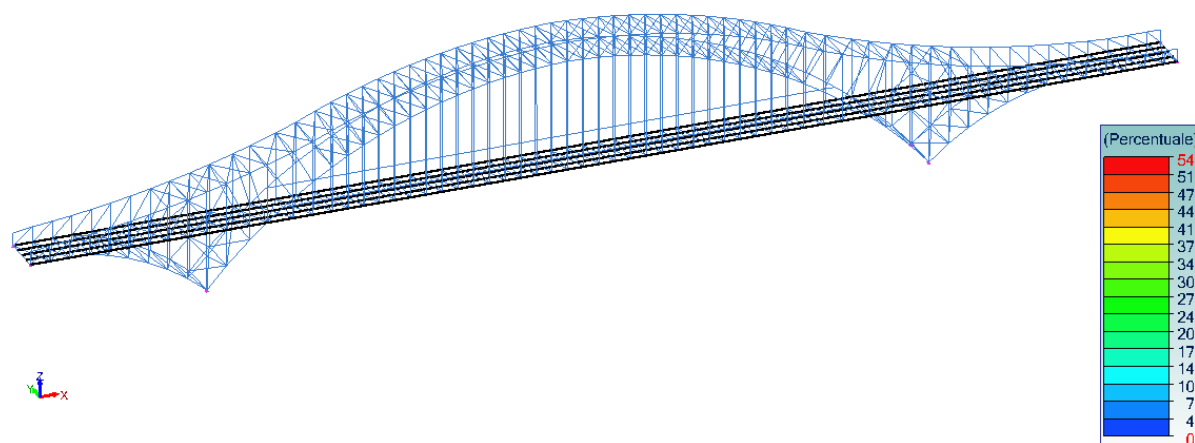


Figure 49: : Stability utilization rate

Scheda sezione - Elemento lineare no.1603	
Sezione	Freccia (10%)
Resistenza sezioni (8%)	Stabilità elementi (54%)
Stabilità e Resistenza al fuoco ()	
Instabilità Snell. E Lung.	$\Lambda_{Fy} = 0.649$ $\Lambda_{Fz} = 2.314$ $L_{fy} = 3.26 \text{ m}$ $L_{fz} = 3.26 \text{ m}$
Inst.flesso-torsionale	$\Lambda_{LT} = 1.324$ $L_{di} = 3.26 \text{ m}$ $L_{ds} = 3.26 \text{ m}$
Caso sfavorevole	Caso n°146 : $1.35x[1 \text{ G}] + 1.5x[2 \text{ G}] + 1.5x[9 \text{ V}] + 0.6x[4 \text{ Q}]$ Sezione : Classe 1
Fattore di amplificazione	$k_z = 1.00$ $k_w = 1.00$ $C_1 = 1.13$ $C_2 = 0.45$ $X_y = 0.87$ $X_z = 0.16$ $X_{LT} = 1.00$ $k_{yy} = 1.54$ $k_{yz} = 1.78$ $k_{zy} = 0.79$ $k_{zz} = 1.46$ $z_g = 0.00 \text{ m}$ $M_{cr} = 25.08 \text{ kN}\cdot\text{m}$ $M_{bRd} = 41.88 \text{ kN}\cdot\text{m}$ $N_{crT} = 792.87 \text{ kN}$
Verifica (6.61)	$\frac{N_{ed}}{(X_y N_{rk} / gM1)} + k_{yy} \left(\frac{M_{y,Ed} + DM_{y,Ed}}{(X_{LT} M_{y,Rk} / gM1)} + k_{yz} \left(\frac{M_{z,Ed} + DM_{z,Ed}}{(M_{z,Rk} / gM1)} \right) \right) < 1$ $0.093 + 0.048 + 0.016 = 0.157 < 1 \quad (16\%)$
Verifica (6.62)	$\frac{N_{ed}}{(X_z N_{rk} / gM1)} + k_{zy} \left(\frac{M_{y,Ed} + DM_{y,Ed}}{(X_{LT} M_{y,Rk} / gM1)} + k_{zz} \left(\frac{M_{z,Ed} + DM_{z,Ed}}{(M_{z,Rk} / gM1)} \right) \right) < 1$ $0.502 + 0.025 + 0.013 = 0.540 < 1 \quad (54\%)$

3.5.8 Hangers

The hangers were designed using solid round bars with a diameter of six centimeters.

In the structural analysis software, they were modeled as tie rods, and therefore only tensile checks were carried out.

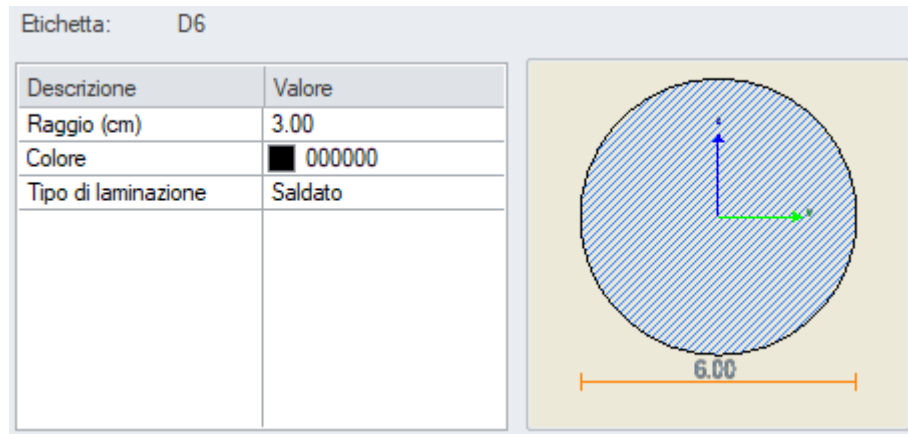


Figure 50: Circular section taken from Advance Design profiler

Vista FRONTALE
 Analisi: 138 (1.35x[1 G]+1.5x[2 G]+1.5x[4 Q]+0.9x[9 V])
 Lineare : Fx
 Assi locali

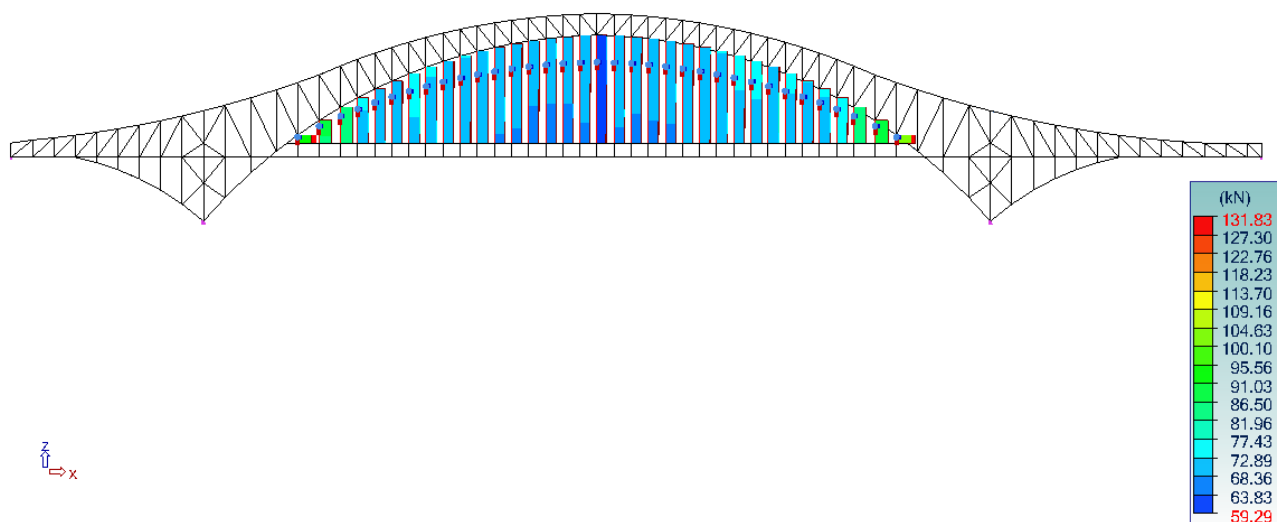


Figure 51: Axial force acting on hangers

Vista FRONTALE
Tasso di lavoro massimo
Lineare : Tasso di lavoro massimo - Resistenza

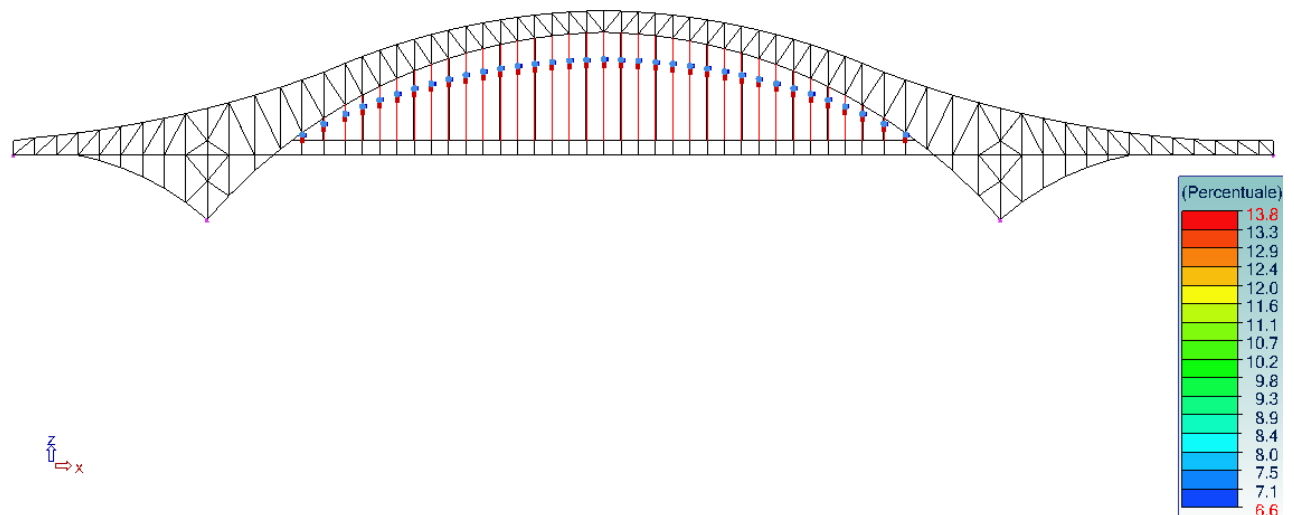


Figure 52: : Resistance utilization rate

$$N_{Ed} := 131,83 \text{ kN}$$

Design axial force

$$\gamma_{M0} := 1,05$$

Partial safety coefficient

$$A = 28,27 \text{ cm}^2$$

Section area

$$f_{yk} := 355 \text{ MPa}$$

Yield strength

$$N_{c,Rd} := \frac{A \cdot f_{yk}}{\gamma_{M0}} = 956 \text{ kN}$$

Plastic axial resistance

$$\rho := \frac{N_{Ed}}{N_{c,Rd}} = 0,14$$

Utilization ratio

	Caso sfavore...	Sezione Classe	Verifica	Tasso di l...
Trazione Compressione (6.2.3)	n*138	Classe 1	$F_x < N_{t,Rd}$ $131.83 < 955.94 \text{ kN}$	14%

Stability verification is not required for these elements, since they are subjected to axial tension only and therefore not susceptible to instability phenomena.

To take a further step in BIM-based design, a search was carried out for companies manufacturing tie rod systems. The choice fell on Macalloy, a company specialized in the production of high-strength

steel tie rods and post-tensioning systems. Macalloy provides not only the tie rods themselves but the entire suspension system, which is verified in-house. An additional advantage is that the company supplies both .dwg and .rvt files, facilitating integration into BIM workflows. Below is the technical data sheet of one of their products.

Macalloy 460 Carbon Bars.

The Macalloy 460 bar has the following mechanical properties:

- Minimum Yield Stress 460 N/mm²
- Minimum Breaking Stress 610 N/mm²
- Minimum Elongation 19%
- Minimum charpy Impact Value 27J @-20°C
- Nominal Young's Modulus 205 kN/mm²

The standard diameter range for this system is from M10 to M100. In addition, other diameters can be supplied but are subject to longer lead times. Tendons up to and including M16 diameters can be supplied in lengths of 6m. For larger diameter, lengths of up to 11.95m are available. Greater lengths are possible using couplers and turnbuckles. These fittings are designed to take the full load of the bar.

Adjustments within each fork or spade are:

- M10 to M56: +/- 1/2 thread diameter
- M64 to M100: +/-25mm

Turnbuckles give additional adjustments of:

- M10 to M24: +/-25mm
- M30 to M100: +/-50mm

Special turnbuckles, with a greater adjustment are available on request. [Contact a Macalloy agent today](#) to or use our live chat option to discuss your requirements.

TABLE 1					
Product Name	Material	Characteristic Yield Stress N/mm ²	Ultimate Tensile Stress N/mm ²	Min. Elongation %	Min. Charpy Impact J@-20°C
Macalloy 460	Carbon Steel	460	610	19	27

TABLE 5																					
TENDON CAPACITIES FOR CARBON AND *STAINLESS 550																					
THREAD (CARBON)	M10	M12	M16	M20	M24	M30	M36	M42	M48	M56	M64	M70	M76	M80	M85	M90	M95	M100	M105	M110	M120
THREAD (STAINLESS)	M10	M12	M16	M20	M24	M30	M36	M42	M48	M56	M64	M70	M76	*CONTACT MACALLOY FOR FURTHER DETAILS							
Nominal Bar Dia. (mm)	10	11	15	19	22	28	34	39	44	52	59	67	71	78	83	87	93	98	103	110	120
Design Resistance to EC3 NR,d (kN)	27	40	75	119	171	273	399	549	723	999	1319	1608	1924	2152	2453	2775	3114	3475	3856	4257	5117
Min. Yield Load (kN)	30	44	82	129	186	298	435	599	789	1090	1439	1754	2100	2348	2677	3028	3399	3792	4208	4645	5584
Min. Break Load (kN)	38	56	104	165	237	379	554	763	1004	1387	1832	2233	2673	2988	3407	3854	4325	4827	5356	5912	7107
Nominal Bar Weight (kg/m)	0.6	0.8	1.5	2.5	3.1	5.2	7.3	9.9	12.5	16.7	22.2	27.7	32.9	37.5	42.5	49.9	53.3	59.2	68.0	74.6	88.8

Tension Bars

The Macalloy tension structures range includes a 460N/mm², 520N/mm² and the new 550N/mm², available in carbon and stainless steel. For more details, please refer to the data sheet.

All systems are ISO 9001 accredited and meet European technical approval document ETA 21/0053, which is available on request.

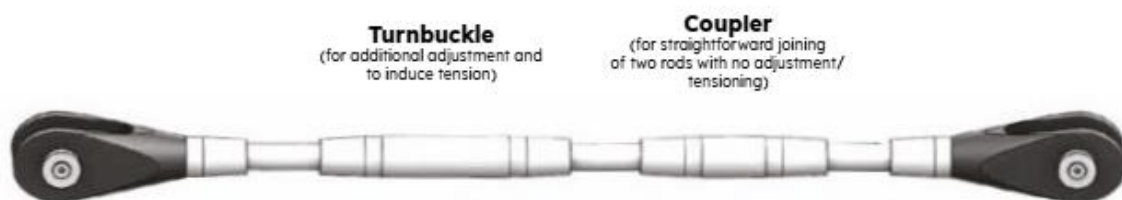
Carbon bars can be supplied primed and ready for paint, painted, powder-coated or hot-dipped/galvanised to BS EN 1461:2009.

Fittings are designed to give the maximum amount of flexibility and adjustment, and special fittings can be designed to suit customer requirements.

All fittings (forks, pins, turnbuckles, couplers and lock covers) are supplied with a galvanised coating.

Cast fittings are UT and MPI tested in accordance with European technical approval – ETA21/0053.

FINAL ASSEMBLY EXAMPLE



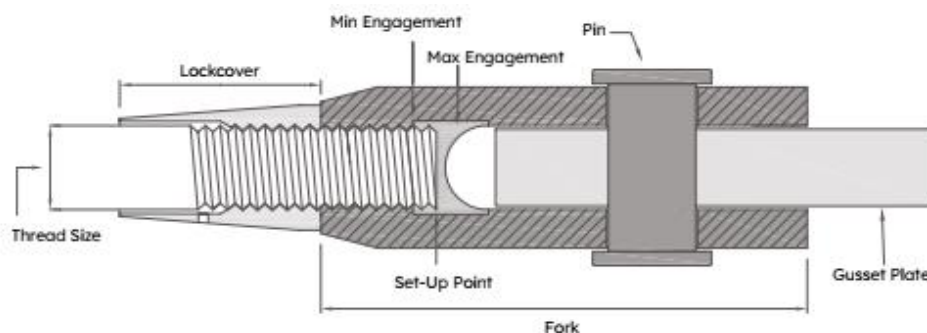
FORK ADJUSTMENT AND SET UP POINTS

Fork Adjustment – M10 to M56: +/- ½ thread diameter in each fork end.

Fork Adjustment – M64 to M105: +/- 25 mm in each fork end.

Set-Up Point – M10 to M56: 1 ½ x thread diameter in each fork end.

Set-Up Point – M64 to M105: 1 x thread diameter plus 25mm in each fork end.



TURNBUCKLE ADJUSTMENT AND SET UP POINTS

Turnbuckle Adjustment – M10 to M24: +/- 25mm.

Turnbuckle Adjustment – M30 to M105: +/- 50mm.

Set-Up Point – M10 to M24: 1 x thread diameter +12.5mm in each end of the turnbuckle.

Set-Up Point – M30 to M105: 1 x thread diameter + 25mm in each end of the turnbuckle.

3.5.9 Timber decking

The final element to be verified is the timber decking, positioned on the top flange of the deck structure. It is fastened to the secondary IPE beams using self-drilling screws, in order to make the walkway accessible.

The material chosen is chestnut wood; it is valued for its durability, resistance to moisture, and is easy to work with. Due to its high tannin content, chestnut wood is naturally resistant to weathering and pests, even without chemical treatment.

The corresponding verification is presented below.

$h := 5 \text{ cm}$	thickness
$b := 20 \text{ cm}$	width
$I := \frac{b \cdot h^3}{12} = 208 \text{ cm}^4$	moment of inertia
$W := \frac{b \cdot h^2}{6} = 83 \text{ cm}^3$	resistant modulus
$L := 1,5 \text{ m}$	length
$A := b \cdot L = 0,3 \text{ m}^2$	area
$\rho_k := 4,6 \frac{\text{kN}}{\text{m}^3}$	characteristic density
$G_1 := h \cdot b \cdot \rho_k = 0,05 \frac{\text{kN}}{\text{m}}$	dead load
$Q := 5 \frac{\text{kN}}{\text{m}^2} \quad q := Q \cdot b = 1 \frac{\text{kN}}{\text{m}}$	variable load
$\gamma_G := 1,35 \quad \gamma_Q := 1,5$	safety coefficients
$q_{tot} := \gamma_G \cdot G_1 + \gamma_Q \cdot q = 1,56 \frac{\text{kN}}{\text{m}}$	total load
$M_{Ed} := 0,1 \cdot q_{tot} \cdot L^2 = 0,35 \text{ kN m}$	bending moment
$\sigma_{Ed} := \frac{M_{Ed}}{W} = 4,22 \text{ MPa}$	bending stress
$f_{m,k} := 28 \text{ MPa}$	characteristic bending strength

$f_{m,k} := 28 \text{ MPa}$ characteristic bending strenght

$k_{mod} := 0,6$ correction factor

$\gamma := 1,5$ safety material factor

$f_d := \frac{f_{m,k} \cdot k_{mod}}{\gamma} = 11,2 \text{ MPa}$ design bending strength

$\frac{\sigma_{Ed}}{f_d} = 0,38$ work ratio

$V_{Ed} := 1,14 \cdot q_{tot} \cdot L = 2,67 \text{ kN}$ shear force

$\tau_{Ed} := V_{Ed} \cdot \frac{W}{I \cdot b} = 0,53 \text{ MPa}$ shear stress

$f_{v,k} := 2 \text{ MPa}$ shear strenght

$f_{v,d} := \frac{f_{v,k} \cdot k_{mod}}{\gamma} = 0,8 \text{ MPa}$ design shear strength

$\frac{\tau_{Ed}}{f_{v,d}} = 0,67$ work ratio

$f := \frac{5 \cdot (G_1 + q) \cdot L^4}{384 \cdot E_{0,mean} \cdot I} = 3 \text{ mm}$

$f_{lim} := \frac{L}{200} = 8 \text{ mm}$

The working rate is less than one at both bending moment and shear, and the deformations are acceptable, so it is considered verified.

3.6 SLS verifications

Deflection Check

The pedestrian bridge under design is a steel arch structure with a free span of 100 m. In accordance with the provisions of the Italian Building Code (NTC 2018, § 4.1.10.1.2) and the Explanatory Circular No. 7/2019, the vertical deflection has been verified at the Serviceability Limit State (SLS).

As the bridge is exclusively for pedestrian use, reference is also made to the recommendations in Eurocode EN 1993-2, Annex C, which suggest limiting vertical deflections to values between $L/300$ and $L/500$. In this project, a conservative limit of $L/500$ was adopted.

Thus, the maximum allowable deflection is:

$$f_{\max} = 100 \text{ m} / 500 = 20 \text{ cm}$$

From numerical analysis under SLS load combinations (permanent + pedestrian live loads), the calculated vertical deflection is:

$$f_{\text{calculated}} = 17 \text{ cm}$$

Since $f_{\text{calculated}} \leq f_{\max}$ the deflection check is satisfied.

Vista UTENTE
Analisi: 168 (1x[1 G]+1x[2 G]+1x[5 V]+0.8x[3 N]+0.4x[4 Q])
Lineare : D
Assi locali

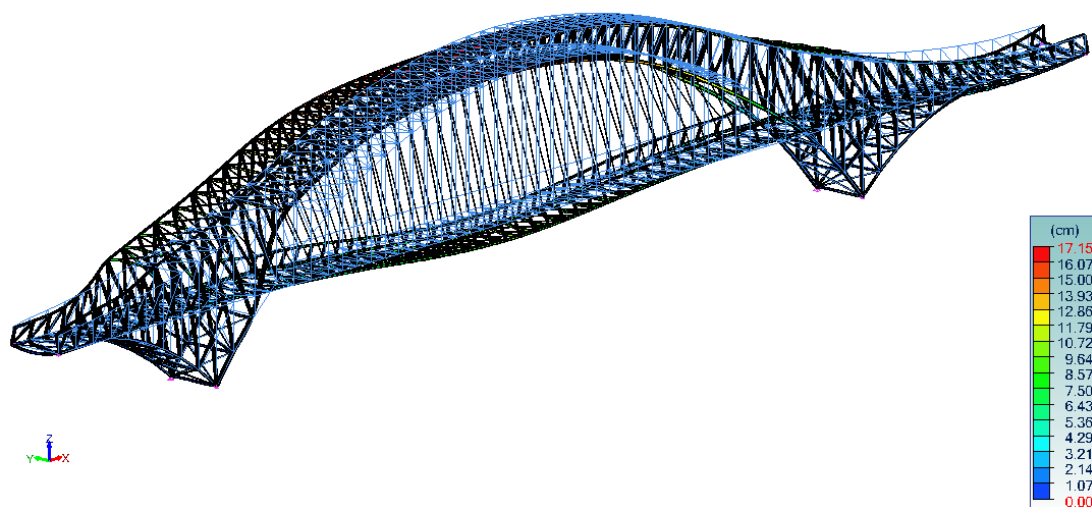


Figure 53: Displacements under SLE combination

3.7 Human comfort

The issue of vibrations induced by the dynamic interaction between pedestrians and structures represents a significant concern for footbridges, particularly those of more recent construction. The use of innovative materials has enabled the design of increasingly slender and flexible structures, which can be more susceptible to dynamic excitation. Among the most well-known examples is the Millennium Bridge in London, inaugurated on June 10, 2000, but closed just a few days later due to vibration issues. The bridge swayed unexpectedly when crowded with pedestrians, as a result of a pedestrian-induced resonance phenomenon. This phenomenon is called “Lock in”, by which a pedestrian crowd, with frequencies randomly distributed around an average value and with random phase shifts, will gradually coordinate at common frequency (that of the footbridge) and enters in phase with the footbridge motion. The phenomenon can be attributed to the instinctive response of pedestrians, who tend to adjust their walking pace upon perceiving the lateral oscillations of the footbridge, which begin to cause discomfort. In the attempt to maintain balance, they unconsciously synchronize their walking frequency with that of the structural motion. This behaviour induces a resonance effect, which becomes progressively amplified as more individuals follow the same pattern. Theoretically, this can lead to large-scale synchronization within the crowd, further exacerbating the problem. In practice, however, the degree of synchronization is generally limited. Moreover, when the amplitude of the footbridge's motion reaches a level that impairs the ability to walk safely, pedestrians are forced to stop, thereby interrupting the development of the phenomenon.

Therefore to prevent the structure from being perceived as unstable or unsafe, thereby discouraging its use, it is essential to thoroughly assess the effects of dynamic phenomena induced by pedestrian traffic.

According to EN 1990:2002 + A1:2005/AC:2010 – Annex A2, supported by Eurocode EN 1991-2 and EN 1993-2, the fundamental vertical frequency must be ≥ 5 Hz to avoid resonance with walking frequencies ($\sim 1.6\text{--}2.4$ Hz), and the fundamental lateral frequency must be ≥ 2.5 Hz. However, the Eurocodes adopt a highly conservative approach, setting vibration limits that are significantly high in order to ensure that resonance conditions are safely avoided. Nevertheless, they do not provide detailed guidance on the effects of lower-level vibrations. In practice, it is often difficult—if not impossible—to comply with these stringent limits. For this reason, and to enable a more detailed analysis, reference is made to the following standard, which specifically addresses the vibration behaviour of pedestrian footbridges: “Sétra - Technical guide. Footbridges: Assessment of vibration behaviour of footbridges (October 2006)”.

3.7.1 Pedestrian loading

Pedestrian loading—whether due to walking or running—has been extensively investigated. Although several parameters can influence and alter the nature of this load, experimental data confirm that it exhibits a predominantly periodic behavior. This periodicity is characterized by a fundamental parameter: the frequency, defined as the number of steps per second. Estimated values for this frequency are reported in Table 1.1.

Designation	Specific features	Frequency range (Hz)
Walking	Continuous contact with the ground	1.6 to 2.4
Running	Discontinuous contact	2 to 3.5

Under conventional assumptions for normal, unobstructed walking, the step frequency can be modeled using a Gaussian distribution with a mean value of approximately 2.0 Hz and a standard deviation around 0.20 Hz (ranging from 0.175 Hz to 0.22 Hz, depending on the reference source). However, recent studies and experimental investigations suggest slightly lower average frequencies, typically in the range of 1.8 Hz to 1.9 Hz.

The periodic force function, denoted as $F(t)$, can be expressed as a Fourier series—consisting of a constant component plus an infinite series of harmonic terms. The combined effect of the periodic action is obtained by summing all unit contributions of these harmonics.

$$F(t) = G_0 + G_1 \sin 2\pi f_m t + \sum_{i=2}^{\infty} G_i \sin(2\pi i f_m t - \varphi_i)$$

with

- G_0 : static force (pedestrian weight for the vertical component),
- G_1 : first harmonic amplitude,
- G_i : i-th harmonic amplitude,
- f_m : walking frequency,
- φ_i : phase angle of the i-th harmonic in relation to the first one,
- n : number of harmonics taken into account.

For practical design purposes, this force is typically resolved into three components: a vertical component, a longitudinal horizontal component (in the direction of motion), and a transverse horizontal component (perpendicular to the walking direction). The following values, generally limited to the first harmonic, are recommended for use in structural dimensioning.

Vertical component of one-pedestrian load:

$$F_v(t) = G_0 + 0,4 G_0 \sin(2\pi f_m t)$$

Transverse horizontal component of one-pedestrian load:

$$F_{ht}(t) = 0,05 G_0 \sin\left(2\pi \left(\frac{f_m}{2}\right) t\right)$$

Longitudinal horizontal component of one-pedestrian load:

$$F_{hl}(t) = 0,2 G_0 \sin(2\pi f_m t)$$

It is important to highlight that, during a single walking cycle, the frequency of the transverse load is half that of the vertical and longitudinal loads. This difference arises from the nature of how forces are applied. In the vertical and longitudinal directions, each individual step—left or right—generates a force in the same direction, making the load period equal to the time interval between two consecutive steps. In contrast, the transverse load is influenced by alternating left and right steps, which apply forces in opposite directions. As a result, a complete period for the transverse load corresponds to two consecutive steps of the same foot (e.g., two right or two left steps). Consequently, the period of the transverse load is twice that of the vertical and longitudinal components, and therefore its frequency is half as high.

In real-world conditions, footbridges are subjected to the simultaneous actions of multiple pedestrians, significantly increasing the complexity of the resulting dynamic response. Each pedestrian is characterized by distinct parameters—such as weight, walking frequency, and speed—which contribute to a non-uniform and variable loading pattern. Depending on the number of individuals present on the structure, the loads they induce may exhibit varying degrees of synchrony, both among themselves and with the dynamic response of the footbridge. Furthermore, initial phase differences arise from the staggered entry times of pedestrians, introducing additional variability in the overall loading scenario. As a result, accurately simulating the actual dynamic action of a crowd remains highly challenging.

Given the complexity of crowd dynamics, it is only possible to adopt reasonable and simplifying assumptions, grounded in studies of pedestrian behaviour. Typically, the overall effect of the crowd is estimated by scaling the elementary response induced by a single pedestrian, potentially adjusted by a reduction factor to account for desynchronization or variability. Various conceptual approaches to modeling crowd effects have been proposed, many of which were developed prior to the well-known Solférino and Millennium Bridge incidents.

The following section presents these concepts in detail, along with a more comprehensive statistical analysis, which serves as the foundation for the loading recommendations proposed in Setra guidelines.

Fundamentally, the approach consists in determining an equivalent number of pedestrians, N_{eq} , uniformly distributed and synchronized with the natural frequency of the structure, capable of

generating dynamic effects comparable to those produced by a random distribution of real pedestrians.

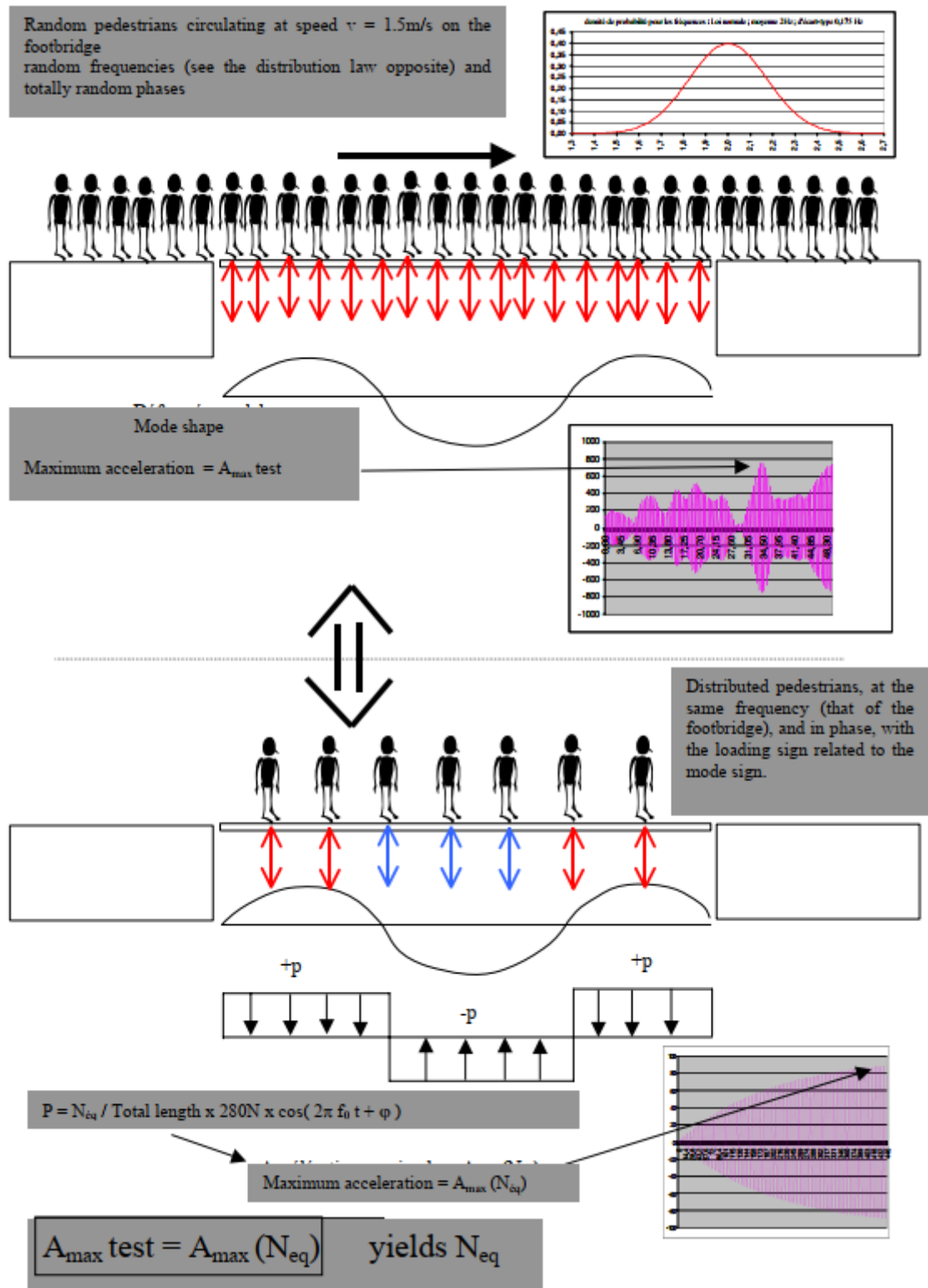


Figure 54: Methodology for calculating the equivalent number of pedestrians

This model is significantly simplified for calculation purposes. It requires only the distribution of N_{eq} pedestrians along the bridge, the application of a force to each pedestrian with a sign consistent with the corresponding mode shape, and the assumption that this force is applied at the natural frequency of the structure. The resulting maximum acceleration is then computed at resonance.

3.7.2 Workflow

The methodology proposed by Setra Guidelines is summarised in the organisation chart below.

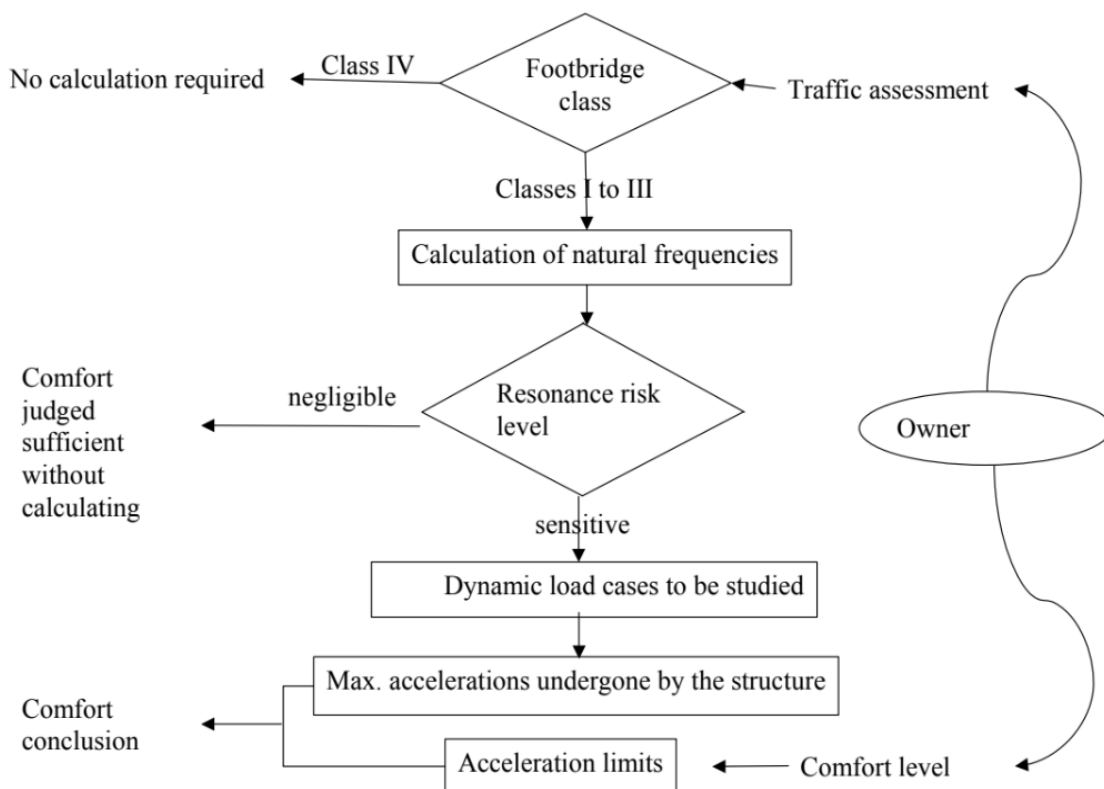


Figure 55: Methodology organization chart

As can be seen, the first step is the determination of the footbridge class. Each classification corresponds to a specific level of pedestrian traffic.

“Class IV: seldom used footbridge, built to link sparsely populated areas or to ensure continuity of the pedestrian footpath in motorway or express lane areas.

Class III: footbridge for standard use, that may occasionally be crossed by large groups of people but that will never be loaded throughout its bearing area.

Class II: urban footbridge linking up populated areas, subjected to heavy traffic and that may occasionally be loaded throughout its bearing area.

Class I: urban footbridge linking up high pedestrian density areas (for instance, nearby

presence of a rail or underground station) or that is frequently used by dense crowds (demonstrations, tourists, etc.), subjected to very heavy traffic.

It is for the Owner to determine the footbridge class as a function of the above information and taking into account the possible changes in traffic level over time.”

The selection of the appropriate class may also be influenced by additional criteria the designer chooses to consider. For example, opting for a higher class can enhance the structure’s resistance to vibrations, which may be desirable in contexts with heightened public or media sensitivity. Conversely, a lower class may be deemed acceptable in order to reduce construction costs or to allow greater architectural freedom. In such cases, the associated risk is typically limited to the possibility that, under exceptional conditions—when pedestrian traffic and intensity exceed typical levels—some users may experience discomfort.

Footbridges classified as Class IV are generally considered exempt from the need for dynamic performance verification. However, for very lightweight footbridges, it is advisable to adopt at least a Class III classification to ensure a basic level of vibration control. This recommendation arises from the fact that lightweight structures may experience significant accelerations even in the absence of resonance phenomena. In accordance with the established classification criteria, the footbridge under consideration is designated as Class III.

3.7.3 Dynamic analysis

The second step is the calculation of natural frequencies. These frequencies concern vibrations in each of 3 directions: vertical, transverse horizontal and longitudinal horizontal. To this end, a modal analysis of the structure is performed. This analysis consists in identifying the natural vibration modes of the structure, along with their corresponding periods, frequencies, and modal masses—parameters that fundamentally govern the overall dynamic behavior of the footbridge. The modal analysis is carried out using the structural analysis software Advance Design. In order to initiate the analysis, it is necessary to define the dynamic mass, that is the portion of the structure’s mass (and thus the loads) that is effectively involved in the response to dynamic actions. The guideline proposes two mass assumptions: empty footbridge (only dead load and permanent loads) and footbridge loaded throughout its bearing area, to the tune of one 700 N pedestrian per square metre (70 kg/m²). Since the study on human comfort specifically concerns pedestrian crossing on the footbridge, the frequency values obtained under a pedestrian load of 0.7 kN/m² are reported below, directly from the software report.

<i>Modal values</i>								
<i>Modo N°</i>	<i>Angular frequency (Rad/s)</i>	<i>Period (s)</i>	<i>frequency (Hz)</i>	<i>Energy (J)</i>	<i>Modal masses</i>			<i>Dam ping (%)</i>
					<i>X T (%)</i>	<i>Y T (%)</i>	<i>Z T (%)</i>	
1	5.05	1.25	0.80	12.73	0.00 (0.00)	250.59 (59.82)	0.00 (0.00)	4
2	7.35	0.86	1.17	26.99	0.00 (0.00)	23.10 (5.51)	0.00 (0.00)	4
3	10.49	0.60	1.67	55.06	153.13(36.5)	0.00 (0.00)	0.75 (0.18)	4
4	10.83	0.58	1.72	58.66	0.08 (0.02)	0.82 (0.20)	0.00 (0.00)	4
5	15.50	0.41	2.47	120.12	0.00 (0.00)	0.29 (0.07)	0.00 (0.00)	4
6	16.80	0.37	2.67	141.08	0.00 (0.00)	0.00 (0.00)	135.8(32.43)	4
7	19.08	0.33	3.04	181.98	0.00 (0.00)	88.24 (21.06)	0.00 (0.00)	4
8	20.96	0.30	3.34	219.74	0.03 (0.01)	2.17 (0.52)	0.01 (0.00)	4
9	21.78	0.29	3.47	237.09	132.6(31.66)	0.00 (0.00)	0.03 (0.01)	4
10	23.03	0.27	3.67	265.20	0.00 (0.00)	0.37 (0.09)	0.00 (0.00)	4
11	24.81	0.25	3.95	307.76	0.00 (0.00)	8.45 (2.02)	0.00 (0.00)	4
12	25.75	0.24	4.10	331.40	12.49 (2.98)	0.00 (0.00)	4.00 (0.95)	4
13	27.47	0.23	4.37	377.17	0.00 (0.00)	6.91 (1.65)	0.01 (0.00)	4
14	27.70	0.23	4.41	383.64	3.42 (0.82)	0.00 (0.00)	69.78(16.66)	4
15	28.79	0.22	4.58	414.54	0.00 (0.00)	2.92 (0.70)	0.01 (0.00)	4
16	28.84	0.22	4.59	415.85	0.68 (0.16)	0.00 (0.00)	15.02 (3.58)	4
17	29.97	0.21	4.77	449.11	0.05 (0.01)	0.00 (0.00)	3.00 (0.72)	4
18	31.30	0.20	4.98	489.87	0.02 (0.00)	0.00 (0.00)	1.36 (0.33)	4
19	32.06	0.20	5.10	514.02	0.00 (0.00)	1.10 (0.26)	0.00 (0.00)	4
20	32.65	0.19	5.20	533.04	0.00 (0.00)	0.01 (0.00)	2.67 (0.64)	4
21	33.70	0.19	5.36	567.81	0.01 (0.00)	0.04 (0.01)	2.41 (0.58)	4
22	34.58	0.18	5.50	597.93	0.02 (0.00)	0.01 (0.00)	2.70 (0.64)	4
23	34.63	0.18	5.51	599.58	0.00 (0.00)	5.80 (1.38)	0.02 (0.01)	4
24	35.89	0.18	5.71	643.88	0.21 (0.05)	0.38 (0.09)	0.47 (0.11)	4
25	37.33	0.17	5.94	696.78	1.99 (0.48)	1.14 (0.27)	0.60 (0.14)	4
26	37.62	0.17	5.99	707.69	1.41 (0.34)	1.21 (0.29)	1.40 (0.34)	4
27	38.21	0.16	6.08	729.85	9.42 (2.25)	0.00 (0.00)	1.98 (0.47)	4
28	41.06	0.15	6.53	842.93	0.44 (0.10)	0.39 (0.09)	6.92 (1.65)	4
29	42.23	0.15	6.72	891.75	0.02 (0.01)	1.86 (0.44)	2.31 (0.55)	4
30	43.99	0.14	7.00	967.71	2.07 (0.49)	0.12 (0.03)	0.01 (0.00)	4
31	46.06	0.14	7.33	1060.99	3.25 (0.78)	0.23 (0.05)	19.89 (4.75)	4
32	48.67	0.13	7.75	1184.33	2.12 (0.51)	0.21 (0.05)	35.70 (8.52)	4
33	51.79	0.12	8.24	1341.32	19.04 (4.55)	0.00 (0.00)	4.41 (1.05)	4
34	52.94	0.12	8.43	1401.18	0.16 (0.04)	2.04 (0.49)	2.77 (0.66)	4
35	58.61	0.11	9.33	1717.35	0.20 (0.05)	0.77 (0.18)	18.12 (4.33)	4
36	62.13	0.10	9.89	1929.88	19.07 (4.55)	1.52 (0.36)	2.54 (0.61)	4
37	62.29	0.10	9.91	1939.94	19.83 (4.73)	1.67 (0.40)	1.53 (0.36)	4
38	70.09	0.09	11.16	2456.54	0.00 (0.00)	0.23 (0.05)	9.84 (2.35)	4
39	70.75	0.09	11.26	2502.65	11.32 (2.70)	0.01 (0.00)	0.03 (0.01)	4
40	86.76	0.07	13.81	3763.50	0.03 (0.01)	3.50 (0.84)	0.38 (0.09)	4
41	92.95	0.07	14.79	4320.12	7.01 (1.67)	0.01 (0.00)	0.02 (0.01)	4
42	100.96	0.06	16.07	5096.61	0.04 (0.01)	0.06 (0.01)	26.83 (6.41)	4
43	127.54	0.05	20.30	8133.38	11.09 (2.65)	0.00 (0.00)	0.01 (0.00)	4
44	133.72	0.05	21.28	8940.97	0.00 (0.00)	7.65 (1.83)	0.53 (0.13)	4
45	157.55	0.04	25.07	12410.88	0.00 (0.00)	0.10 (0.02)	29.32 (7.00)	4
46	271.35	0.02	43.19	36816.40	5.41 (1.29)	0.00 (0.00)	0.00 (0.00)	4
Total				107797	416.71 (99.48)	413.94 (98.82)	403.30 (96.28)	

The first three vibration modes are highlighted in yellow; these are the ones that excite the largest percentage of mass along the y, x, and z directions, respectively. The three modes are graphically shown here.

Vista UTENTE
 Modo 1 Periodo (s) = 1.25 Pulsazione (Rad/s) = 5.05 Freqenza (Hz) = 0.80

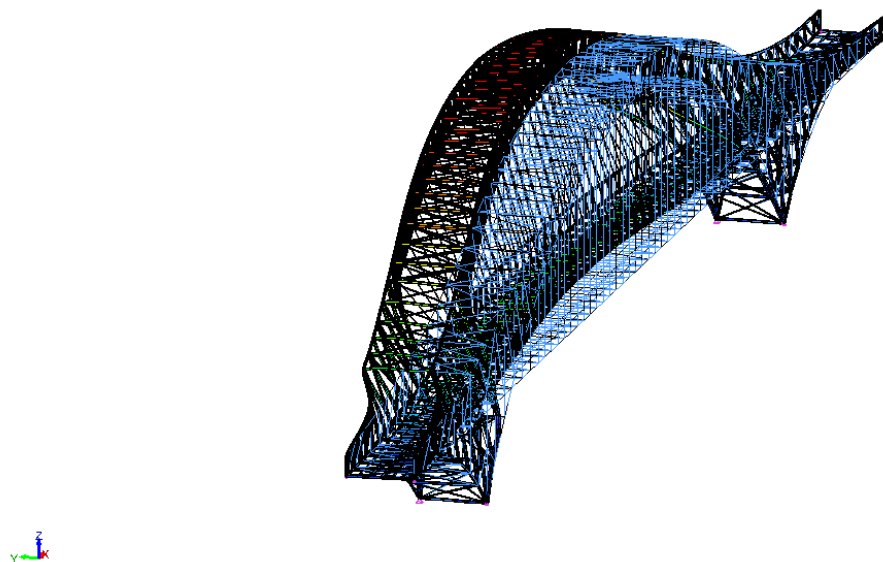


Figure 56: First mode of vibration

Vista UTENTE
 Modo 3 Periodo (s) = 0.60 Pulsazione (Rad/s) = 10.49 Freqenza (Hz) = 1.67

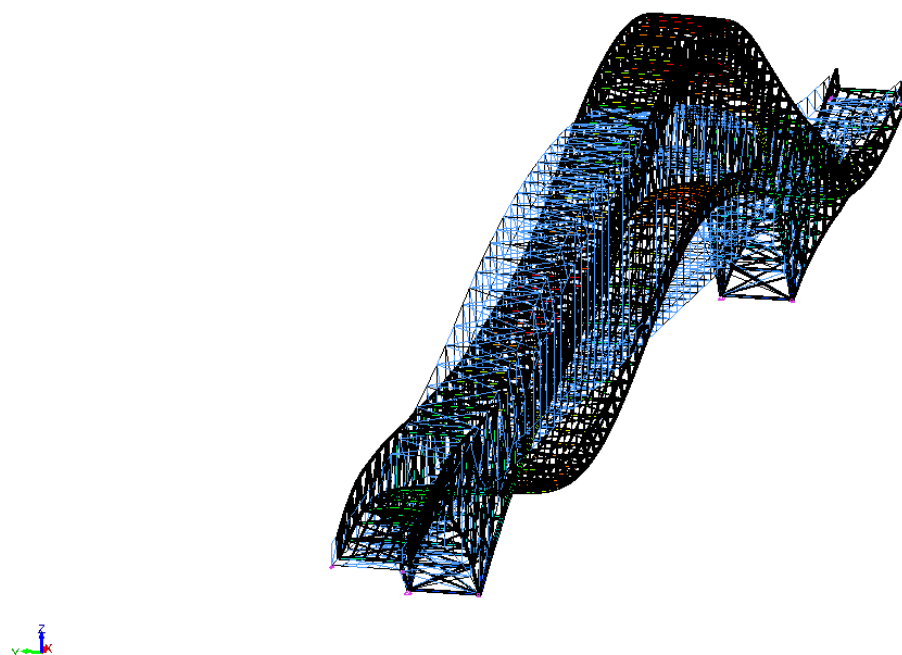


Figure 57: Second mode of vibration

Vista UTENTE
 Modo 6 Periodo (s) = 0.37 Pulsazione (Rad/s) = 16.80 Frequenza (Hz) = 2.67

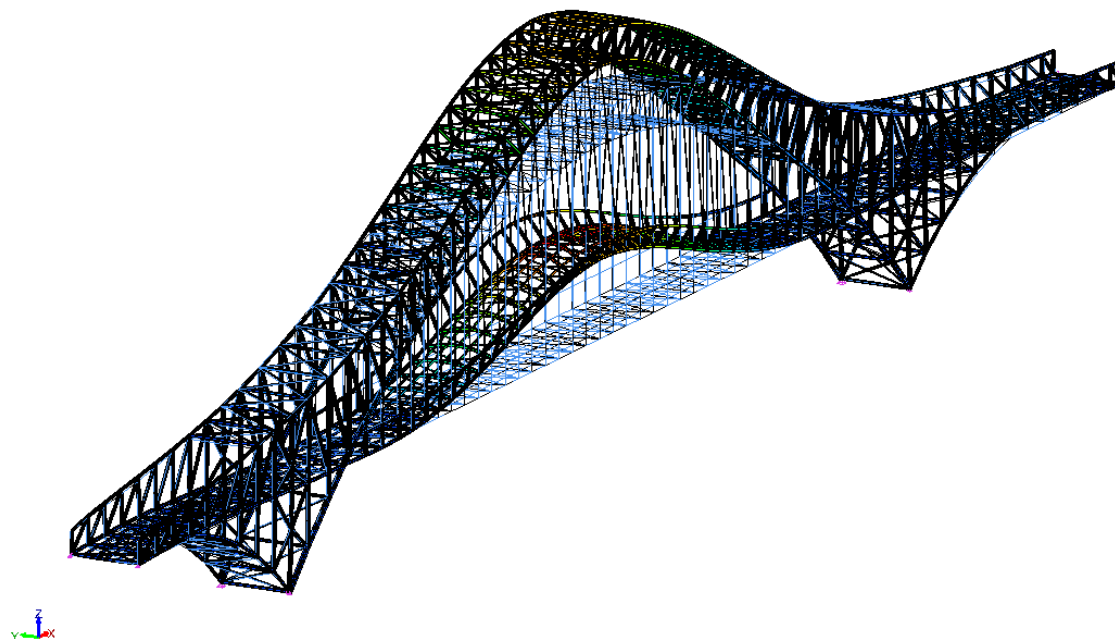


Figure 58: Third mode of vibration

Once the natural frequencies have been determined, the resonance risk level must be assessed. This is done by comparing the calculated frequencies with those provided in Table 2.3 and Table 2.4 of the Setra guidelines.

Frequency	0	1	1.7	2.1	2.6	5
Range 1						
Range 2						
Range 3						
Range 4						

Figure 59: Frequency ranges (Hz) of the vertical and longitudinal vibrations

Frequency	0	0.3	0.5	1.1	1.3	2.5
Range 1						
Range 2						
Range 3						
Range 4						

Figure 60: Frequency ranges (Hz) of the transverse horizontal vibrations

We can see defined four frequency ranges, noted 1, 2, 3 and 4 and represented in different colors, for vertical and horizontal vibrations respectively. In ascending order, the first 3 correspond to the maximum, medium and low risk of resonance. The 4th range corresponds to negligible risk of resonance, which corresponds to the frequencies' limits proposed by Eurocodes.

Mode	Frequency [Hz]	Range	Risk of resonance
Vertical vibrations	2,67	3	Low
Longitudinal vibrations	1.67	2	Medium
Transversal vibrations	0.80	1	High

Any higher mode falls within higher ranges; therefore, it is not necessary to study them.

Now that the ranges in which the natural frequencies of interest fall have been identified, it is necessary to determine whether dynamic verification is required and how it should be carried out. To this end, reference can be made to the table below, which indicates the type of dynamic load to be adopted based on the class of the footbridge and the range in which it falls.

		Load cases to select for acceleration checks		
Traffic	Class	Natural frequency range		
		1	2	3
Sparse	III	Case1	Nil	Nil
Dense	II		Case 1	Case 3
Very dense	I	Case 2	Case 2	Case 3

Case No. 1: Sparse and dense crowd Case No. 3: Crowd complement (2nd harmonic)
Case No. 2: Very dense crowd

It is recalled that the footbridge has been assigned to Class III. For the vertical and longitudinal modes, it falls within Ranges 2 and 3, respectively, which correspond to the 'Nil' cell—meaning no further dynamic analysis is required. The transverse mode, however, falls within Range 1 and therefore requires a dynamic analysis with Load Case No. 1 (Sparse and dense crowd). Nevertheless, both for educational purposes and safety considerations, it was decided to carry out the dynamic verification for all the principal modes.

The density of the crowd to be considered is uniformly distributed over the total area of the footbridge S and it's defined as:

Class	Density d of the crowd
III	0.5 pedestrians/m ²
II	0.8 pedestrians/m ²

The dynamic verification consists in ensuring that the acceleration of the footbridge does not exceed the established comfort threshold.

We can see defined four value ranges, noted 1, 2, 3 and 4, for vertical and horizontal accelerations respectively. In ascending order, the first 3 correspond to the maximum, mean and minimum comfort levels. The 4th range corresponds to uncomfortable acceleration levels that are not acceptable.

Acceleration ranges	0	0.5	1	2.5
Range 1	Max			
Range 2		Mean		
Range 3			Min	
Range 4				

Figure 61: Acceleration ranges (m/s²) for vertical vibrations

Acceleration ranges	0	0.1	0.15	0.3	0.8
Range 1	Max				
Range 2		Mean			
Range 3			Min		
Range 4					

Figure 62: Acceleration ranges (m/s²) for horizontal vibrations

As can be seen, for the horizontal vibrations the highest level of comfort is achieved with accelerations of less than 0.15 m/s², but it is recommended to limit them to 0.1 m/s² to avoid the “lock-in” effect explained before.

In order to calculate the accelerations, the load per unit area must be evaluated. The starting data are:

$L := 159 \text{ m}$ deck length

$d := 6 \text{ m}$ width deck

$S := L \cdot d = 954 \text{ m}^2$ area of the footbridge

$d_{\text{crowd}} := \frac{0,5}{2} \text{ m}$ density crowd uniformly distributed over the total area S

$\zeta := 0,004$ critical damping ratio

$N := S \cdot d_{\text{crowd}} = 477$ number of pedestrian

$P := 70 \text{ kg}$ pedestrian load

$m_{\text{pedestrial}} := \frac{N \cdot P}{L} = 210 \frac{\text{kg}}{\text{m}}$ $m_{\text{deck}} := \frac{244000}{L} \text{ kg} + G_2 \cdot 100 \cdot d \frac{\text{kg}}{\text{kN}} = 2106,59 \cdot \frac{1}{\text{m}} \text{ kg}$

$m_{\text{tot}} := m_{\text{pedestrial}} + m_{\text{deck}} = 2317 \frac{\text{kg}}{\text{m}}$ total linear mass

The damping factor depends on the material; CEB information bulletin No. 209 (Ref. [7]), an important summary document dealing with the general problem of structure vibrations, provides the following values:

Type of deck	Critical damping ratio	
	Minimum value	Average value
Reinforced concrete	0.8%	1.3%
Prestressed concrete	0.5%	1.0%
Metal	0.2%	0.4%
Mixed	0.3%	0.6%
Timber	1.5%	3.0%

The number of equivalent pedestrians, in other words the number of pedestrians who, being all at the same frequency and in phase, would produce the same effects as random pedestrians, in frequency and in phase is: $10,8 \times (\xi \times N)^{1/2}$. The load to be considered is adjusted by a reduction factor, denoted as ψ , which accounts for the decreasing likelihood of resonance as the footbridge's natural frequency moves away from critical frequency ranges. Specifically, the risk of resonance becomes negligible outside the 1.7–2.1 Hz range for vertical accelerations and the 0.5–1.1 Hz range for horizontal accelerations. The factor ψ drops to zero when the natural frequency is below 1 Hz for vertical action

and below 0.3 Hz for horizontal action. Similarly, it becomes zero beyond 2.6 Hz for vertical and 1.3 Hz for horizontal action.

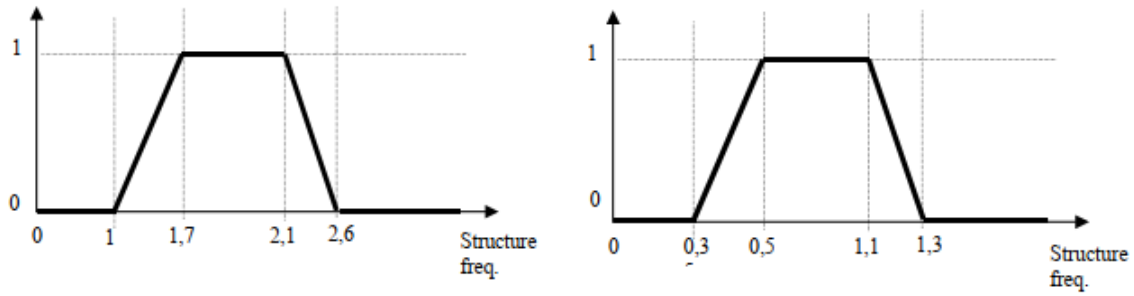


Figure 63: Values of factor ψ depending on frequencies

The load per unit area to be applied for each direction of vibration results to be:

Direction	Load per m ²
Vertical (v)	$d \times (280\text{N}) \times \cos(2\pi f_v t) \times 10.8 \times (\xi/n)^{1/2} \times \psi$
Longitudinal (l)	$d \times (140\text{N}) \times \cos(2\pi f_l t) \times 10.8 \times (\xi/n)^{1/2} \times \psi$
Transversal (t)	$d \times (35\text{N}) \times \cos(2\pi f_t t) \times 10.8 \times (\xi/n)^{1/2} \times \psi$

Where ξ represents the critical damping ratio (no unit) and n the number of pedestrians on the footbridge ($d \times S$). Here there are the calculations:

$$f_y := 0,80$$

$$\psi_y := 1$$

$$F_{s,y} := d_{\text{crowd}} \cdot 35 \text{ N} \cdot 10,8 \cdot \left(\frac{\xi}{N}\right)^{0,5} \cdot \psi_y \cdot \cos(2 \cdot \pi \cdot f_y) = 0,17 \text{ Pa}$$

$$F_{1,y} := F_{s,y} \cdot d = 1,01 \frac{\text{N}}{\text{m}}$$

The actual acceleration of the footbridge can be calculated as follows:

$$a_y := \frac{F_{1,y}}{\pi \cdot m_{\text{tot}}} \cdot \frac{4}{2 \cdot \xi} = 0,07 \frac{\text{m}}{\text{s}^2}$$

The analytically calculated acceleration is less than 0.10 m/s^2 ; it falls within the 'maximum comfort' category. For this reason, the verification with respect to vibrations is considered more than satisfactory.

3.8 Support devices

The design of bearing devices depends on:

- reactions to be transmitted to the foundation
- maximum displacement or rotation allowed
- type of displacement that the device must block or leave free

For the bridge under consideration, the following bearings configuration was chosen:

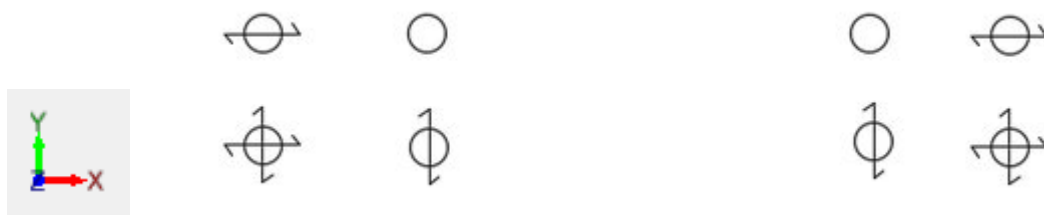


Figure 64: Bearing's articulation

Symbol	Freedom
	Translation fixed, rotation free.
	Translation in one direction, rotation free.
	Translation free, rotation free.

Figure 65: Bearings symbol legend

The bearing configuration is designed in such a way that horizontal and transversal sliding are permitted, in order to prevent stresses resulting from thermal loads. In this way, as can be seen from the image above, we have 4 types of constraints:

-2 fixed constraints

-4 guided, two of which sliding in the longitudinal direction and two in the transverse direction

-2 free sliding

The maximum reactions are shown below:

Vista UTENTE
Analisi:128-135, 137, 138, 141, 142, 145, 146, 149-169, 180-287 (Inviluppo grafico - MaxAbs)
Vincolo puntuale : FX Vincolo lineare : FX Vincolo superficiale : FX
Assi locali

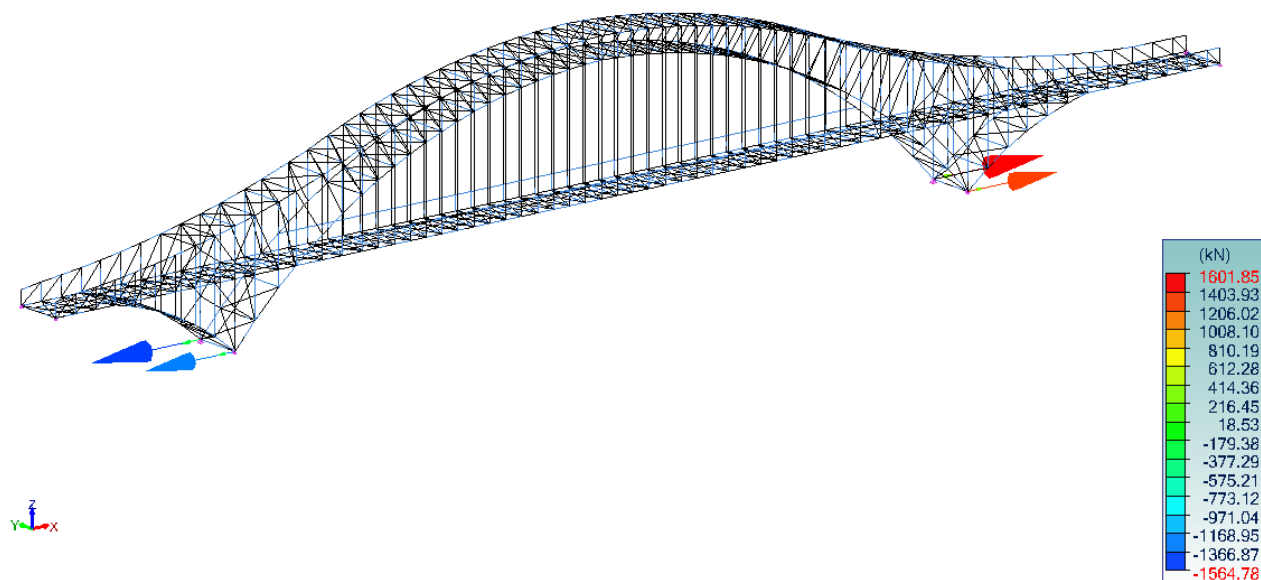


Figure 66: Reactions in x direction

Vista UTENTE
Analisi:128-135, 137, 138, 141, 142, 145, 146, 149-169, 180-287 (Inviluppo grafico - MaxAbs)
Vincolo puntuale : FY Vincolo lineare : FY Vincolo superficiale : FY
Assi locali

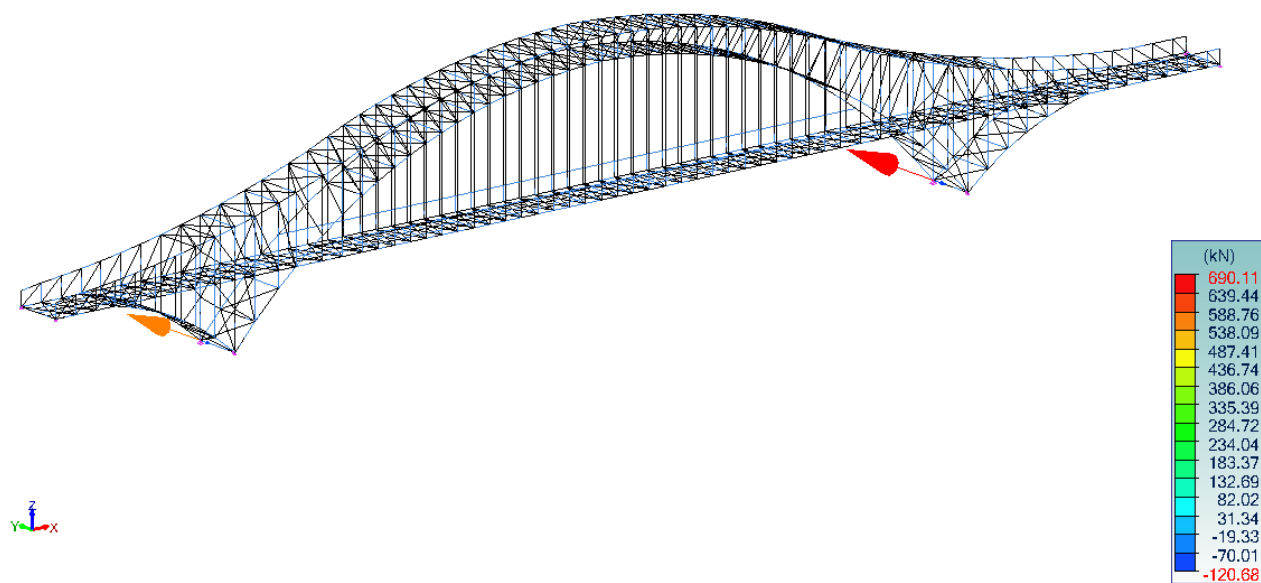


Figure 67: Reactions in y direction

Vista UTENTE
Analisi: 128-135, 137, 138, 141, 142, 145, 146, 149-169, 180-287 (Involuppo grafico - MaxAbs)
Vincolo puntuale : FZ Vincolo lineare : FZ Vincolo superficiale : FZ
Assi locali

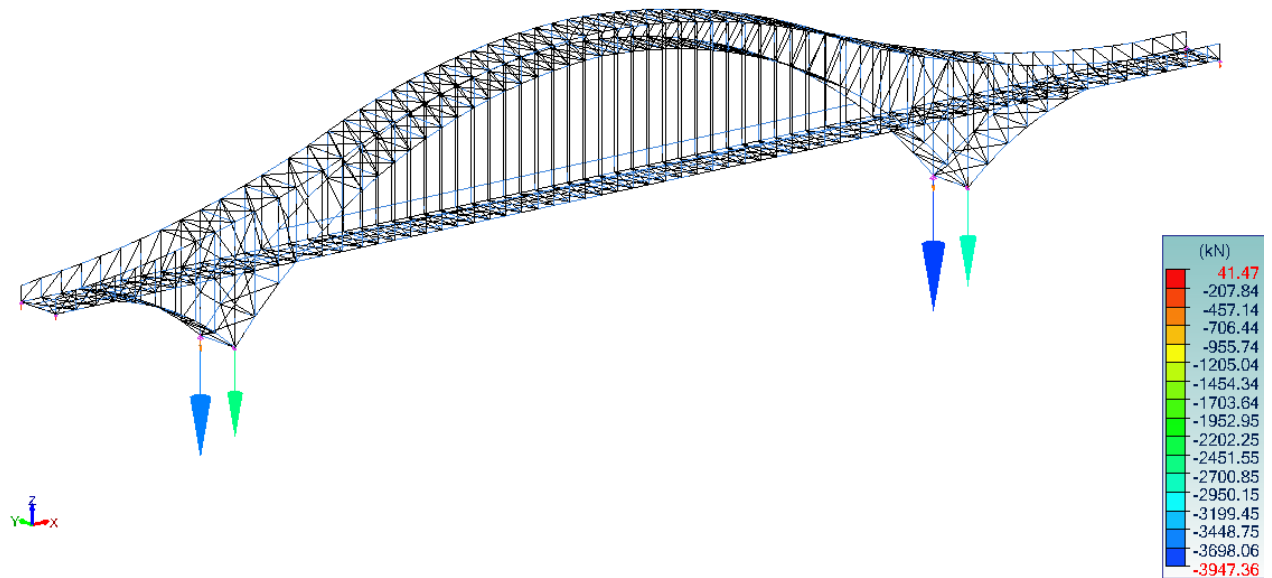


Figure 68: Reactions in z direction

It is important to note that certain load combinations result in tensile forces acting on the bearings (positive F_x components, thus oriented upward). In such cases, it is necessary to use bearings capable of withstanding uplift forces. These consist of standard fixed, guided, or multidirectional bearings, enhanced with mechanical devices designed to prevent separation when subjected to axial tensile actions.

The maximum displacement in the two horizontal directions is calculated, considering the maximum thermal variation, in §3.3.5 of this document. In detail:

- Longitudinal direction - 109 millimeters
- Transverse direction - 4 millimeters

The deformations obtained by calculation software for the load case 'Temperature' are shown:

Vista UTENTE
Analisi: 10 tempo
Vincolo : DY
Assi locali

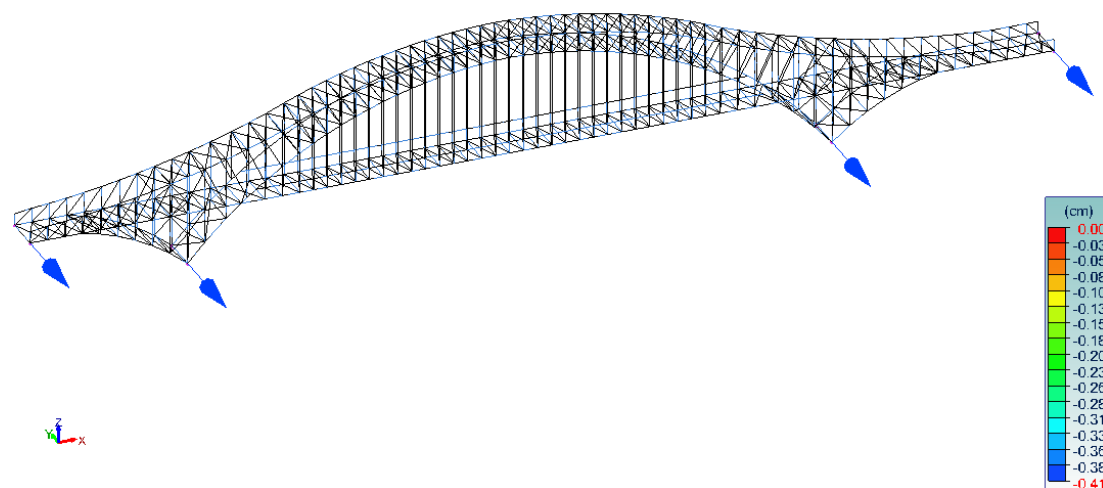


Figure 69: Displacements in y direction

Vista UTENTE
Analisi: 10 tempo
Vincolo : DX
Assi locali

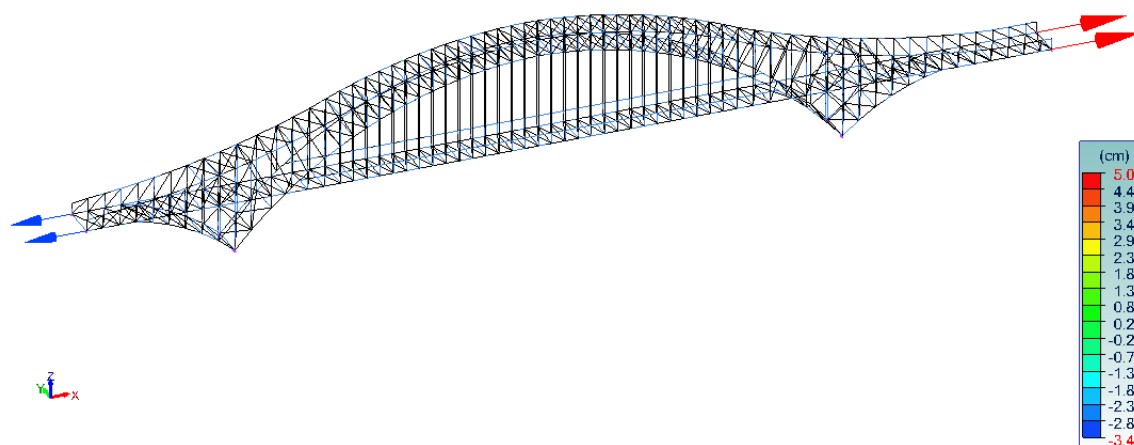


Figure 70: Reactions in x direction

As can be seen, the maximum transverse displacement obtained by the software is consistent with the one manually calculated; on the other hand, the longitudinal displacement differs slightly from that calculated by hand ($5.01 + 3.42 = 84 \text{ mm}$ instead of 109 mm); this is due to the fact that the manual calculation is approximate and does not take into account the fact that the bridge is not simply

supported at the ends but has intermediate constraints, which partially block the longitudinal displacement; the result is a lower longitudinal displacement.

The maximum stresses are given for each support so that an appropriate device can be chosen:



N°	Type	Fx [kN]	Fy [kN]	Fz [kN]
2, 3	Fixed	1601	691	3948
1, 4	Guided, longitudinally sliding	-	33	380
6, 7	Guided, transversally sliding	1292	-	2856
5, 8	Free sliding	-	-	330

The type of support was chosen from the range of the company “Fip Mec,” a manufacturer of supports, earthquake-resistant devices and dissipators. In particular, the products considered are Vasoflon® bearings; they’re structural pot bearings, in which the rotations about any horizontal axis are ensured by the deformability of the elastomeric pad confined in a monolithic steel pot.

“The elastomer behaves like a fluid that, under a tri-axial pressure, offers low resistance to deformations but high vertical stiffness. In addition to vertical compressive loads, Vasoflon® bearings are capable of transferring forces and/or permit sliding in one or more directions of the horizontal plane depending on the different bearing types. In the sliding bearings, translational movements are achieved through the mutual sliding of two flat mating surfaces, one of stainless steel and the other of PTFE.”

The following models were chosen:

- Fixed type: VF 600-180, with a vertical capacity of 6000 kN able to transfer both longitudinally and transversally horizontal forced of 1800 kN;
- Guided type, longitudinally sliding: VU 50/100-5, with a vertical capacity of 500 kN, that permits longitudinal movements of +/- 50mm and is able to transfer transversally horizontal forced of 50 kN;
- Guided type, transversally sliding: VU 450/100-135, with a vertical capacity of 4500 kN, that permits longitudinal movements of +/- 50 mm and is able to transfer transversally horizontal forced of 1350 kN;
- Free sliding type: VM 50/100/50, with a vertical capacity of 500 kN, that permits longitudinal movements of +/- 50 mm and transverse movements of +/- 25 mm;

VF
HIGH

BEARING TYPE	DESIGN VERTICAL LOAD	MAXIMUM HORIZONTAL LOAD	BASE ELEMENT DIAMETER	DOWELS (UPPER/LOWER)		UPPER ELEMENT DIAMETER	UPPER OVERALL DIMENSIONS		LOWER OVERALL DIMENSIONS		BEARING TOTAL HEIGHT	BEARING WEIGHT (EXCEPT ANCHORINGS)
	$N_{sd\ ULS}$ kN	V_{ULS} kN	D_o mm	n	type	B mm	C mm	D mm	G mm	F mm	H_{tot} mm	W kg

VF 600-180	6.000	1.800	570	6/6	3	500	670	730	730	810	108	178
------------	-------	-------	-----	-----	---	-----	-----	-----	-----	-----	-----	-----

VU
NORMAL

VU NORMAL	DESIGN VERTICAL LOAD	MAXIMUM HORIZONTAL LOAD	BASE ELEMENT DIAMETER	DOWELS (UPPER/LOWER)	UPPER OVERALL DIMENSIONS		LOWER OVERALL DIMENSIONS		BEARING TOTAL HEIGHT	BEARING WEIGHT (EXCEPT ANCHORINGS)
					TRANSVERSAL	LONGITUDINAL	TRANSVERSAL	LONGITUDINAL		
BEARING TYPE	N_{sd} ULS kN	V ULS kN	D_o mm	n_o <div><div>n</div><div>type</div></div>	C mm	D mm	G mm	F mm	H_{tot} mm	W kg
VU 50/100-5	500	50	160	4/2 1	270	300	270	160	108	29

VU 50/100-5	500	50	160	4/2	1	270	300	270	160	108	29
-------------	-----	----	-----	-----	---	-----	-----	-----	-----	-----	----

VU 450/100-135	4.500	1.350	570	6/6	3	530	770	730	810	160	339
----------------	-------	-------	-----	-----	---	-----	-----	-----	-----	-----	-----

VM

BEARING TYPE	DESIGN VERTICAL LOAD	BASE ELEMENT DIAMETER	UPPER OVERALL DIMENSIONS		BEARING TOTAL HEIGHT	BEARING WEIGHT (EXCEPT ANCHORINGS)
	$N_{sd\ ULS}$ kN	D_o mm	C mm	D mm	H_{tot} mm	W kg

VM 50/100/50	500	160	270	270	89	22
--------------	-----	-----	-----	-----	----	----

4 CONNECTIONS

In steel structures, connections play a crucial role, as their design has a significant impact on both the overall cost and the quality of the structural solution. The type and behaviour of connections affect the performance of the entire structure—locally, as potential zones of damage concentration, and globally, in terms of the structural response.

They can be designed using different solutions involving welded joints, bolted joints or both techniques. The economic cost associated with joints can have a significant impact on the overall cost of the structure. The nodes of a steel structure are divided into full-strength joint and partial-strength joint. A partial-strength joint is when the connection is only able to transfer a portion of the resistance of the weakest element among those connected (obviously not less than the stress to which the joint is subjected). Vice versa, a connection is referred to as a full-strength joint when the connection is able to transfer the strength of the weakest element among those connected completely, regardless of the stresses to which it is subjected.

In general, bolted connections offer several practical advantages, including:

- fast preparation in the workshop and simple assembly on site, where welding operations may present greater technical challenges;
- ease of maintenance and inspection over the service life of the structure;
- no specific skill requirements for on-site personnel;
- no need for particular environmental conditions during installation.

Conversely, welded joints require more specialized and qualified labor, but still offer notable advantages, such as:

- structural continuity between connected elements, ensuring direct force transmission and a more homogeneous structural behaviour;
- reduction in the overall weight of the structure (no plates, bolts, etc.)
- higher stiffness compared to bolted connections, which helps to minimize relative displacements between components;
- the possibility to realize complex and customized shapes;
- watertightness, which is particularly beneficial in hydraulic structures, tanks, or bridges exposed to weather conditions;
- suitability for workshop fabrication under controlled conditions, contributing to higher final product quality.

In the following sections, the theoretical approach adopted for the verification of the connections is explained. As an example, three joints were analyzed in detail, and the related drawings are included.

These representations were produced during the design phase to visually assess the most suitable solution for each connection. The checks were mainly carried out using the structural software IDEA StatiCa, but to validate the results, some manual calculations were also performed.

The use of BIM methodology and the interoperability between different analysis software tools make it possible to evaluate the internal forces at joints with great precision. In particular, the integration between Advance Design, used for the global structural analysis, and IDEA StatiCa allows for the direct export of the joint of interest along with the corresponding internal forces, enabling detailed modelling and accurate verification of the connection.

4.1 Theory of Bolted Joints

A bolt consists of a screw—composed of a head and a shank—and a nut. The tightening of the nut can be performed either in a simple manner or by applying a specific torque. The use of controlled tightening torque improves the mechanical performance of the connection. When a defined torque is applied, tensile forces are induced along the shank of the bolt. This allows the joint to transfer loads not only through direct bearing but also through friction between the contact surfaces, thereby enhancing the load-carrying capacity of the bolted connection.

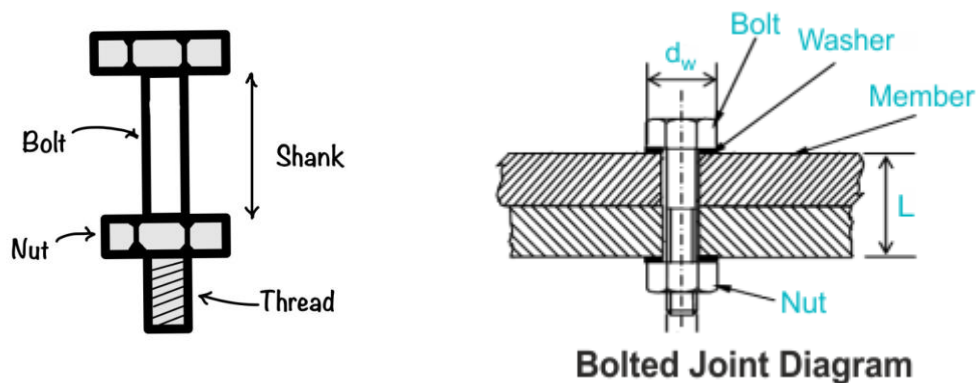


Figure 71: Main components of bolted joints

Bolts are categorized into various strength classes, which define their mechanical properties. These classifications will be discussed in the following sections. The shank of a bolt can be either smooth or threaded, and this distinction directly affects the calculation of the bolt's net area, which is crucial for resistance checks. A good general practice is to ensure that the length of the unthreaded portion of the bolt is equal to the total thickness of the connected plates (i.e., the start of the threading should lie within the thickness of the washer). Moreover, when the connection is subject to vibrations, it is

advisable to use a spring washer (or equivalent devices) to prevent the loosening of the nut and to long-term integrity of the joint.

Table 3.1: Nominal values of the yield strength f_{yb} and the ultimate tensile strength f_{ub} for bolts

Bolt class	4.6	4.8	5.6	5.8	6.8	8.8	10.9
f_{yb} (N/mm ²)	240	320	300	400	480	640	900
f_{ub} (N/mm ²)	400	400	500	500	600	800	1000

Only bolt assemblies of classes 8.8 and 10.9 conforming to the requirements given in 1.2.4 Reference Standards: Group 4 for High Strength Structural Bolting for preloading with controlled tightening. It follows that the bolts used in bridge structures are typically high-strength bolts, belonging to class 8.8 or 10.9.

Using simplified behavioral models, bolts are assumed to be subjected only to axial tensile forces (tension), transverse forces perpendicular to the shank (shear), or a combination of both actions.

Eurocode 3 classifies shear-resistant bolted connections as follows:

- **Shear connections (Category A)**
Bolts of class 4.6 to 10.9 are used, without preloading and with no specific requirements for the contact surfaces.
- **Slip-resistant connections at the Serviceability Limit State (Category B)**
High-strength preloaded bolts are used, tightened with a controlled torque to prevent slip at the serviceability limit state (as per EN 1090-2).
- **Slip-resistant connections at the Ultimate Limit State (Category C)**
High-strength preloaded bolts are used, tightened with a controlled torque to prevent slip at the ultimate limit state (as per EN 1090-2).

Tension-resistant bolted connections are instead classified as:

- **Non-preloaded bolted connections (Category D)**
Ordinary or high-strength bolts are used, without preloading.
- **Preloaded high-strength bolted connections (Category E)**
High-strength bolts are used with preloading, in accordance with EN 1090-2.

During installation, it is essential that the fit between bolts and holes complies with specified tolerances to minimize relative movement between the connected components. In this regard,

Eurocode 3 prescribes specific clearance values between the hole and the bolt, depending on the bolt diameter, in order to ensure the proper functioning of the connection.

According to UNI EN 1090-2, the permissible tolerances are as follows:

- For bolts with a diameter of 12–14 mm $\rightarrow \varphi - d = 1 \text{ mm}$
- For bolts with a diameter of 16–24 mm $\rightarrow \varphi - d = 2 \text{ mm}$
- For bolts with a diameter $\geq 27 \text{ mm} \rightarrow \varphi - d = 3 \text{ mm}$

Similarly, the Italian Building Code (NTC 2018) also specifies allowable tolerances: for bolts with a diameter less than 20 mm, the hole clearance should be 1 mm, while for diameters greater than 20 mm, a clearance of 1.5 mm is permitted.

Compliance with these tolerances is essential to ensure effective force transmission between connected elements and to prevent loosening or deformation during the service life of the structure. To guarantee a proper stress distribution within the connection plates, bolts must be arranged appropriately. For this reason, specific standards provide guidance on the correct layout of bolts. These provisions must be followed unless validated experimental evidence supports alternative configurations.

The main geometric requirements for bolted connections are outlined in Section 4.2.8 of the NTC 2018. These specifications refer to the hole diameter d_{0d0} , from which all minimum and maximum spacing requirements are derived, in order to ensure both the safety and efficiency of the connection.

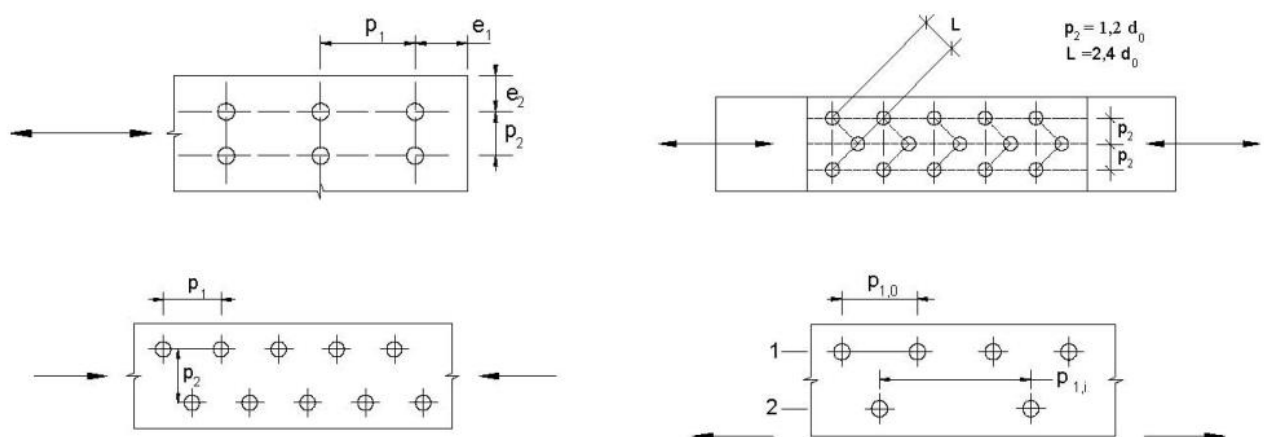


Figure 72: Rules for the arrangement of holes for bolted connections

Table 4.2.XVIII – Hole positioning for bolted and riveted connections

Distances and Spacings	Minimum	Connections exposed to corrosive or environmental effects	Connections not exposed to corrosive or environmental effects	Connections made of corrosion-resistant steel (UNI EN 10025-5)
e_1	$1.2 d_o$	$4t + 40 \text{ mm}$	–	$\max(8t; 12 \text{ mm})$
e_2	$1.2 d_o$	$4t + 40 \text{ mm}$	–	$\max(8t; 125 \text{ mm})$
p_1	$2.2 d_o$	$\min(14t; 200 \text{ mm})$	$\min(14t; 200 \text{ mm})$	$\min(14t; 175 \text{ mm})$
$p_{1,o}$	–	$\min(14t; 200 \text{ mm})$	–	–
$p_{1,i}$	–	$\min(28t; 400 \text{ mm})$	–	–
p_2	$2.4 d_o$	$\min(14t; 200 \text{ mm})$	$\min(14t; 200 \text{ mm})$	$\min(14t; 175 \text{ mm})$

Note:

Local instability of the plate between bolts/rivets should not be considered if $(p_1/t) < [9(235/f_y)^{0.5}]$; otherwise, a free buckling length equal to $0.6 \cdot p_1$ will be assumed.

t is the minimum thickness of the outer connected elements.

From a construction standpoint, it is essential to account for the space required by workers to properly perform manual assembly operations on site. This space, known as the *clearance space* or *working space*, allows for the insertion and tightening of bolts and ensures both safety and efficiency during the structural assembly phases. Therefore, in addition to technical requirements, it is always advisable to provide adequate distances between bolts and between bolts and plate edges to facilitate all on-site operations.

Tensile resistance

The tensile resistance is divided into two contributions, the first being $F_{t,Rd}$, i.e. the tensile strength of a bolt, while the second contribution is given by $B_{p,Rd}$ which consists of the punching resistance of the plate, the actual resistant value being the lower of the two:

$$F_{t,Rd} = \frac{k_2 \cdot f_{ub} \cdot A_s}{\gamma_{M2}}$$

$$B_{p,Rd} = \frac{0.6 \cdot \pi \cdot d_m \cdot t_p \cdot f_u}{\gamma_{M2}}$$

Where:

- $k_2 = 0.9$
- f_{ub} : ultimate bolt tension
- A_s : resistant section area of the bolt
- $\gamma_{M2} = 1.25$ Partial safety factor for bolted unions

Shear resistance

Shear unions are the most common in steelwork, the value of shear resistance in the case where the shear plane passes through the threaded zone is given by:

$$F_{vRd} = n_s \cdot \frac{0.6 \cdot f_{ub} \cdot A_s}{\gamma_{M2}}$$
$$F_{vRd} = n_s \cdot \frac{0.5 \cdot f_{ub} \cdot A_s}{\gamma_{M2}}$$

The first formula is for bolt of classes 4.6, 5.6, 8.8. The second one for classes 4.8, 5.8, 6.8, 10.9. While if it does not pass through the threaded area it is equal to:

$$F_{vRD} = n_s \cdot \frac{(0.6 \cdot f_{ub} \cdot A)}{\gamma_{M2}}$$

Shear and tensile strength

In the case of co-presence of shear and tensile forces, the verification is carried out by considering the two contributions $F_{v,Ed}$ and $F_{t,Ed}$, shear and tensile design forces respectively, thus defining a resistance domain, with the following

$$\frac{F_{v,ED}}{F_{v,Rd}} + \frac{F_{t,Ed}}{1,4F_{t,Rd}} \leq 1$$

The resistant values in the denominators are those proposed in the previous paragraphs.

Recasting

Relining consists of plate failure due to ploughing or ovalisation of the hole.

$$F_{b,Rd} = \frac{k_1 \cdot \alpha_b \cdot f_u \cdot d \cdot t}{\gamma_{M2}}$$

Where d is the diameter of the bolt, t and f_u are the thickness and breaking tension of the plate respectively, γ_{M2} is the safety coefficient while the factors k_1 and α_b depend on the geometry of the holes in relation to the direction of the applied load. The coefficient α_b takes into account the arrangement of the holes in the direction parallel to that of the load direction, it is a function of the ratio f_{ub}/f_u and the ratio of the edge distance to the hole diameter d_0 . For edge bolts the coefficients are

$$k_1 = \min \left\{ 2.8 \cdot \frac{e_2}{d_0} - 1.7; 2.5 \right\}$$

$$\alpha_b = \min \left\{ \frac{e_1}{3 \cdot d_0}; \frac{f_{ub}}{f_u}; 1.0 \right\}$$

The coefficient k_1 takes into account the arrangement of the holes in a direction perpendicular to that of the load direction. It is a function of the ratio of edge distance to hole diameter d_0 . For internal bolts, the coefficients are:

$$k_1 = \min \left\{ 1.4 \cdot \frac{p_2}{d_0} - 1.7; 2.5 \right\}$$

$$\alpha_b = \min \left\{ \frac{p_1}{3 \cdot d_0} - \frac{1}{4}; \frac{f_{ub}}{f_u}; 1.0 \right\}$$

Slip

The design creep resistance of a resistant section is given by:

$$F_{sRd} = k_s \cdot \eta \cdot \frac{\mu}{\gamma_{M3}} \cdot F_{p,c}$$

Where $F_{p,c}$ is the design preload force for high-strength bolts with controlled torque.

$$F_{p,c} = 0.7 \cdot f_{ub} \cdot A_{res}$$

n corresponds to the number of sliding surfaces, k_s is a function of the hole type, μ is a friction coefficient.

Block tearing

Since block tearing is a shear failure mechanism at the row of holes along the stressed face where a portion of the object is torn away from the rest of the element, the following verification is required to prevent this phenomenon

$$V_{eff,Rd} = \frac{f_u A_{nt}}{\gamma_{M2}} + \frac{f_y A_{nv}}{\sqrt{3} \gamma_{M0}}$$

When several elements of a structure converge at a node, a connection is made, which may be partial or complete reinstatement, in the first case the joint is capable of transferring, between the two or more elements involved, a part of the actions that the members are able to support; therefore, they represent the weakest point of the structure. On the other hand, when we speak of fully reinforcing joints, they are capable of transferring the maximum values of the stresses that the weakest structural element is able to withstand. Both of these types do not constitute joints, i.e. joints that allow relative displacement between two connected pieces; therefore, an assessment of ductility, i.e. the ability to deform in the plastic field before collapsing, must also be carried out. Compared to welds, bolted joints tend to offer a lower plastic reserve, this also clearly depends on how the bolted joint is made; however, this is due to the fact that welding should provide more continuity between the elements.

4.2 Theory of Welded Joints

Welding is a joining technique that allows a permanent union between the metal elements involved, creating structural continuity. This process consists of the base metal of the elements to be welded and the filler metal, which forms the weld bead. During welding, the filler metal is in a liquid state, forming a melt pool due to the high temperatures developed in the weld zone. At the end of the process, the filler metal cools, solidifying and creating the weld bead.

There are two main types of welding. Full-penetration welding is when a complete fusion of the base material and the filler metal is achieved along its entire thickness. In order to achieve this, proper preparation is required, which involves edge caulking. This technique is carried out using a filler material of the same class as the materials to be joined. The second type is the angle seam weld: there is no penetration of the fusion material, the steel elements form angles of between 60° and 120° , and it is characterised by the groove height of the seam. The resistant section of this type of weld is its throat section. resistance of this weld can be verified by two methods, depending on the position of the throat section and how the forces are distributed over the weld bead.

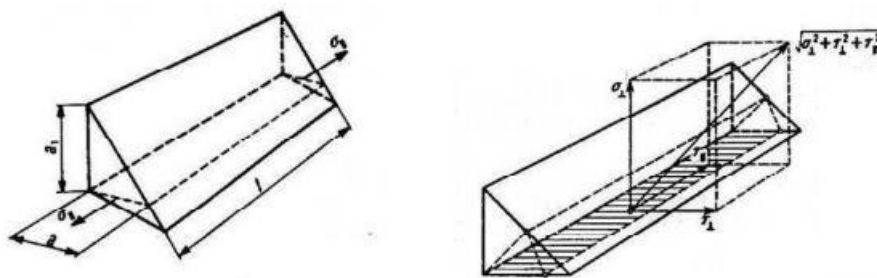


Figure 73: Throat planes - NTC 18

Different stresses can be identified on the throat sections of the weld seam:

- σ_{\perp} : the normal component of the throat section, which acts perpendicular to the direction of the seam.
- τ_{\perp} : the tangential component orthogonal to the bead axis, acting in the plane of the throat section.
- $\tau_{//}$: the tangential component parallel to the bead axis, also acting in the plane of the throat section.
- $\sigma_{//}$: the normal component parallel to the axis, which, however, does not influence the behaviour of the joint and is not considered in the strength checks.

The first verification method proposed is the directional method, which is the most 'complete', in which the tensional state relative to the non-tilted throat section is determined. The verification requires the following conditions to be met:

$$\sqrt{(\sigma_{\perp}^2 + 3(\tau_{\perp}^2 + \tau_{\parallel}^2))} \leq \frac{f_{tk}}{\beta_w \gamma_{M2}}$$

$$\sigma_{\perp} < \frac{0.9 f_{tk}}{\gamma_{M2}}$$

Acciaio	f_u [MPa]	β_w
S235	360	0.80
S275	430	0.85
S355	510	0.90
S420	520	1.00
S460	540	1.00

Where f_u is the nominal tensile breaking strength of the weakest element constituting the joint, β_w is the correlation coefficient, $\gamma_{(M2)}$ the partial safety coefficient.

The second criterion, referred to as simplified, is based on the following criterion.

$$F_{w,Ed}/F_{w,Rd} \leq 1$$

Where $F_{w,Ed}$ represents the design force acting on the corner bead per unit length, while $F_{w,Rd}$ is the design resistance of the corner bead per unit length.

$$F_{w,Rd} = a f_{tk} / (\sqrt{3} \beta \gamma_{M2})$$

Finally, the third method, which will be adopted in the following paragraphs, assumes that the weld throat section is overturned. In this case, the normal and tangential stresses perpendicular to the weld axis are indicated by n and τ . The verification is satisfied if the following conditions are met:

$$\sqrt{n_{\perp}^2 + \tau_{\perp}^2 + \tau_{\parallel}^2} \leq \beta_1 f_{yk}$$

$$|n_{\perp}| + |\tau_{\perp}| \leq \beta_2 f_{yk}$$

	S235	S275 - S355	S420 - S460
β_1	0,85	0,70	0,62
β_2	1,0	0,85	0,75

4.3 Connection Design Using IDEA StatiCa

4.3.1 Joint 1: Longitudinal beams – Vertical members – Diagonals – Bracings – Transversal beams

Several elements converge at this joint. The vertical members have been conceived as single continuous elements, also considering that their height rarely exceeds 12 meters (except for the tallest one), allowing them to be transported to the construction site as single units. The joint is designed with stiffeners having the same cross-section as the connected elements, all assembled in the workshop and then transported to the site. Flanged connections are used to join the stiffeners to the longitudinal and transverse beams, as well as to the diagonal members. The deck bracings (only one is shown here, as they are symmetrical) are bolted to the transverse beams using connection plates. These bracings converge at the center of the joint to avoid the generation of parasitic moments.

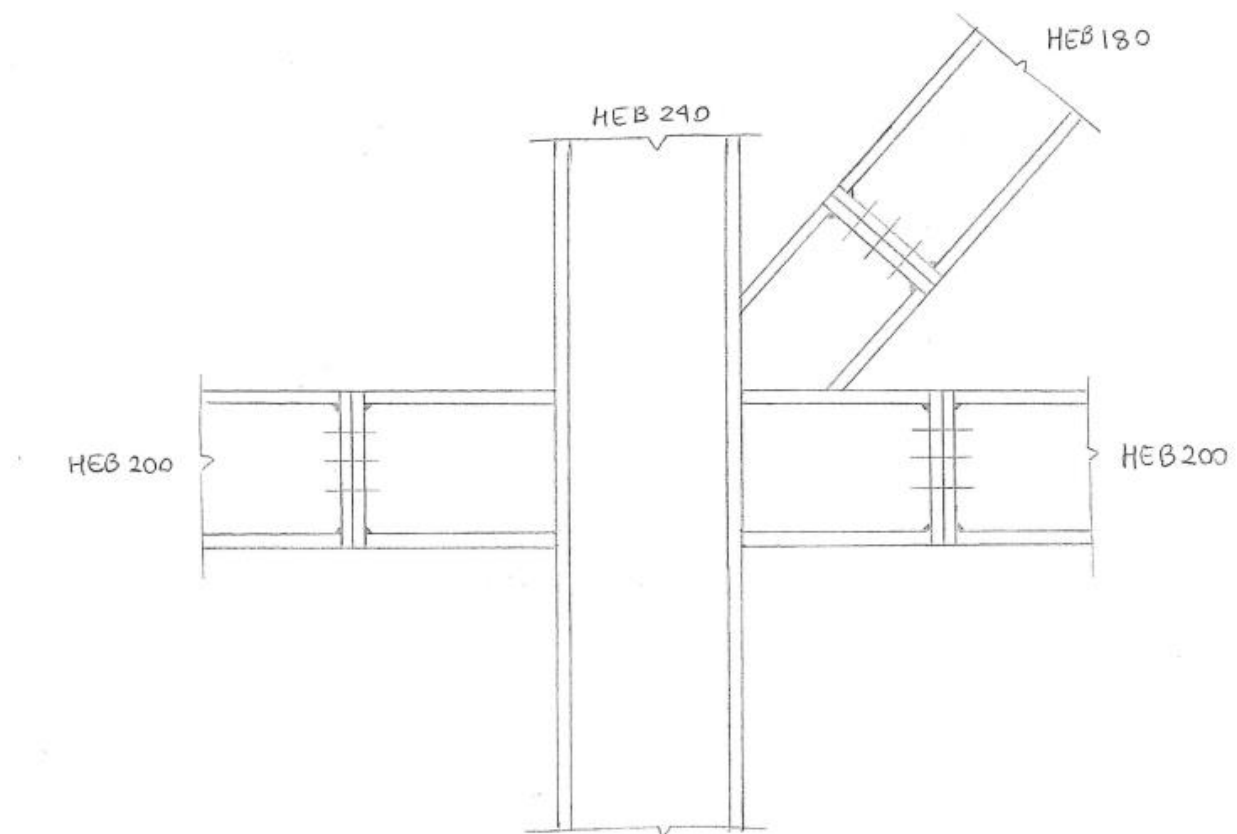


Figure 74: Sketch n. 1- Vertical members, longitudinal beams, diagonals

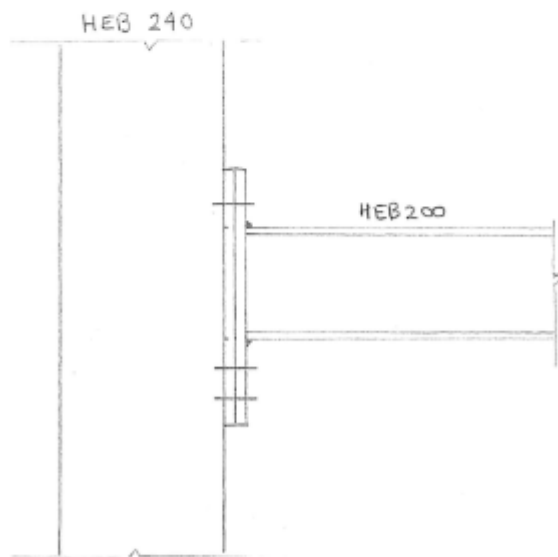
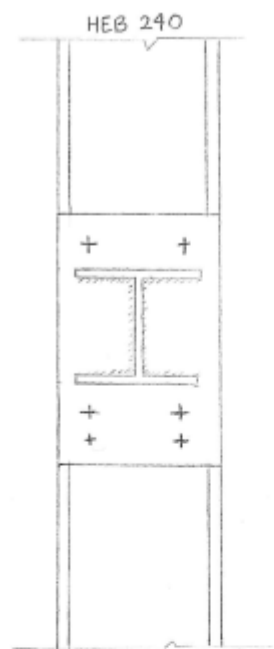


Figure 75: Sketch n.2 -Vertical members, transversal beams

Analysis	✓	100.0%
Plates	✓	2.1 < 5.0%
Bolts	✓	93.9 < 100%
Welds	✓	98.1 < 100%
Buckling		Not calculated

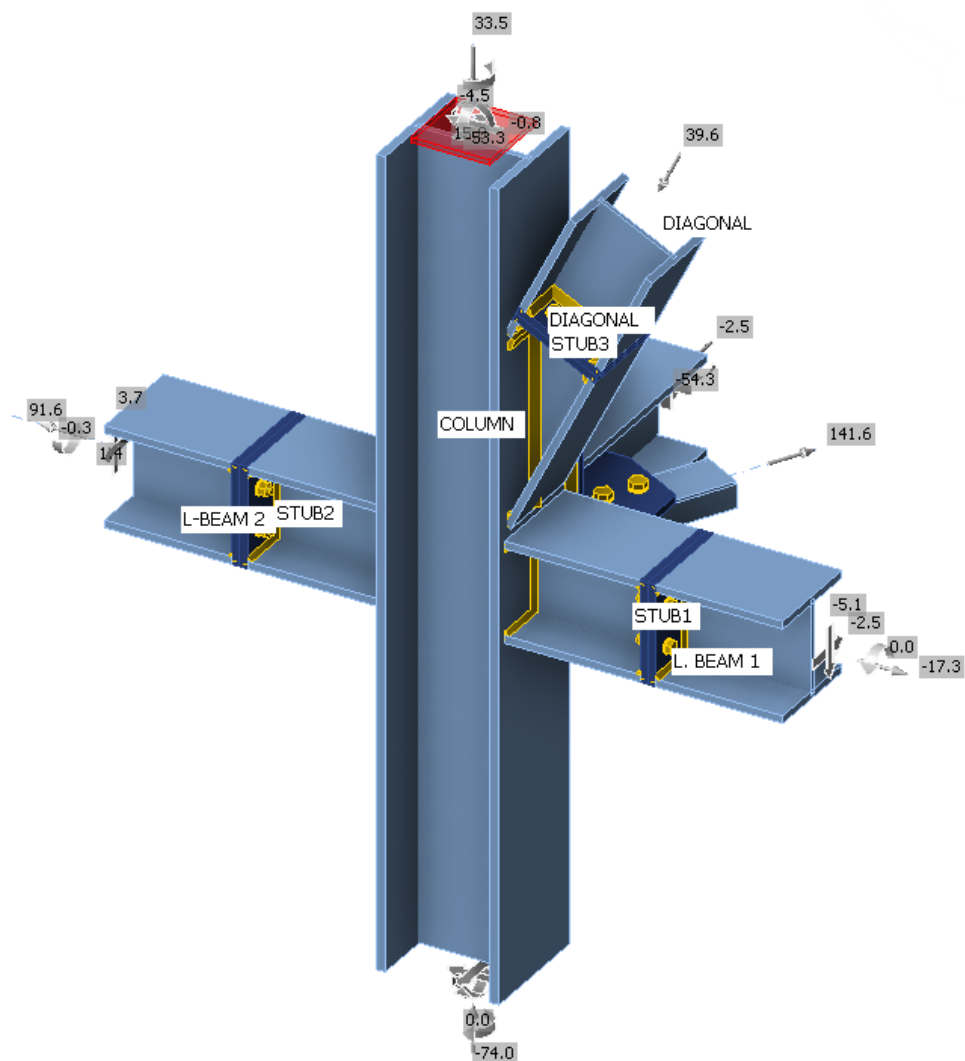
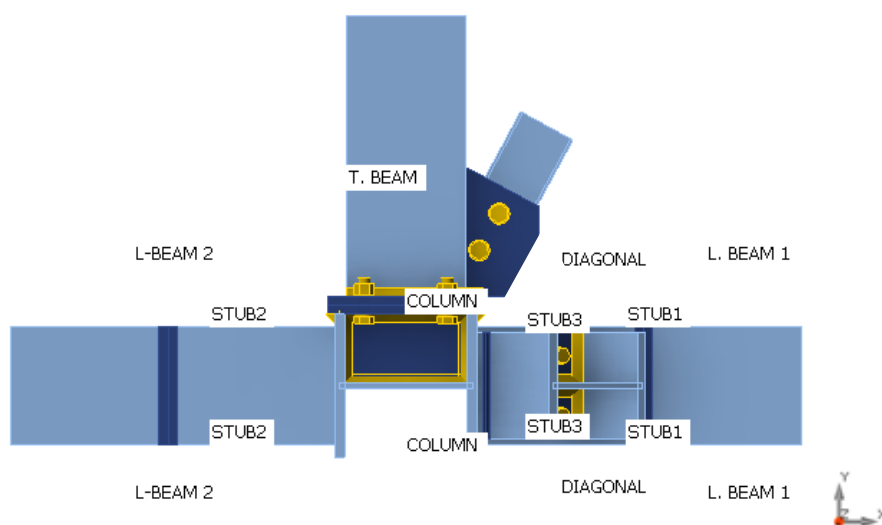
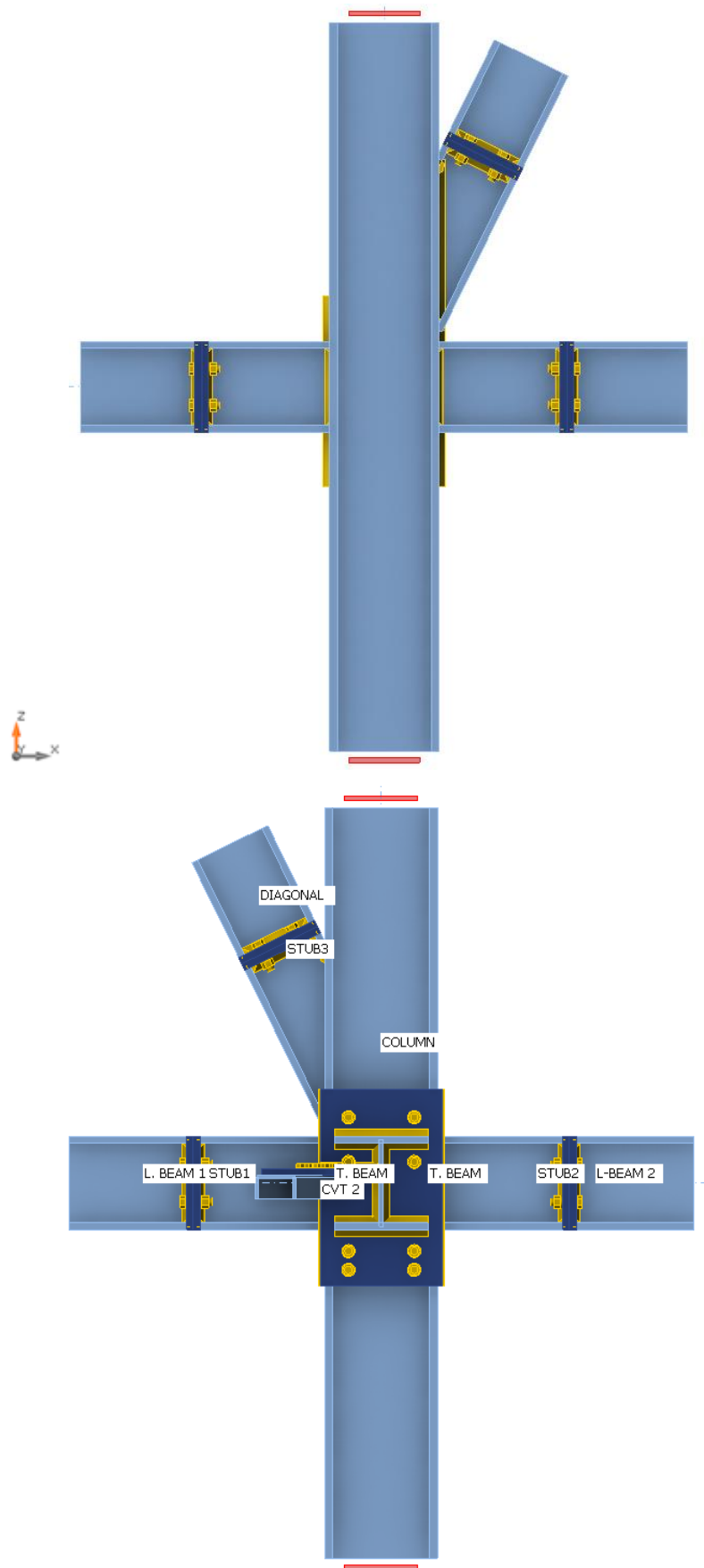


Figure 76: Joint n.1 in IDEA Statica





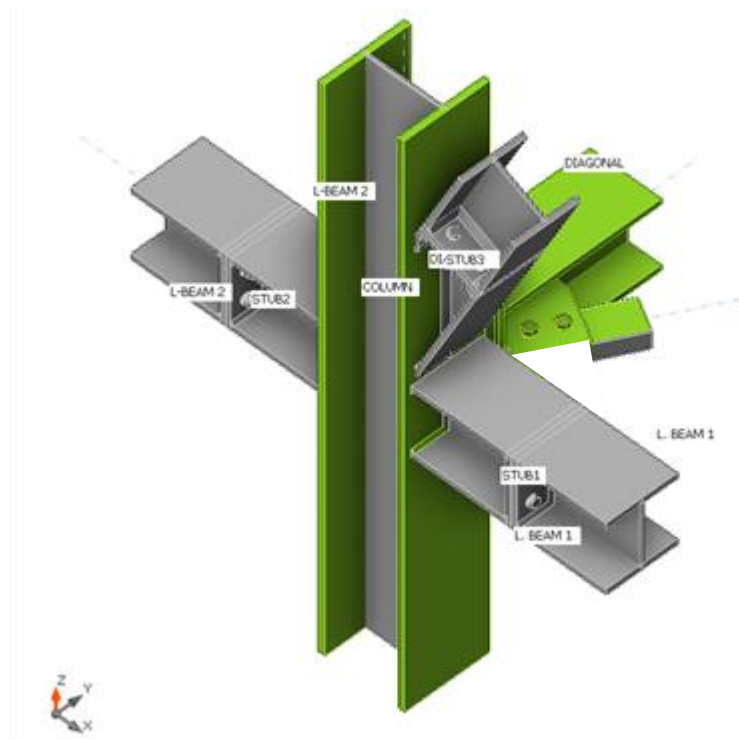
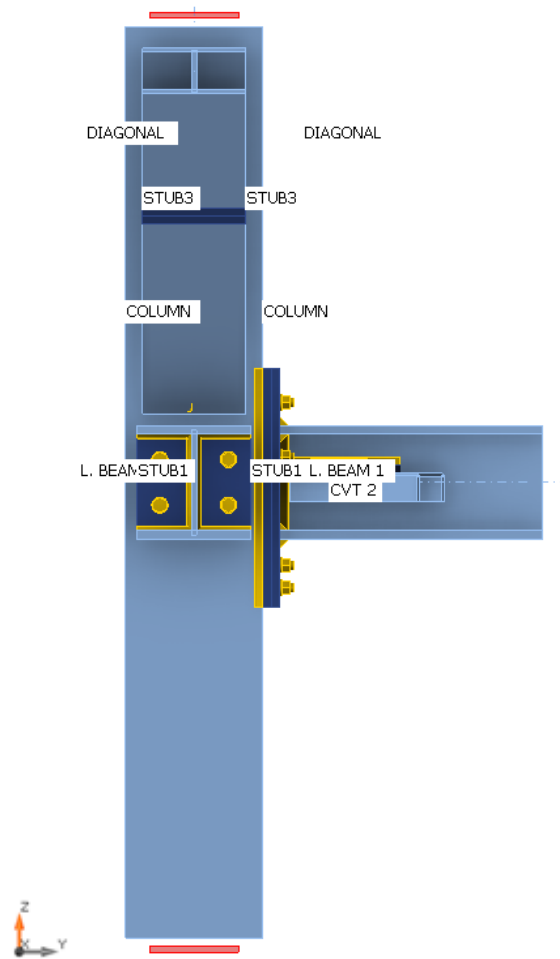
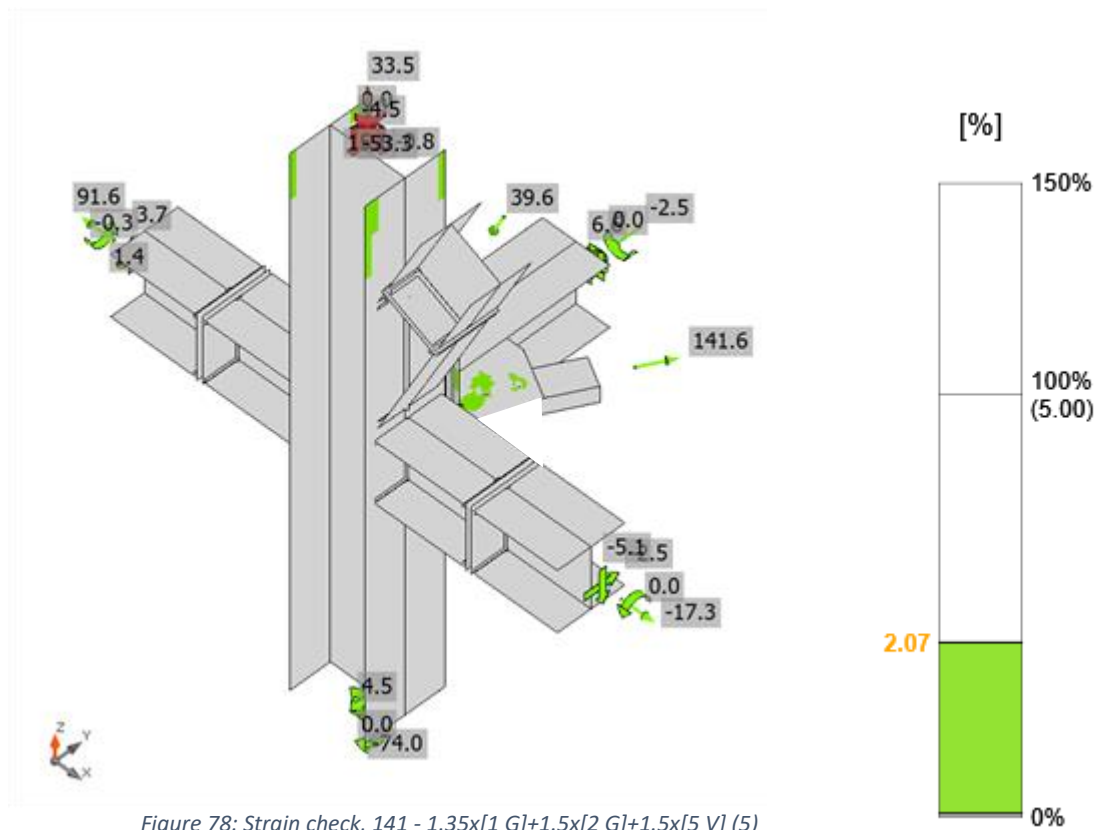
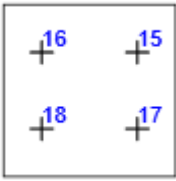


Figure 77: Overall check, $141 - 1.35 \times [1 \text{ G}] + 1.5 \times [2 \text{ G}] + 1.5 \times [5 \text{ V}] (5)$



Bolts

Shape	Item	Grade	Loads	$F_{t,Ed}$ [kN]	$F_{v,Ed}$ [kN]	$F_{b,Rd}$ [kN]	U_{t_i} [%]	U_{t_s} [%]	$U_{t_{ts}}$ [%]	Detailing	Status
	B1	M16 8.8 - 1	142 - 1.35x[1 G]+1.5x[2 G]+1.5x[9 V] (54)	41.0	0.5	174.2	45.3	0.9	33.2	OK	OK
	B2	M16 8.8 - 1	142 - 1.35x[1 G]+1.5x[2 G]+1.5x[9 V] (54)	32.4	2.1	235.2	35.8	3.4	29.0	OK	OK
	B3	M16 8.8 - 1	142 - 1.35x[1 G]+1.5x[2 G]+1.5x[9 V] (54)	23.3	0.2	177.3	25.8	0.4	18.8	OK	OK
	B4	M16 8.8 - 1	142 - 1.35x[1 G]+1.5x[2 G]+1.5x[9 V] (54)	25.6	2.0	235.2	28.4	3.3	23.6	OK	OK
	B5	M16 8.8 - 1	116 - 1x[7 EY]-0.3x[6 EX]+0.3x[8 EZ][Newmark] (4)	15.1	0.1	174.2	16.7	0.1	12.0	OK	OK
	B6	M16 8.8 - 1	116 - 1x[7 EY]-0.3x[6 EX]+0.3x[8 EZ][Newmark] (4)	14.6	0.1	174.2	16.1	0.1	11.6	OK	OK

	B7	M16 8.8 - 1	116 - 1x[7 EY]-0.3x[6 EX]+0.3x[8 EZ][Newmar k] (4)	14.5	0.0	234.6	16.0	0.1	11.5	OK	OK
	B8	M16 8.8 - 1	142 - 1.35x[1 G]+1.5x[2 G]+1.5x[9 V] (54)	19.5	1.1	235.1	21.5	1.9	17.2	OK	OK
	B9	M20 8.8 - 2	135 - 1.35x[1 G]+1.5x[2 G]+1.5x[4 Q] (1)	117. 3	15.4	275.5	83.2	16.4	75.8	OK	OK
	B10	M20 8.8 - 2	142 - 1.35x[1 G]+1.5x[2 G]+1.5x[9 V] (54)	132. 4	3.4	158.4	93.8	3.6	70.6	OK	OK
	B11	M20 8.8 - 2	142 - 1.35x[1 G]+1.5x[2 G]+1.5x[9 V] (54)	100. 3	10.2	129.4	71.0	10.8	61.6	OK	OK
	B12	M20 8.8 - 2	135 - 1.35x[1 G]+1.5x[2 G]+1.5x[4 Q] (1)	117. 7	13.5	270.1	83.4	14.3	73.9	OK	OK
	B13	M20 8.8 - 2	142 - 1.35x[1 G]+1.5x[2 G]+1.5x[9 V] (54)	127. 7	16.8	158.4	90.5	17.9	82.6	OK	OK
	B14	M20 8.8 - 2	142 - 1.35x[1 G]+1.5x[2 G]+1.5x[9 V] (54)	77.5	30.0	114.1	54.9	31.9	71.1	OK	OK
	B15	M16 8.8 - 1	135 - 1.35x[1 G]+1.5x[2 G]+1.5x[4 Q] (1)	77.5	0.0	178.0	85.7	0.0	61.3	OK	OK
	B16	M16 8.8 - 1	135 - 1.35x[1 G]+1.5x[2 G]+1.5x[4 Q] (1)	77.4	0.1	174.2	85.6	0.1	61.3	OK	OK
	B17	M16 8.8 - 1	135 - 1.35x[1 G]+1.5x[2 G]+1.5x[4 Q] (1)	77.4	0.0	177.7	85.6	0.1	61.2	OK	OK
	B18	M16 8.8 - 1	135 - 1.35x[1 G]+1.5x[2 G]+1.5x[4 Q] (1)	77.5	0.0	174.7	85.7	0.1	61.3	OK	OK

To validate the results obtained from IDEA StatiCa, an example of manual verification is provided for bolt no. B16.

TENSION RESISTANCE CHECK

$d_b := 16 \text{ mm}$	Diameter
$f_{ub} := 800 \text{ MPa}$	Ultimate tensile strenght of the bolt
$f_{yb} := 640 \text{ MPa}$	Tensile stress strenght of the bolt
$A_s := 157 \text{ mm}^2$	Tensile stress area of the bolt
$Y_{M2} := 1,25$	Safety factor
$F_{t,Rd} := \frac{0,9 \cdot f_{ub} \cdot A_s}{Y_{M2}} = 90,4 \text{ kN}$	Tensile resistance
$F_{t,Ed} := 77,4 \text{ kN}$	Tensile force
$\frac{F_{t,Ed}}{F_{t,Rd}} = 0,86$	Work ratio < 1 OK

SHEAR RESISTANCE CHECK

$F_{v,Ed} := 0,1 \text{ kN}$	Shear force
$F_{v,Rd} := \frac{0,6 \cdot f_{ub} \cdot A_s}{1,25} = 60,3 \text{ kN}$	Shear resistance
$\frac{F_{v,Ed}}{F_{v,Rd}} = 0$	Work ratio < 1 OK

INTERACTION OF TENSION AND SHEAR

$\frac{F_{v,Ed}}{F_{v,Rd}} + \frac{F_{t,Ed}}{1,4 \cdot F_{t,Rd}} = 0,61$	Work ratio < 1 OK
--	-------------------

PUNCHING RESISTANCE CHECK

$$t_p := 15 \text{ mm}$$

Plate thickness

$$f_u := 490 \text{ MPa}$$

Ultimate strength (plate)

$$d_m := 25 \text{ mm}$$

The mean of the across points and across flats dimensions of the bolt head of the nut (the smaller)

$$B_{p,Rd} := \frac{0,6 \cdot \pi \cdot d_m \cdot t_p \cdot f_u}{Y_{M2}} = 277,1 \text{ kN}$$

Punching resistance

$$\frac{F_{t,Ed}}{B_{p,Rd}} = 0,28$$

Work ratio < 1 OK

BEARING RESISTANCE CHECK

$$e_1 := 40 \text{ mm}$$

Distance to the plate edge in the direction of the shear force

$$e_2 := 41 \text{ mm}$$

Distance to the plate edge perpendicular to the shear force

$$d_0 := 18 \text{ mm}$$

Bolt hole diameter

$$k_1 := \min \left(2,8 \cdot \frac{e_2}{d_0} - 1,7; 2,5 \right) \quad k_1 := 2,5$$

Factor for edge distance and bolt spacing perpendicular to the direction of load transfer

$$\alpha_b := \min \left(\frac{e_1}{3 \cdot d_0}; \frac{f_{ub}}{f_u}; 1 \right) \quad \alpha_b := 0,74$$

Factor for edge distance and bolt spacing in direction of load transfer

$$F_{b,Rd} := \frac{\alpha_b \cdot f_u \cdot d_b \cdot t_p \cdot k_1}{1,25} = 174 \text{ kN}$$

Work ratio < 1 OK

$$\frac{F_{v,Ed}}{F_{b,Rd}} = 0$$

4.4.2 Joint 2: Beam-beam connection

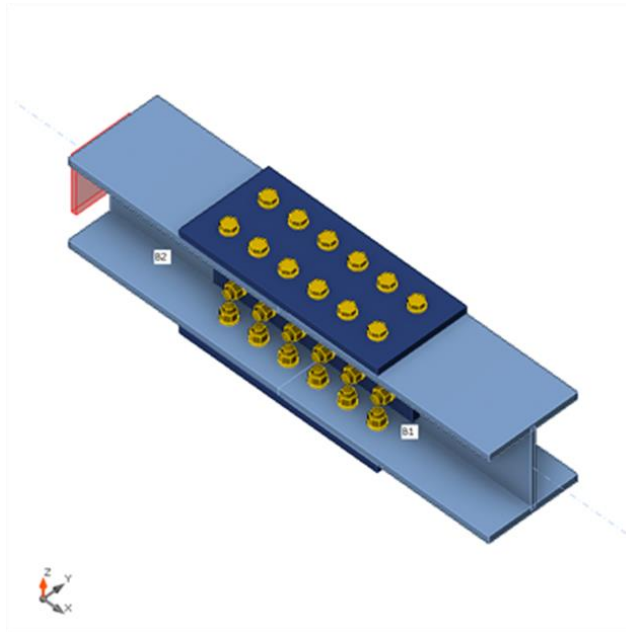


Figure 79: Joint n.2 in IDEA Statica

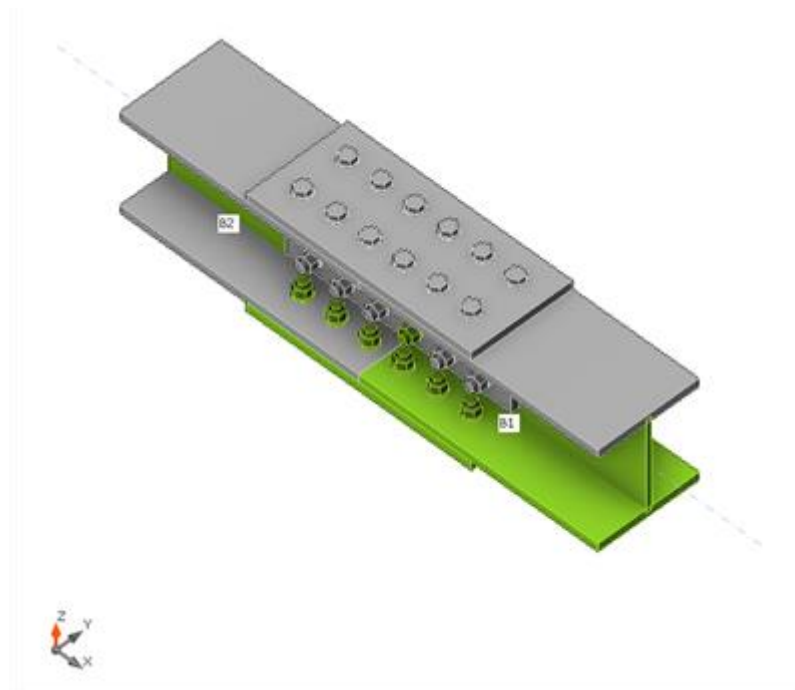


Figure 80: Overall check, LE3

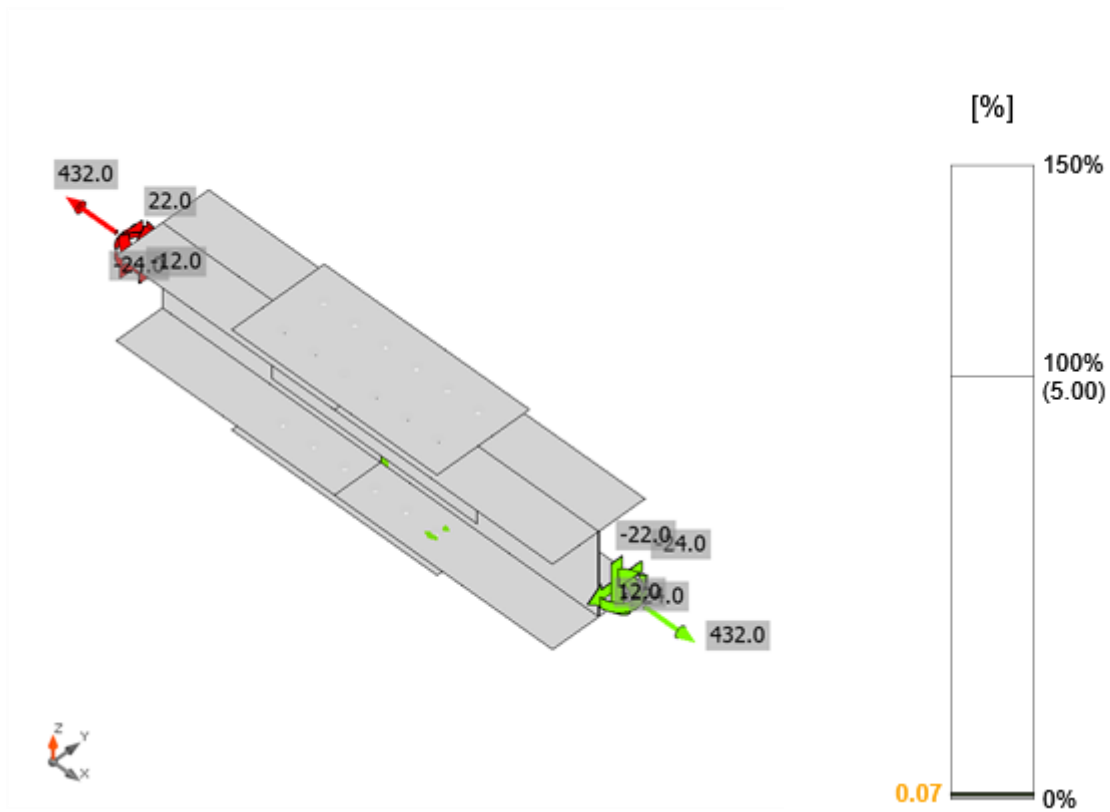


Figure 81: Strain check, LE3

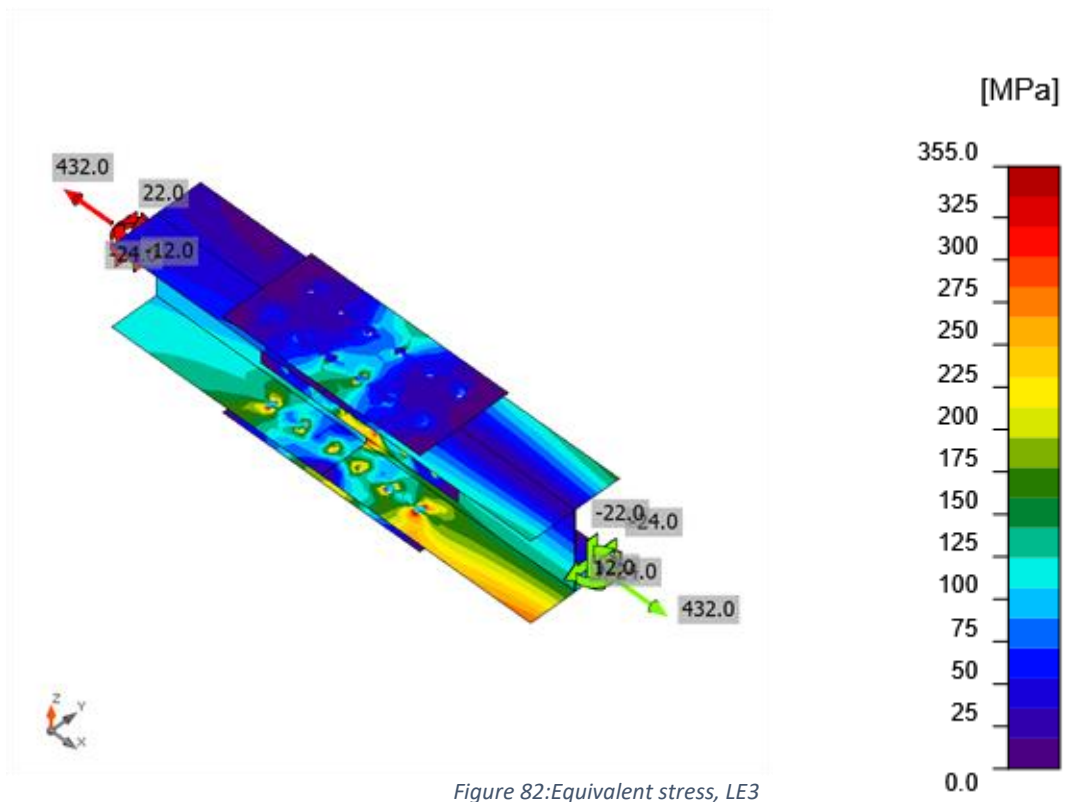

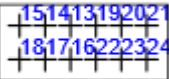
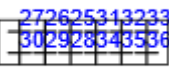


Figure 82: Equivalent stress, LE3

Bolts

Shape	Item	Grade	Loads	F _{t,Ed} [kN]	F _{v,Ed} [kN]	F _{b,Rd} [kN]	U _t [%]	U _{t,s} [%]	U _{t,ts} [%]	Detailing	Status
	B1	M16 8.8 - 1	LE2	3.8	30.6	122.0	4.2	50.8	53.8	OK	OK
	B2	M16 8.8 - 1	LE2	1.9	26.6	189.0	2.1	44.1	45.6	OK	OK
	B3	M16 8.8 - 1	LE2	8.4	29.9	217.8	9.3	49.6	56.3	OK	OK
	B4	M16 8.8 - 1	LE2	4.5	50.8	122.0	5.0	84.3	87.9	OK	OK
	B5	M16 8.8 - 1	LE2	1.8	48.1	189.0	2.0	79.8	81.2	OK	OK
	B6	M16 8.8 - 1	LE2	7.8	51.2	189.0	8.6	84.9	91.0	OK	OK
	B7	M16 8.8 - 1	LE2	4.2	29.6	122.0	4.6	49.1	52.4	OK	OK
	B8	M16 8.8 - 1	LE2	2.2	29.2	189.0	2.5	48.5	50.3	OK	OK
	B9	M16 8.8 - 1	LE2	9.2	32.5	217.8	10.2	53.9	61.2	OK	OK
	B10	M16 8.8 - 1	LE2	3.3	46.0	122.0	3.6	76.4	79.0	OK	OK
	B11	M16 8.8 - 1	LE2	1.7	45.6	189.0	1.9	75.6	77.0	OK	OK
	B12	M16 8.8 - 1	LE2	8.3	48.6	189.0	9.2	80.7	87.3	OK	OK
	B13	M16 8.8 - 1	LE3	3.8	50.4	122.0	4.2	83.7	86.7	OK	OK
	B14	M16 8.8 - 1	LE3	2.0	48.2	189.0	2.2	80.0	81.5	OK	OK
	B15	M16 8.8 - 1	LE3	8.5	51.6	189.0	9.4	85.6	92.3	OK	OK
	B16	M16 8.8 - 1	LE3	3.9	30.1	122.0	4.3	49.9	52.9	OK	OK
	B17	M16 8.8 - 1	LE3	2.0	26.7	189.0	2.2	44.2	45.8	OK	OK
	B18	M16 8.8 - 1	LE3	9.2	30.2	217.8	10.1	50.1	57.4	OK	OK
	B19	M16 8.8 - 1	LE3	3.8	46.5	122.0	4.2	77.1	80.1	OK	OK
	B20	M16 8.8 - 1	LE3	1.6	45.5	189.0	1.8	75.5	76.7	OK	OK
	B21	M16 8.8 - 1	LE3	7.7	48.2	189.0	8.5	80.0	86.0	OK	OK
	B22	M16 8.8 - 1	LE3	4.4	30.2	122.0	4.9	50.1	53.6	OK	OK
	B23	M16 8.8 - 1	LE3	2.1	29.2	189.0	2.3	48.4	50.0	OK	OK
	B24	M16 8.8 - 1	LE3	8.6	32.1	217.8	9.5	53.3	60.1	OK	OK
	B25	M16 8.8 - 2	LE2	2.9	18.6	64.8	3.2	55.7	33.2	OK	OK
	B26	M16 8.8 - 2	LE2	0.6	19.2	100.5	0.6	34.3	32.3	OK	OK
	B27	M16 8.8 - 2	LE2	3.7	21.0	116.7	4.1	34.8	37.7	OK	OK
	B28	M16 8.8 - 2	LE3	3.0	20.1	64.8	3.4	60.5	35.8	OK	OK
	B29	M16 8.8 - 2	LE3	0.7	20.1	100.5	0.8	36.2	34.0	OK	OK
	B30	M16 8.8 - 2	LE3	3.7	21.9	116.7	4.1	36.3	39.3	OK	OK
	B31	M16 8.8 - 2	LE2	2.9	20.6	64.8	3.2	60.4	36.5	OK	OK
	B32	M16 8.8 - 2	LE2	1.2	20.1	100.5	1.3	36.2	34.2	OK	OK
	B33	M16 8.8 - 2	LE2	3.0	21.5	116.7	3.3	35.7	38.1	OK	OK

	B34	M16 8.8 - 2	LE3	2.7	19.1	64.8	2.9	55.7	33.8	OK	OK
	B35	M16 8.8 - 2	LE3	1.0	19.1	100.5	1.1	34.3	32.5	OK	OK
	B36	M16 8.8 - 2	LE3	2.9	20.7	116.7	3.3	34.3	36.6	OK	OK

4.4 Joint 3: Bracing connection

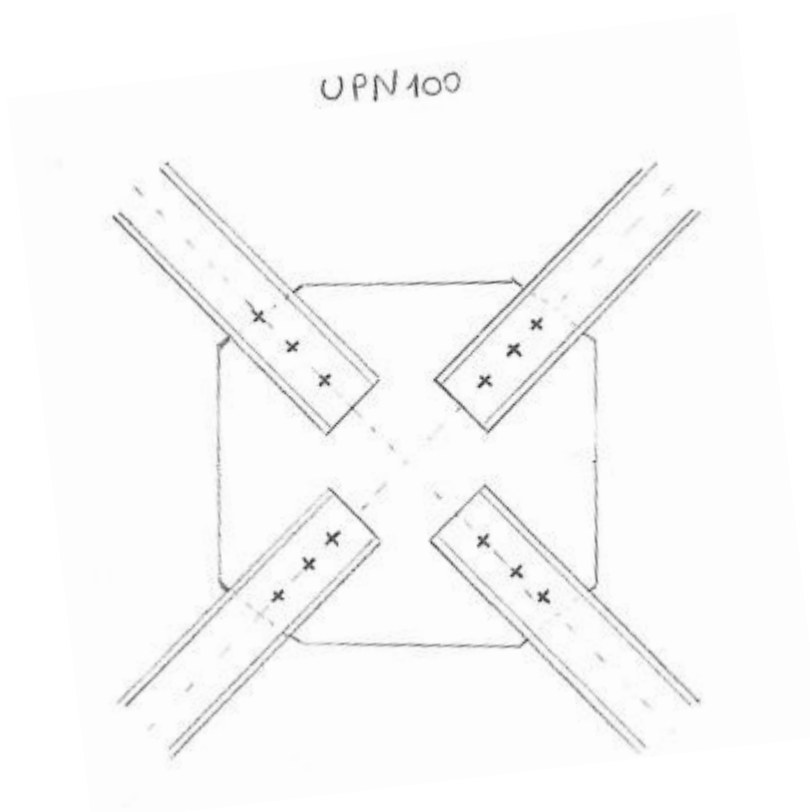


Figure 83: Sketch n.3 -Bracings

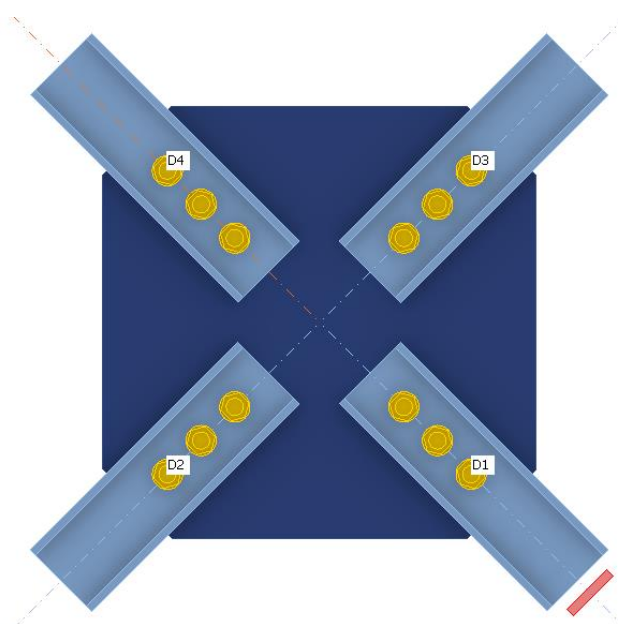


Figure 84: Joint n.3 in IDEA Statica

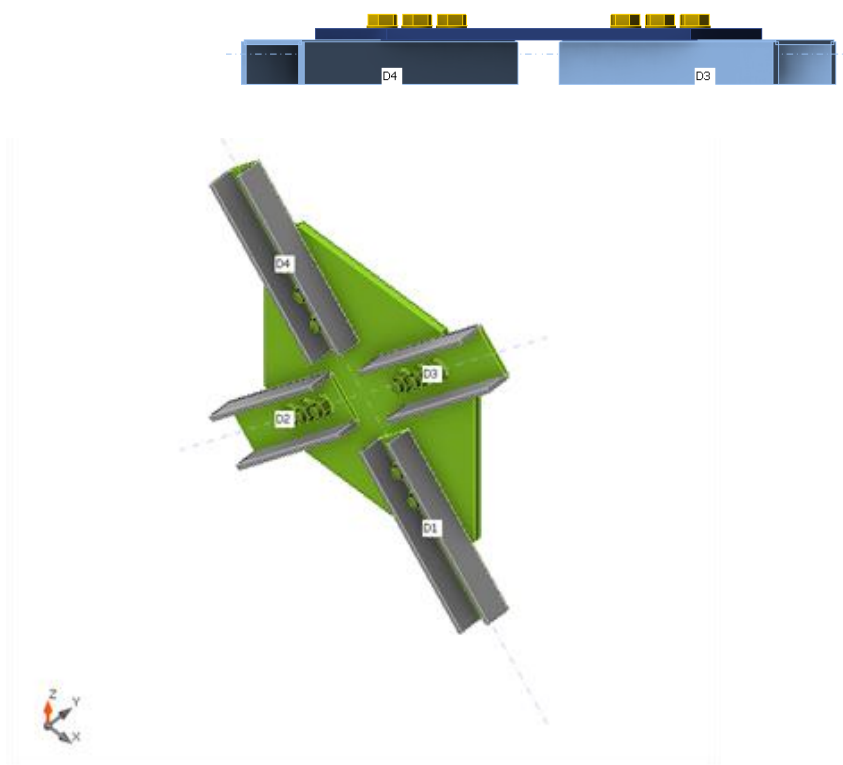


Figure 85: Overall check, LE1

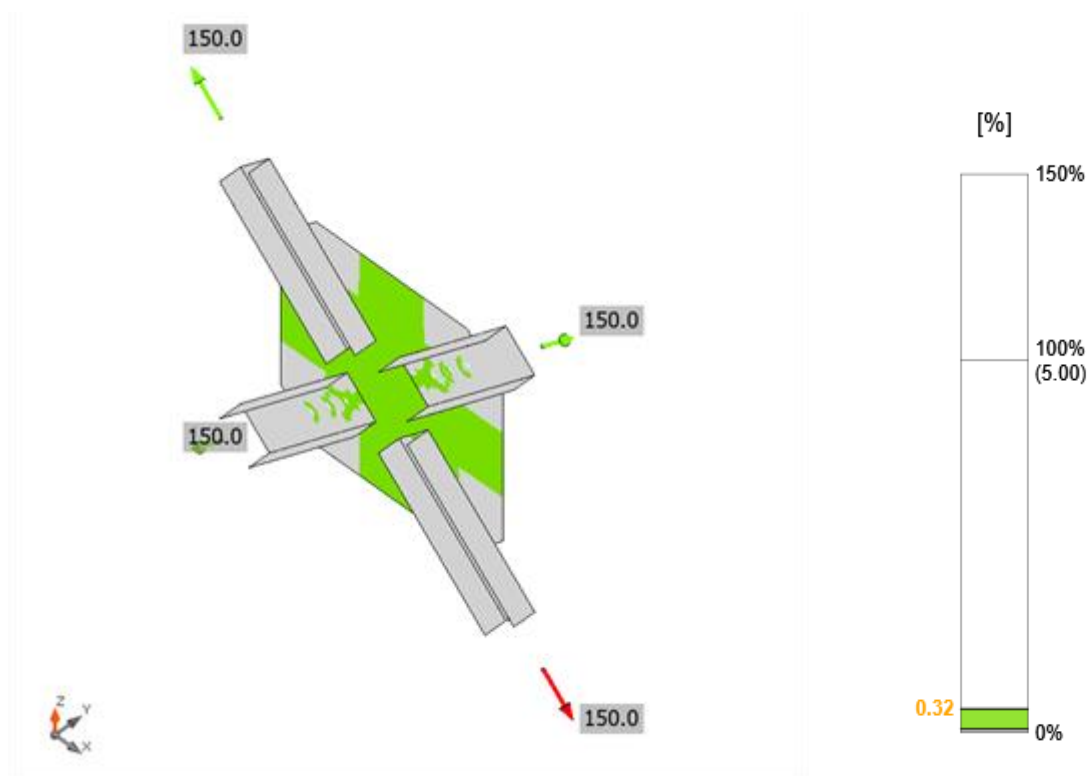


Figure 86: Strain check, LE1

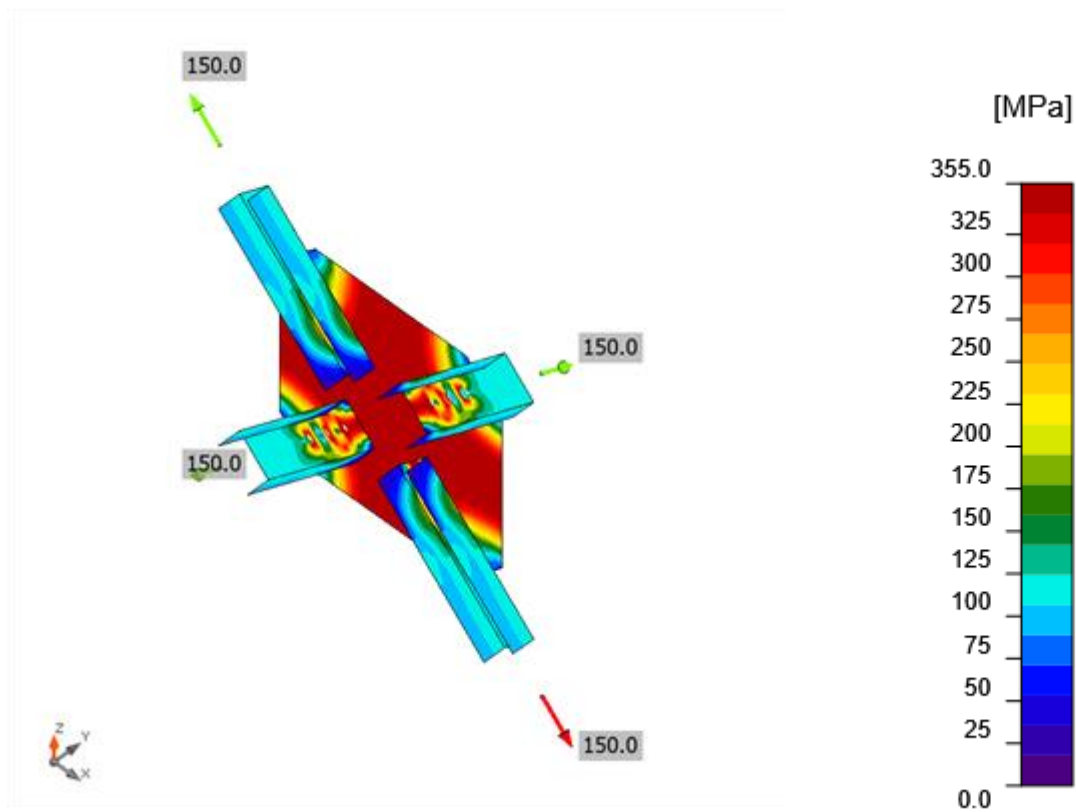
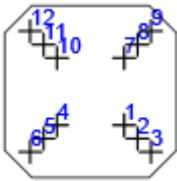


Figure 87: Equivalent stress, LE1

Bolts

Shape	Item	Grade	Loads	$F_{t,Ed}$ [kN]	$F_{v,Ed}$ [kN]	$F_{b,Rd}$ [kN]	U_{t_i} [%]	U_{t_s} [%]	$U_{t_{ts}}$ [%]	Detailing	Status
	B1	M20 8.8 - 1	LE1	71.2	51.6	98.0	50.6	54.8	90.9	OK	OK
	B2	M20 8.8 - 1	LE1	3.7	49.3	68.6	2.6	71.9	54.3	OK	OK
	B3	M20 8.8 - 1	LE1	4.5	49.1	68.6	3.2	71.5	54.4	OK	OK
	B4	M20 8.8 - 1	LE1	71.2	51.6	98.0	50.6	54.8	90.9	OK	OK
	B5	M20 8.8 - 1	LE1	3.7	49.4	68.6	2.7	71.9	54.4	OK	OK
	B6	M20 8.8 - 1	LE1	4.6	49.1	68.6	3.2	71.5	54.5	OK	OK
	B7	M20 8.8 - 1	LE1	71.3	51.6	98.0	50.6	54.8	90.9	OK	OK
	B8	M20 8.8 - 1	LE1	3.7	49.4	68.6	2.6	72.0	54.4	OK	OK
	B9	M20 8.8 - 1	LE1	4.5	49.1	68.6	3.2	71.5	54.5	OK	OK
	B10	M20 8.8 - 1	LE1	71.2	51.6	98.0	50.6	54.8	90.9	OK	OK
	B11	M20 8.8 - 1	LE1	3.7	49.3	68.6	2.6	71.9	54.3	OK	OK
	B12	M20 8.8 - 1	LE1	4.5	49.1	68.6	3.2	71.5	54.4	OK	OK

Design data

Grade	$F_{t,Rd}$ [kN]	$B_{p,Rd}$ [kN]	$F_{v,Rd}$ [kN]
M20 8.8 - 1	141.1	140.8	94.1

5 ARCHITECTURAL MODEL

The architectural model was created in Revit by importing the .gtcx file from Advance Design. The following operations were performed in Revit:

- positioning the secondary longitudinal beams at their correct height
- adding the wooden deck to the secondary beams
- positioning the asphalt before and after the walkway to facilitate the cycle-pedestrian path and road markings
- adding Revit files for the Macalloy hangers, which were also added

The architectural model is useful for us to then carry out the subsequent steps of rendering and metric calculation.

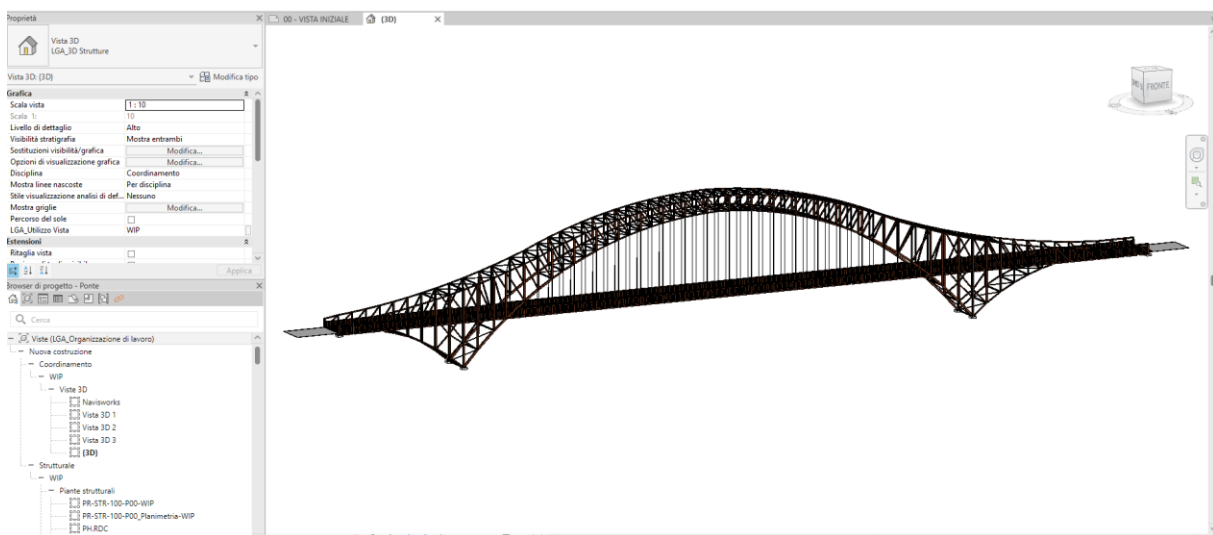


Figure 88: 3D Model in Revit

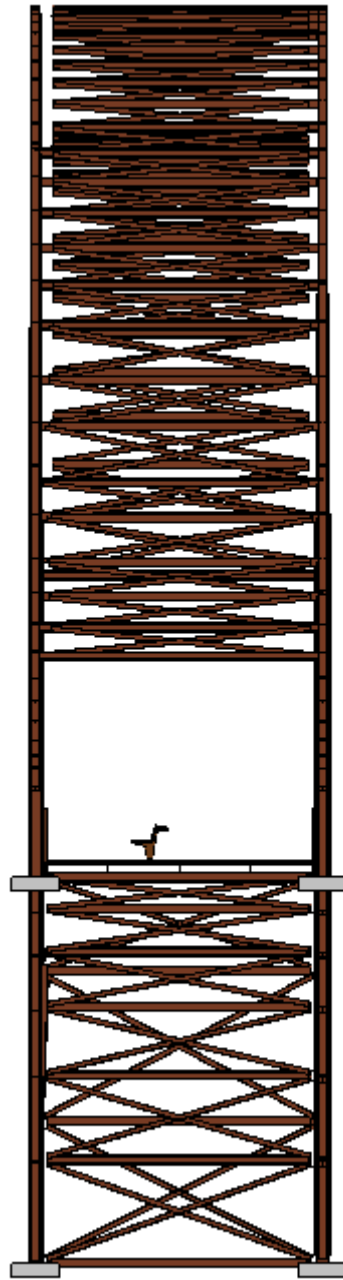


Figure 89: 3D Model lateral view in Revit

6 COST ANALYSIS (5th Dimension)

The economic aspect of BIM is what is known as the fifth dimension. In fact, this section contains a cost estimate related exclusively to the elements analyzed in this thesis. It is therefore not a complete calculation of the entire project, but rather an assessment focused on the structural parts that have been studied: metal carpentry, connections, supports. It was then decided to add an indicative calculation dedicated to excavation and site preparation; in the absence of data, assumptions were made. The objective is twofold: on the one hand, to offer an idea of the economic impact of the solutions adopted, but above all to link the economic aspect directly to the BIM model. In this way, if a change occurs in the three-dimensional model, it is possible to vary the metric calculation almost automatically. This is done using the architectural model created on Revit, from which it is possible to extrapolate the quantities of materials. Once the quantities are known, they are entered into Primus, a software program suitable for creating metric calculations. All prices for materials, labor, etc., were taken from the Piedmont 2025 Price List.

<Computo dei materiali per più categorie 2>				
A	B	C	D	E
Famiglia e tipo	Materiale: Nome	Materiale: Volume	Materiale: Costo	Peso
Flangia larga ad H-Pilastro: HE	Acciaio Corten	3,76 m³	2,00	29532,47 kg
Flangia larga ad H-Pilastro: HE	Acciaio Corten	2,51 m³	2,00	19735,53 kg
Trave H: HE180B	Acciaio Corten	10,73 m³	2,00	84254,09 kg
Trave H: HE200B	Acciaio Corten	4,99 m³	2,00	39170,89 kg
Trave H: HE240B	Acciaio Corten	0,38 m³	2,00	2963,55 kg
Trave H: HE320B	Acciaio Corten	1,39 m³	2,00	10926,90 kg
Trave IPE: IPE160	Acciaio Corten	1,58 m³	2,00	12369,84 kg
Trave UPN: UPN100	Acciaio Corten	2,47 m³	2,00	19367,67 kg
Acciaio Corten: 1514		27,81 m³		218320,94 kg
Sezioni circolari cave-Pilastro:	Acciaio S355	0,04 m³	0,00	350,66 kg
Sezioni circolari cave: TRON2	Acciaio S355	0,00 m³	0,00	14,81 kg
Acciaio S355: 37		0,05 m³		365,47 kg
Totale generale: 1551		27,86 m³		218686,41 kg

Figure 90: Quantity take-off related to materials using schedules in Revit

The cost estimate done in Primus is reported below (all the items are in Italian because the Price List is Italian).

N°	CODICE	DESIGNAZIONE DEI LAVORI	MISURAZIONI:				Quantità	IMPORTI	
			Par.ug	Lung.	Larg.	H/peso		unit ario	TOTALE
1	01.A02.E 10.005	<p>Allestimento di cantiere comprendente la collocazione di una unita' di decontaminazione provvista di almeno tre aree quali locale spogliatoio, locale doccia con acqua calda e fredda, locale equipaggiamento e di una unita' di filtraggio acqua oltre a tutto quanto richiesto dalla legislazione vigente in materia. Compreso il trasporto e il noleggio per tutta la durata dei lavori</p> <p>MISURAZIONI:</p> <p>2.00</p> <p>SOMMANO cad</p>					2.00		
							2.00	1674.47	3348.94
2	28.A05.D 05.005	<p>NUCLEO ABITATIVO per servizi di cantiere. Prefabbricato monoblocco ad uso ufficio, spogliatoio e servizi di cantiere. Caratteristiche: Struttura di acciaio, parete perimetrale realizzata con pannello sandwich, dello spessore minimo di 40 mm, composto da lamiera preverniciata esterna ed interna e coibentazione di poliuretano espanso autoestinguente, divisioni interne realizzate come le perimetrali, pareti pavimento realizzato con pannelli in agglomerato di legno truciolare idrofugo di spessore mm 19, piano di calpestio in piastrelle di PVC, classe 1 di reazione al fuoco, copertura realizzata con lamiera zincata con calatoi a scomparsa nei quattro angoli, serramenti in alluminio preverniciato, vetri semidoppi, porta d'ingresso completa di maniglie e/o maniglione antipanico, impianto elettrico a norma di legge da certificare. Sono compresi: l'uso per la durata delle fasi di lavoro che lo richiedono al fine di garantire la sicurezza e l'igiene dei lavoratori; il montaggio e lo smontaggio anche quando, per motivi legati alla sicurezza dei lavoratori, queste azioni vengono ripetute più volte durante il corso dei lavori a seguito della evoluzione dei medesimi; il documento che indica le istruzioni per l'uso e la manutenzione; i controlli periodici e il registro di manutenzione programmata; il trasporto presso il cantiere; la preparazione della base di appoggio; i collegamenti necessari (elettricità, impianto di terra acqua, gas, ecc) quando previsti; l'uso dell'autogru per la movimentazione e la collocazione nell'area predefinita e per l'allontanamento a fine opera. Arredamento minimo: armadi, tavoli e sedie [Note: La previsione degli apprestamenti proposti negli articoli seguenti (baraccamenti di cantiere), dovrà essere correttamente condotta in relazione alle caratteristiche ed alla localizzazione del cantiere, risultando di norma già riconosciuta nell'ambito delle spese generali (rif. D.P.R. 207/10 art. 32 c.4). Il Coordinatore per la Sicurezza in Fase di Progettazione valuterà l'eventuale inclusione di tali apprestamenti nel computo metrico della sicurezza in funzione delle esigenze ulteriori (rispetto a condizioni ordinarie) derivanti dal cantiere specifico.] Dimensioni esterne massime m 2,40 x 6,40 x 2,45 circa (modello base) -Costo primo mese o frazione di mese</p> <p>MISURAZIONI:</p> <p>2.00</p> <p>SOMMANO cad</p>					2.00		
							2.00	412.72	825.44

3	28.A05.D 05.010	<p>NUCLEO ABITATIVO per servizi di cantiere. Prefabbricato monoblocco ad uso ufficio, spogliatoio e servizi di cantiere. Caratteristiche: Struttura di acciaio, parete perimetrale realizzata con pannello sandwich, dello spessore minimo di 40 mm, composto da lamiera preverniciata esterna ed interna e coibentazione di poliuretano espanso autoestinguente, divisioni interne realizzate come le perimetrali, pareti pavimento realizzato con pannelli in agglomerato di legno truciolare idrofugo di spessore mm 19, piano di calpestio in piastrelle di PVC, classe 1 di reazione al fuoco, copertura realizzata con lamiera zincata con calatoi a scomparsa nei quattro angoli, serramenti in alluminio preverniciato, vetri semidoppi, porta d'ingresso completa di maniglie e/o maniglione antipanico, impianto elettrico a norma di legge da certificare. Sono compresi: l'uso per la durata delle fasi di lavoro che lo richiedono al fine di garantire la sicurezza e l'igiene dei lavoratori; il montaggio e lo smontaggio anche quando, per motivi legati alla sicurezza dei lavoratori, queste azioni vengono ripetute più volte durante il corso dei lavori a seguito della evoluzione dei medesimi; il documento che indica le istruzioni per l'uso e la manutenzione; i controlli periodici e il registro di manutenzione programmata; il trasporto presso il cantiere; la preparazione della base di appoggio; i collegamenti necessari (elettricità, impianto di terra acqua, gas, ecc) quando previsti; l'uso dell'autogru per la movimentazione e la collocazione nell'area predefinita e per l'allontanamento a fine opera. Arredamento minimo: armadi, tavoli e sedie [Note: La previsione degli apprestamenti proposti negli articoli seguenti (baraccamenti di cantiere), dovrà essere correttamente condotta in relazione alle caratteristiche ed alla localizzazione del cantiere, risultando di norma già riconosciuta nell'ambito delle spese generali (rif. D.P.R. 207/10 art. 32 c.4). Il Coordinatore per la Sicurezza in Fase di Progettazione valuterà l'eventuale inclusione di tali apprestamenti nel computo metrico della sicurezza in funzione delle esigenze ulteriori (rispetto a condizioni ordinarie) derivanti dal cantiere specifico.] costo per ogni mese o frazione di mese successivo al primo</p> <p>M I S U R A Z I O N I:</p>	2.00		12.00	24.00			
		SOMMANO cad				24.00	166.70	4000.80	
4	28.A05.D 25.005	<p>BAGNO CHIMICO PORTATILE per cantieri edili, in materiale plastico, con superfici interne ed esterne facilmente lavabili, con funzionamento non elettrico, dotato di un WC alla turca ed un lavabo, completo di serbatoio di raccolta delle acque nere della capacità di almeno 200 l, di serbatoio di accumulo dell'acqua per il lavabo e per lo scarico della capacità di almeno 50 l, e di connessioni idrauliche acque chiare e scure. Dimensioni orientative 120 x 120 x 240 cm. Il WC dovrà avere una copertura costituita da materiale che permetta una corretta illuminazione interna, senza dover predisporre un impianto elettrico. Compreso trasporto, montaggio, smontaggio, preparazione della base, manutenzione e spostamento durante le lavorazioni. Compreso altresì servizio di pulizia periodica settimanale (4 passaggi/mese) e il relativo scarico presso i siti autorizzati. nolo primo mese o frazione di mese</p> <p>M I S U R A Z I O N I:</p>	2.00			2.00			

		SOMMANO cad					2.00	179.11	358.22
5	28.A05.D 25.010	BAGNO CHIMICO PORTATILE per cantieri edili, in materiale plastico, con superfici interne ed esterne facilmente lavabili, con funzionamento non elettrico, dotato di un WC alla turca ed un lavabo, completo di serbatoio di raccolta delle acque nere della capacità di almeno 200 l, di serbatoio di accumulo dell'acqua per il lavabo e per lo scarico della capacità di almeno 50 l, e di connessioni idrauliche acque chiare e scure. Dimensioni orientative 120 x 120 x 240 cm. Il WC dovrà avere una copertura costituita da materiale che permetta una corretta illuminazione interna, senza dover predisporre un impianto elettrico. Compreso trasporto, montaggio, smontaggio, preparazione della base, manutenzione e spostamento durante le lavorazioni. Compreso altresì servizio di pulizia periodica settimanale (4 passaggi/mese) e il relativo scarico presso i siti autorizzati. nolo per ogni mese o frazione di mese successivo al primo M I S U R A Z I O N I:	2.00		12.00	24.00			
		SOMMANO cad				24.00		161.47	3875.28
6	18.A65.A 25.005	Decespugliamento di aree boscate con pendenza media inferiore al 50%, invase da rovi, arbusti ed erbe infestanti con salvaguardia dell'eventuale rinnovazione arborea ed arbustiva naturale su aree ad alta densità di infestanti (altezza superiore a m 1 e copertura dei terreno superiore al 90%) con raccolta e trasporto ad impianto di trattamento autorizzato o altro luogo indicato dalla D. L. dei materiali di risulta M I S U R A Z I O N I: SPALLA SX	120.00	3.00		360.00			
		SOMMANO m²				360.00		0.74	266.40
7	18.A65.A 25.005	Decespugliamento di aree boscate con pendenza media inferiore al 50%, invase da rovi, arbusti ed erbe infestanti con salvaguardia dell'eventuale rinnovazione arborea ed arbustiva naturale su aree ad alta densità di infestanti (altezza superiore a m 1 e copertura dei terreno superiore al 90%) con raccolta e trasporto ad impianto di trattamento autorizzato o altro luogo indicato dalla D. L. dei materiali di risulta M I S U R A Z I O N I: SPALLA DX	40.00	50.00	0.50	1000.00			
		SOMMANO m²				1000.00		0.74	740.00
8	23.A00.A 22.015	Interventi su vegetazione ripariale - taglio manutentivo della vegetazione ripariale dei corsi d'acqua principali e secondari all'interno dell'alveo attivo, sulle sponde e delle piante instabili nella fascia di 10 metri esterna al ciglio superiore di sponda, comprensivo di abbattimento, sramatura, allestimento, esbosco ed accatastamento del legname in zona di sicurezza, con rilascio della vegetazione flessibile come da Regolamento Forestale. Voce comprensiva di ogni altro onere accessorio per dare l'opera compiuta a regola d'arte secondo le indicazioni della DL. Presenza di formazioni lineari con copertura arborea continua, ma a tratti (alberi ed arbusti a gruppi, per lunghezze di almeno 30 metri). Diametro alberi medio-piccolo							

		(indicativamente, diametro medio inferiore a 15 cm). Condizioni operative difficili							
		MISURAZIONI:							
		SPALLA DX	30.00	10.00		300.00			
		SPALLA SX	30.00	10.00		300.00			
		SOMMANO m²				600.00	0.85	510.00	
9	07.A01.A 05.010	Scavo generale di sbancamento o splateamento, a qualsiasi scopo destinato, a qualsiasi profondità, eseguito con escavatore meccanico; compreso eventuale completamento a mano; con trasporto del materiale di risulta ad impianto di smaltimento autorizzato, escluso onere di trattamento dello stesso							
		MISURAZIONI:	30.00	9.00	2.50	675.00			
		SOMMANO m³				675.00	12.61	8511.75	
10.00	01.A01.C 50.005	Formazione di rampe accesso in rilevato e relative isole di lavoro nell'alveo di torrenti o fiumi, per l'esecuzione di opere di fondazione, di arginatura, pilastri e spalle di manufatti etc, eseguite con materiali ghiaio - terrosi opportunamente spianati e costipati, successiva rimozione delle stesse con idonei mezzi meccanici trasporto nei siti indicati dalla direzioe lavori e ripristino degli alvei e delle sponde eventualmente manomesse Con materiale provvisto dalla ditta							
		MISURAZIONI:							
		RAMPA ACCESSO SPALLA DX	30.00	5.00	1.00	150.00			
		PASSAGGIO IN ALVEO	100.00	5.00	1.00	500.00			
		RAMPA ACCESSO SPALLA SX	30.00	5.00	1.00	150.00			
		SOMMANO m³				800.00	44.38	35504.00	
11.00	18.A30.A 05.005	Ricostruzione di difese in massi e/o di prismi di calcestruzzo con rimozione della parte che si trova in posizione non più utile per variazione della conformazione idraulica e ricollocazione in opera nelle immediate vicinanze in posizione utile per il nuovo assetto idraulico							
		MISURAZIONI:							
		RACCORDI			100.00	100.00			
		SOMMANO m³				100.00	15.91	1591.00	
12.00	18.A30.A 10.005	rie terrose e ghiaiose anche con trovanti di e dimensione e durezza sino alla profondità di sotto il pelo delle acque di magra, compresa e rimozione lo spostamento in opera dei di cui prima e degli eventuali prismi di zzo di difese preesistenti, per apertura di , deviazione di acque, formazione di isolotti, per o alla posa di massi naturali, compresa la pne delle pareti e del fondo degli scavi, il							

		ento delle materie di risulta che dovranno e essere utilizzate esclusivamente secondo le ni della Direzione dei Lavori, il riempimento dei nenti ad opera finita e lo spianamento in alveo aterie eccedenti, il loro trasporto e la one entro l'area di cantiere, o rinterro e ad ento di sponda MISURAZIONI: RAMPA A SCENDERE RAMPA ACCESSO SPALLA SX		20.00 30.00	8.00 8.00	2.00 2.00	320.00 480.00			
		SOMMANO m³					800.00	4.43	3544.00	
13.00	01.P24.A 10.015	Nolo di escavatore con benna rovescia compreso manovratore, carburante, lubrificante, trasporto in loco ed ogni onere connesso per il tempo di effettivo impiego, della capacita' di m³ 1,500 MISURAZIONI:		2.00 2.00		30.00 30.00	60.00 60.00			
		SOMMANO h					120.00	118.2 9	14194.8 0	
14.00	18.A30.A 40.005	Esecuzione di scogliere con massi provenienti da cave disposti in sagoma prestabilita di volume comunque non inferiore a m³ 0,30 e di peso superiore a Kg 800 compresa la preparazione del fondo, l'allontanamento delle acque ed ogni altro onere per dare l'opera finita a regola d'arte. MISURAZIONI: SPONDA DX SPONDA DX		30.00 30.00	3.00 3.00	1.50 1.50	135.00 135.00			
		SOMMANO m³					270.00	74.80	20196.0 0	
15.00	01.A01.B 10.032	Scavo di materiali di qualsiasi natura in ambito urbano, fino ad una profondità massima di cm 60, compreso l'eventuale dissodamento e/o disfacimento della pavimentazione bituminosa, l'accumulo, il carico ed il trasporto ad impianto di trattamento autorizzato del materiale per profondità fino a Cm 60 eseguito a macchina MISURAZIONI:		30.00	2.00		60.00			
		SOMMANO m²					60.00	22.90	1374.00	
16.00	01.P26.A 60.030	Trasporto e scarico di materiale di scavo, demolizione e/o rifiuto ad impianto di trattamento autorizzato, esclusi i relativi oneri e tributi se dovuti. In impianto di trattamento autorizzato, da 10 km fino a 30 km di distanza MISURAZIONI:	100.00	0.15			15.00			
		SOMMANO m³					15.00	6.00	90.00	
17.00	01.A18.E 06.005	fornitura e posa in opera di parapetto in acciaio CORTEN per sentieri, parchi, piste ciclabili etc.; il tutto costituito da montanti verticali in acciaio del diametro di 114 mm, sp 2 mm, h. 1150 mm, da porre in opera alla distanza di circa 2,50 m, provvisti di due fori passanti per permettere l'inserimento dei correnti orizzontali. I montanti saranno provvisti di linguette pieghevoli con foro per il fissaggio dei correnti orizzontali e coperchi in								

		acciaio CORTEN per la protezione dagli agenti atmosferici per ogni metro lineare							
		MISURAZIONI:							
		SOMMANO m		320.00			320.00		
18.00	04.P83.A 13.015	Segnaletica orizzontale in vernice spartitraffico rifrangente premiscelata (composto di resina alchidica o acrilica) per tracciatura pittogramma "pista ciclabile", "omino" o altro, per ogni elemento verniciato a ripasso Tracciatura o ripasso pittogramma consistente in una freccia direzionale di dimensioni ridotte, per piste ciclabili o ciclo-pedonali, con dimensioni assimilabili a un triangolo avente una base di 60 cm e un'altezza di 70 cm e a un gambo costituito da una striscia avente una larghezza di 12-15 cm e una lunghezza di circa 100 cm. In colore bianco o giallo. MISURAZIONI: FRECCIA DIREZIONALE		6.00			6.00		
		SOMMANO cad					6.00	3.31	19.86
19.00	04.P83.A 02.005	Segnaletica orizzontale in vernice spartitraffico rifrangente premiscelata (composto di resina alchidica o acrilica) per la tracciatura delle linee di mezzzeria e di corsia, marginali, piste risevate, ecc., computabili a metro lineare, da tracciarsi tendenzialmente a ripasso (nuovi manti esclusi). La stesa in opera dovrà essere conforme e dovrà rispettare le prescrizioni della normativa UNI-EN 1436, con particolare riguardo ai criteri di efficienza, rifrangenza e antiskid. Ripasso striscia in vernice spartitraffico rifrangente, in colore bianco o giallo, di larghezza cm 12 MISURAZIONI: SEGNALETICA DI MEZZERIA		320.00			320.00		
		SOMMANO m					320.00	0.55	176.00
20.00	04.P83.A 02.010	Segnaletica orizzontale in vernice spartitraffico rifrangente premiscelata (composto di resina alchidica o acrilica) per la tracciatura delle linee di mezzzeria e di corsia, marginali, piste risevate, ecc., computabili a metro lineare, da tracciarsi tendenzialmente a ripasso (nuovi manti esclusi). La stesa in opera dovrà essere conforme e dovrà rispettare le prescrizioni della normativa UNI-EN 1436, con particolare riguardo ai criteri di efficienza, rifrangenza e antiskid. Ripasso striscia in vernice spartitraffico rifrangente, in colore bianco o giallo, di larghezza cm 15 MISURAZIONI: LINEE DI MARGINE		2.00	320.00		640.00		
		SOMMANO m					640.00	0.64	409.60
21.00	04.P80.D 01.010	Sostegni per segnali stradali in uso nella città di Torino Palina semplice o piantana in tubo di acciaio zincato a caldo, spessore minimo mm 3,25 (pn). può essere richiesta anche con cavallotti saldati alla base per il fissaggio con sistema BAND-IT (prs). Diam. 48 h da 2.81 a 3.80 m MISURAZIONI: NUOVA SEGNALETICA		3.00			3.00		

		SOMMANO cad					3.00	25.80	77.40
22.00	04.P80.A 03.060	Cartelli stradali e pannelli integrativi normalizzati (art.37.1/37.5 C.P.A.) Segnale stradale in lamiera di alluminio o pannello integrativo a forma quadrata o romboidale conforme alle tab. II 5,6,9 art. 80 D.P.R. 495/92. il supporto in alluminio dovrà aver subito le necessarie lavorazioni quali: carteggiatura meccanica, sgrassaggio, lavaggio, fosfocromatazione e lavaggio demineralizzato, quindi, dopo l'applicazione di vernici tipo wash-primer, dovrà essere verniciato in color grigio neutro con processo elettrostatico e polveri termoindurenti cotte al forno a 180 °C per 30'. sul supporto così preparato verrà applicata la pellicola retroriflettente "a pezzo unico" secondo il disciplinare tecnico approvato con D.M. 31/5/95, n.1584 e s. m. i. (Al= supporto in lamiera di alluminio; E.G.= pellicola retroriflettente classe 1; H.I.= pellicola retroriflettente classe 2). Lato 600 mm, sp. 25/10, Al, H.I MISURAZIONI: SEGNALETICA VERTICALE	3.00				3.00		
		SOMMANO cad					3.00	79.46	238.38
23.00	01.A01.A 55.020	Scavo a sezione obbligata o a sezione ristretta per opere di fondazione, in terreni sciolti o compatti, di larghezza minima 30 cm, anche in presenza di acqua fino ad un battente massimo di 20 cm, eseguito con idonei mezzi meccanici, esclusa la roccia da mina, misurato in sezione effettiva, compreso il carico sugli automezzi, trasporto e sistemazione entro l'area del cantiere, escluse eventuali sbadacchiature per scavi oltre 1,50 m di profondità da conteggiare totalmente a parte. Oltre a 3 m di profondità rispetto al piano di sbancamento, solo per la parte eccedente i primi 3 m MISURAZIONI: SPALLA DX SPALLA SX		6.00 6.00	7.00 7.00	2.60 4.00	109.20 168.00		
		SOMMANO m³					277.20	16.10	4462.92
78	01.A24.F 20.010	Fornitura e posa in opera di apparecchi di appoggio per impalcati di ponti, in acciaio e teflon per ogni tonnellata di reazione all'appoggio, compreso ogni onere Di tipo mobile unidirezionale e multidirezionale MISURAZIONI:	2.00 2.00			40.000 300.00	80.00 600.00	6.84	547.20
		SOMMANO t					680.00	6.84	4651.20
25.00	01.A24.F 20.005	Fornitura e posa in opera di apparecchi di appoggio per impalcati di ponti, in acciaio e teflon per ogni tonnellata di reazione all'appoggio, compreso ogni onere Di tipo fisso MISURAZIONI: APPOGGI TIPO FISSO	2.00			400.00	800.00		
		SOMMANO t					800.00	4.99	3992.00
26.00	01.A18.A 10.010	Carpenteria per grandi orditure o industrializzata, capriate, tralicci, pilastri e simili, compresa coloritura ad una ripresa di antiruggine, escluse le sole opere murarie In ferro in profilati normali e lavorazione chiodata o bullonata MISURAZIONI:							

		IMPALCATO				218321	218321		
			* Parziale kg				218321		
		INCREMENTO PIASTRAME		15282.47		0.10	1528.25		
			SOMMANO kg				219849	3.00	659548
27.00	01.P16.A 70.020 c	Rivestimento in tavole lisce o in perline in legno massello, perfettamente piallate, non verniciate (castagno)					960	39	37872
		TOTALE euro							835184

7 RENDER

The render is created with the aim of producing a highly realistic visual representation; this plays a significant role in the presentation of the project, as it allows even non-experts to easily understand its content. The rendering of the model was carried out using Twinmotion, a software developed by Epic Games, specifically designed for rendering and real-time visualization.

The import of files into Twinmotion is enabled through the Plug in Revit, which allows for direct export and synchronization between the two programs. In this way, any modifications made to the Revit model are automatically or manually updated in Twinmotion through synchronization.



Figure 91: Render n.1



Figure 92: Render n.2















Figure 93: Render n.3

Conclusions

The thesis covers the main steps in the design process for a civil engineering project, specifically a cycle-pedestrian bridge. Starting with an introduction to the BIM methodology used and the surrounding context, the geometry and materials to be used were chosen in collaboration with LGA Engineering.

The part relating to the dimensioning and verification of the structural elements is certainly the most extensive and the one that took the most time because, despite the use of software, the design was an iterative process: the elements were modified several times, increasing the sections in order to satisfy the verifications without exceeding the oversizing. A fundamental aspect in the choice of profiles concerned the dynamic behaviour of the walkway in relation to pedestrian comfort. Vibration analysis made it possible to evaluate the response of the structure under pedestrian loads, ensuring that the oscillations were within acceptable limits for safe and comfortable use. The results obtained are very satisfactory, offering a structure that not only meets regulatory requirements for safety and durability but is also aesthetically pleasing.

Part of the thesis work was devoted to evaluating how BIM methodology can facilitate data exchange within a project. As this was a single thesis, it was not possible to investigate the interoperability between different professional figures in depth, but the interoperability between the software used was investigated. The interoperability matrix, which shows the degree of interconnection between the programmes, is shown below.

	To From						
Autocad 2D		✓	✓	✓	/	/	/
Advance Design		✓	✓	!	✓	/	/
Revit 3D		✓	/	✓	/	✓	!
IDEA Statica		/	/	/	✓	/	/
Twinmotion		/	/	✓	/	✓	/
Primus		/	/	/	/	/	✓



 80-100 %
 30-79 %
 / unexamined

Figure 94: Interoperability matrix

As can be seen, the interoperability between the programmes used gave excellent results, with very little data loss. In particular, there is excellent interoperability between Advance Design and IDEA Statica using a special tool, with the possibility of importing all load combinations. It should be noted, however, that this involves a significant computational burden and should therefore be evaluated appropriately when necessary. For exporting from Advance Design to Revit, the .ifc format was initially used, but some information was lost, including profile recognition and therefore the ability to make changes. For this reason, it was decided to export the .gtcx file, on which it was then possible to develop the architectural model. From Revit, importing the model into Twinmotion was a very simple operation using a special tool, with the possibility of synchronising the two models.

In conclusion, BIM certainly brings greater complexity to both project management and computation, which is why it can sometimes be difficult for small projects. However, as the size of the project increases, these advanced calculation tools greatly facilitate design, calculation and communication within the project. The thesis work carried out demonstrates how it is possible to refine and optimise structural solutions, both globally and locally, representing an interesting prospect for the future of civil engineering.

Table of figures

Figure 1: LOD in different countries	8
Figure 2: Workflow	9
Figure 3: Top view of the site of the intervention.....	11
Figure 4: Top view photo of the site taken with a drone	12
Figure 5: Photo of the site taken with a drone	12
Figure 6: Neuer Zollhof complex in Dusseldorf	13
Figure 7: Guggenheim Museum in Bilbao	13
Figure 8: Tyne Bridge, UK	14
Figure 9: Las Llamas Bridge, Spain.....	14
Figure 10: Chaotianmen Bridge, China.....	15
Figure 11: Site plan	16
Figure 12: Stress-strain curve	18
Figure 13: Snow load zones.....	23
Figure 14: Map of the zones into which the Italian territory is divided.....	25
Figure 15: -Evolution of the exposure coefficient c_e as a function of height above ground (for $c_t = 1$)	28
Figure 16: Deck shapes proposed by the CNR -DT 207 R1/2008	30
Figure 17: Force coefficient c_{fx0} for structures and elements with circular cross-section (Fig. G.53 CNR).....	31
Figure 18: Values of $c_m(z)$ for different exposure categories, in case $c_r(z)=1$	33
Figure 19: Maximum and minimum temperatures for bridges	34
Figure 20: Thermal zones according to external air temperature	35
Figure 21: 2D Design in Autocad	46
Figure 22: 2D Design in Advance Design	46
Figure 23: 3D Model in Advance Design.....	47
Figure 24: Axial forces under self-weight.....	48
Figure 25: Bending moment under self-weight	48
Figure 26: 3D Model with loads	49
Figure 27: 3D Model with wind loads	49
Figure 28: 3D Model with wind load, lateral view	50
Figure 29: Advance Design Conventions	50
Figure 30: Maximum resistance utilization ratio.....	52
Figure 31: Maximum stability utilization ratio	52
Figure 32: HEB 320 section taken from Advance Design profiler	62
Figure 33: Axial forces F_x on arch.....	63

Figure 34: Shear forces F_y on the arch.....	63
Figure 35: Shear forces F_z on the arch.....	64
Figure 36: Bending moment on the arch	64
Figure 37: HEB 200 section taken from Advance Design profiler	72
Figure 38: Resistance utilization rate	72
Figure 39: : Stability utilization rate	73
Figure 40: HEB 180 section taken from Advance Design profiler	74
Figure 41: HEB 200 section taken from Advance Design profiler	75
Figure 42: : Resistance utilization rate	75
Figure 43: : Stability utilization rate	76
Figure 44: UPN100 section taken from Advance Design profiler.....	77
Figure 45: : Resistance utilization rate	78
Figure 46: : Resistance utilization rate	79
Figure 47: : Resistance utilization rate	81
Figure 48: : Resistance utilization rate	82
Figure 49: : Stability utilization rate	83
Figure 50: Circular section taken from Advance Design profiler.....	84
Figure 51: Axial force acting on hangers	84
Figure 52: : Resistance utilization rate	85
Figure 53: Displacements under SLE combination	90
Figure 54: Methodology for calculating the equivalent number of pedestrians	94
Figure 55: Methodology organization chart.....	95
Figure 56: First mode of vibration	98
Figure 57: Second mode of vibration	98
Figure 58: Third mode of vibration	99
Figure 59: Frequency ranges (Hz) of the vertical and longitudinal vibrations	99
Figure 60: Frequency ranges (Hz) of the transverse horizontal vibrations	99
Figure 61: Acceleration ranges (m/s^2) for vertical vibrations	101
Figure 62: Acceleration ranges (m/s^2) for horizontal vibrations	101
Figure 63: Values of factor ψ depending on frequencies	103
Figure 64: Bearing's articulation	105
Figure 65: Bearings symbol legend.....	105
Figure 66: Reactions in x direction	106
Figure 67: Reactions in y direction	106
Figure 68: Reactions in z direction	107

Figure 69: Displacements in y direction	108
Figure 70: Reactions in x direction	108
Figure 71: Main components of bolted joints.....	112
Figure 72: Rules for the arrangement of holes for bolted connections.....	114
Figure 73: Throat planes - NTC 18.....	119
Figure 74: Sketch n. 1- Vertical members, longitudinal beams, diagonals	121
Figure 75: Sketch n.2 -Vertical members, transversal beams	122
Figure 76: Joint n.1 in IDEA Statica.....	123
Figure 77: Overall check, 141 - $1.35 \times [1 \text{ G}] + 1.5 \times [2 \text{ G}] + 1.5 \times [5 \text{ V}] (5)$	125
Figure 78: Strain check, 141 - $1.35 \times [1 \text{ G}] + 1.5 \times [2 \text{ G}] + 1.5 \times [5 \text{ V}] (5)$	126
Figure 79: Joint n.2 in IDEA Statica.....	130
Figure 80: Overall check, LE3.....	130
Figure 81: Strain check, LE3.....	131
Figure 82: Equivalent stress, LE3.....	131
Figure 83: Sketch n.3 -Bracings	134
Figure 84: Joint n.3 in IDEA Statica.....	134
Figure 85: Overall check, LE1.....	135
Figure 86: Strain check, LE1.....	135
Figure 87: Equivalent stress, LE1	136
Figure 88: 3D Model in Revit	137
Figure 89: 3D Model lateral view in Revit	138
Figure 90: Quantity take-off related to materials using schedules in Revit.....	139
Figure 91: Render n.1	148
Figure 92: Render n.2	149
Figure 93: Render n.3	149
Figure 94: Interoperability matrix	150

Bibliography and Webography

- [1] Ministero delle Infrastrutture e dei Trasporti, *DECRETO 17 gennaio 2018. Aggiornamento delle «Norme tecniche per le costruzioni»*, Roma, Italia: Gazzetta Ufficiale della Repubblica Italiana, 2018
- [2] Ministero delle Infrastrutture e dei Trasporti, *Istruzioni per l'applicazione dell'«Aggiornamento delle «Norme tecniche per le costruzioni»» di cui al decreto ministeriale 17 gennaio 2018.*, Roma, Italia: Gazzetta Ufficiale della Repubblica Italiana, 2019.
- [3] Footbridges, Assessment of vibrational behaviour of footbridges under pedestrian loading, Technical guide SETRA, Paris, France 2006;
- [4] CNR - Consiglio Nazionale delle Ricerche, *Istruzioni per la valutazione delle azioni e degli effetti del vento sulle costruzioni*, 2019.
- [5] European Committee for Standardization, *EN 1993-1-1:2005: Eurocode 3: Design of steel structures - Part 1-1: General rules and rules for buildings*, 2005.
- [6] European Committee for Standardization, *EN 1993-2: Eurocode 3: Design of steel structures - Part 2: Steel bridges*, 2006.
- [7] European Committee for Standardization, *EN 1993-1-5: Eurocode 3: Design of steel structures - Part 1-5: Plated structural elements*, 2006.
- [8] Anna Osello, Notes from the course “InfraBIM, Design, Construction and Management”, a.a.2023/2024
- [9] Francesco Tondolo, Notes from the course “Theory and design of steel structures”, a.a. 2022/2023
- [10] <https://www.elemka.gr/media/Ozknhcyi/fip-vasoflon.pdf>
- [11] <https://www.fipmec.it/it/prodotti/apparecchi-dappoggio/>
- [12] <https://macalloy.com/>